

The removal and fixing of harmful substances by zeolites and their composites

WATANABE, Yujiro / 渡邊, 雄二郎

(発行年 / Year)

2005-03-24

(学位授与番号 / Degree Number)

32675甲第137号

(学位授与年月日 / Date of Granted)

2005-03-24

(学位名 / Degree Name)

博士(工学)

(学位授与機関 / Degree Grantor)

法政大学 (Hosei University)

(URL)

<https://doi.org/10.15002/00003811>

法政大学院工学研究科物質化学専攻

**THE REMOVAL AND FIXING OF HARMFUL SUBSTANCES
BY ZEOLITES AND THEIR COMPOSITES**

ゼオライト系化合物による有害物質の除去と
固定化に関する研究

02R9201

渡辺 雄二郎

YUJIRO WATANABE

CONTENTS

CHAPTER 1.	
INTRODUCTION.....	4
1-1. General introduction.....	5
1-2. Adsorbent for ammonium ion and radioactive ions: Zeolite	8
1-2-1. Characterization of zeolite	8
1-2-2. The application of zeolite to water and wastewater treatment.....	8
1-3. Material for removing harmful ions and for fixing of radioactive ion: Apatite ...	10
1-3-1. Characterization of apatite	10
1-3-2. The application of apatite for removing of harmful ions and for fixing of radioactive ions.....	11
1-4. References	13
CHAPTER 2.	
ION EXCHANGE BEHAVIOR OF NATURAL ZEOLITES.....	15
Natural zeolites from Shimane, Japan	16
2-1. Introduction.....	16
2-2. Experiment.....	17
2-3. Results and discussion.....	19
2-4. Conclusion.....	23
Natural zeolites from Akita, Japan and Australia	31
2-5. Introduction.....	31
2-6. Experiment.....	32
2-7. Results and discussion.....	33
2-8. Conclusion	35
2-9. References	41
CHAPTER 3.	
AMMONIUM ION EXCHANGE OF SYNTHETIC ZEOLITES.....	43
3-1. Introduction.....	44
3-2. Experiment.....	46
3-3. Results and discussion.....	48
3-4. Conclusion	54
3-5. References	62
CHAPTER 4.	
AMMONIUM IONS EXCHANGE OF SYNTHETIC ZEOLITES OBTAINED FROM HYDROTHERMAL MODIFICATION OF NATURAL ZEOLITES.....	64
4-1. Introduction.....	65
4-2. Experiment.....	66
4-3. Results and discussion.....	68
4-4. Conclusion	72
4-5. References	80
CHAPTER 5.	
HYDROTHERMAL FORMATION OF HYDROXYAPATITE LAYERS ON THE SURFACE OF TYPE-A ZEOLITE.....	82

Preparation of a novel type-A zeolite with hydroxyapatite layers on its surface by a hydrothermal method	83
5-1. Introduction	83
5-2. Experiment	83
5-3. Results and discussion	84
5-4. Conclusion	88
Ion exchange ability in NaCl solution and stability of its structure in the process of the ion exchange for the type-A zeolite with hydroxyapatite surface layers	93
5-5. Introduction	93
5-6. Experimental methods	93
5-7. Results and discussion	95
5-8. Conclusion	98
HAp thin layers synthesized on the LTA surface by hydrothermal treatments at different temperatures and durations in the reactions	101
5-9. Introduction	101
5-10. Experimental	102
5-11. Results and discussion	103
5-12. Conclusion	107
5-13. References	116
 CHAPTER 6.	
THE DENIFICATION OF ZEOLITE/APATITES COMPOSITES USING PULSE ELECTRIC CURRENT SINTERING METHOD	118
6-1. Introduction	118
6-2. Experimental methods	120
6-3. Results and discussion	122
6-4. Conclusion	126
6-5. References	137
 CHAPTER 7.	
CONCLUSIONS	139
7-1. GENERAL CONCLUSION	140
7-2. Ammonium adsorption on various zeolites	140
7-3. The preparation of zeolite/apatite composites for removing of harmful ions and for fixing radioactive ions	141
 LIST OF PUBLICATIONS	144
ACKNOWLEDGMENTS	152

CHAPTER 1

INTRODUCTION

1-1. GENERAL INTRODUCTION

The world is faced with increasing demands for removal of contaminants from municipal, agricultural, and industrial wastewaters. The most common cation in the waters affecting human and animal health is ammonium ion (NH_4^+). To achieve better NH_4^+ treatment, the use of activated carbon, which is comparatively expensive, is proposed. Zeolites have been proposed as an alternative to the activated carbon, and can also be used as a pretreatment material prior to biological processing to ensure a constant concentration feed to a biological treatment plant. The use of natural zeolites in removal of NH_4^+ from wastewaters has been reported by many authors. But the characterization, synthesis, and chemical behavior of various zeolites for improvement of NH_4^+ removal from wastewaters have not been investigated in detail. Therefore, it is very important to investigate about NH_4^+ behaviors on various zeolites. In this study, the characterization, synthesis, and NH_4^+ exchange behaviors of natural zeolites, synthetic zeolites, and modified zeolite were carried out by using various methods (XRD, SEM, EDS, ICP, electric specific (NH_4^+), and BET).

The disposal of radioactive waste generated by the nuclear fuel cycle also is among the most pressing and potentially costly environmental problems of the 21st century. Proposed disposal strategies are complicated, not only because of the large volumes and high radioactivities of the waste, but also because of the political and public-policy issues associated with a long period of time of storage in containment (10^4 to 10^6 years).

Zeolites have been proposed as a material for removing heavy metal ions such as Cd^{2+} and Pb^{2+} , and radioactive ions such as Cs^+ , Sr^{2+} , and I^- . But the stability in alkali solution is lower than other materials for fixation. Hydroxyapatite [$\text{Ca}_{10}(\text{PO}_4)_6(\text{OH})_2$] also has a high cation exchange capacity for Cd^{2+} and very low solubility products of under 5.4×10^{-119} (K_{sp} ; $\text{mol}^{18}\text{I}^{-18}$), and shows particularly high stability in alkaline solution. Therefore, the apatite solidification is expected to be stable for a longer period of time than cement solidification or glassification. For these reasons, we focused on zeolite/apatite composites as a material for removal of these harmful ions and radioactive ions. In this study, the synthesis and sintering of zeolite/apatite composites were carried out under various conditions, and the characterization of the obtained materials was investigated by using various methods (XRD, SEM, EDS, TEM, STEM, ICP, Electric specific (NH_4^+), BET, Dynamic-ultra-microhardness tester, and Universal tester).

This thesis is composed of 6 chapters. Chapter 1 describes about characterization of zeolites and their application in water and wastewater treatment, and about characterization of apatite and its application for removing of harmful ions and for fixing of radioactive ions.

Chapter 2 describes about ion exchange behavior of natural zeolites from Shimane and Akita prefectures, Japan and Mount Gipps, Australia in distilled water, hydrochloric acid, and ammonium chloride solution. The results were compared with published adsorption values of other zeolites.

Chapter 3 describes about ammonium ion exchange of synthetic zeolites (Lide Type A zeolite, Faujasite, Sodalite, and rho zeolite) in regard to the effect of their open-window sizes, pore structures, and cation exchange capacities.

Chapter 4 describes about hydrothermal modification of natural zeolites (natural clinoptilolite and mordenite) to improve up-take of ammonium ions.

Chapter 5 describes about hydrothermal formation of hydroxyapatite layers on the surface of type-A zeolite.

Chapter 6 describes about the sintered bodies of LTA with HAp thin layers and FAp fabricated by using the pulse electronic current sintering (PECS) method.

Chapter 7 concludes the results obtained in this study.

1-2. ADSORBENT FOR AMMONIUM IONS AND RADIOACTIVE IONS:

ZEOLITE

1-2-1. Characterization of zeolite

Zeolite is defined by the requirements of Smith (1963) for a zeolite.¹ These requirements include: (a) a three-dimensional framework of tetrahedral, more than 50% of which is occupied by Si and Al; (b) an 'open' structure with a framework density (i.e. the number of tetrahedral atoms per 1000 \AA^3) lower than 20 (Brunner and Meier, 1989) and hence enclosing cavities connected by windows larger than regular six-membered rings; and (c) an extraframework content represented by cations and water molecules.²

In the general formula $M_x D_y [Al_{x+2y} Si_{n-(x+2y)} O_{2n}] \cdot mH_2O$, where M_x are monovalent and D_y are divalent cations, it is possible to distinguish two parts, although they are very different, which are mutually dependent and form a homogeneous complex endowed with exclusive chemico-physical properties. A portion in the square brackets represents the tetrahedral framework and is characterized by an overall negative charge which increases as the Si/Al ratio decreases. The area outside the square brackets consists of exchangeable extraframework cations, which neutralize the framework negative charge, and finally water molecules which often coordinate with the extraframework cations.

1-2-2. The application of zeolite to water and wastewater treatment

The world is faced with increasing demands for removal of contaminants from municipal, agricultural, and industrial wastewaters. The use of natural zeolites in removal

of impurities from drinking water or wastewater have been reported by many authors (Murphy et al. 1978, Tarasevich 1994, Kallo 1995).³⁻⁵

Most technologies using natural zeolites for water purification are based on the unique cation-exchange behavior of zeolites through which dissolved cations can be removed from water by exchanging with cations on zeolites exchange sites. The most common cation in water affecting human and animal health is NH_4^+ . It can be removed by exchanging with biologically acceptable cations such as Na^+ , K^+ , Mg^{2+} , Ca^{2+} or H^+ residing on the exchange sites of the zeolites. Fortunately, many natural zeolites (e.g. clinoptilolite, mordenite, phillipsite, and chabazite) are selective for NH_4^+ , meaning that they exchange NH_4^+ even in the presence of larger amounts of competing cations. Clinoptilolite and mordenite are also selective for transition metals (e.g. Cu^{2+} , Ag^+ , Zn^{2+} , Cd^{2+} , Hg^{2+} , Pb^{2+} , Cr^{3+} , Mo^{2+} , Mn^{2+} , Co^{2+} , and Ni^{2+}), which are often present in industrial wastes, and can be very toxic even in a concentration as low as several mg/L. As emphasized in discussion of radioactive waste treatment, both clinoptilolite and mordenite have very high selectivity for Cs^+ and Sr^{2+} , and can therefore be used to remove minute amounts of radioactive ^{137}Cs and ^{90}Sr from nuclear process wastewater.

The quality of water prior to treatment can vary considerably. Simple purification technologies, such as the use of chemical additives, may not meet demands for quality water. This is particularly so in cases where too much chemicals are applied, which may result in hazardous water (e.g. excess organic coagulants may increase the biological

oxygen demand (BOD) in the effluent, or surplus Al added for phosphate removal may become a harmful contaminant to humans). Fortunately, the use of natural zeolites has a potential to eliminate this problem by removing contaminants from the water via an ion-exchange or adsorption process. Furthermore, abundant deposits of natural zeolites in near-surface sedimentary deposits make their use in the treatment of drinking water and wastewater very attractive.

1-3. MATERIAL FOR REMOVING HARMFUL IONS AND FOR FIXING OF RADIOACTIVE IONS: APATITE

1-3-1. Characterization of apatite

The apatite-group minerals of the general formula of $M_{10}(ZO_4)_6X_2$ ($M = Ca, Sr, Pb, Na...$, $Z = P, As, Si, V...$, and $X = F, OH, Cl...$) are remarkably tolerant to structural distortion and chemical substitution, and consequently are extremely diverse in composition (e.g., Kreidler and Hummel 1970; McConnell 1973; Roy et al. 1978; Elliott 1994).⁶⁻⁹ Of particular interest is that a number of important geological, environmental/paleoenvironmental, and technological applications of the apatite-group minerals are directly linked to their chemical compositions. It is therefore fundamentally important to understand the substitution mechanism, and other intrinsic and external factors that control the compositional variation in apatites.

Phosphate apatites, particularly fluorapatite and hydroxyapatite, are by far the most

common in nature, and are often synonymous with “apatite(s)”. For example, fluorapatite is a ubiquitous accessory phase in igneous, metamorphic, and sedimentary rocks, and major constituent in phosphorites, and certain carbonates and anorthosites (McConnell 1973; Dymek and Owens 2001).^{7,10} Of particular importance in a biological system is hydroxylapatite and fluorapatite (and their carbonate-bearing varieties) which are important mineral components of bones, teeth, and fossils.

1-3-2. The application of apatite for removing of harmful ions and for fixing of radioactive ions

The disposal of radioactive waste generated by the nuclear fuel cycle is among the most pressing and potentially costly environmental problems of the 21st century. Proposed disposal strategies are complicated, not only because of the large volume and high radioactivity of the waste, but also because of the political and public-policy issues associated with a long period of time of storage in containment (10^4 to 10^6 years).

To keep the waste in a highly durable form, materials that have a high chemical durability and resistance to radiation damage effects contribute to the disposal strategy.

An interest in a phosphate-based form of waste has been aroused because the waste with a high radioactivity level generated by reprocessing of used nuclear fuel contains a substantial amount of phosphate (up to 15wt % P_2O_5) that results from processing technology utilized either a bismuth phosphate or tributylphosphate process (Bunker et al. 1995).¹¹ In addition to the high phosphate content, other metal oxides may account for a

significant proportion (Lambert and Kim 1994).¹² These complex compositions have presented special challenge in developing crystalline ceramics that can accommodate the full compositional range of the waste stream.

The early work on phosphate glasses led to the idea that crystalline phosphate might make extremely durable waste forms, particularly for actinides. The earliest suggestion was for the use of monazite (Boatner 1978, Boatner et al. 1980, McCarthy et al. 1978, 1980).¹³⁻¹⁶ The attractive features of monazite as a nuclear waste form are: (1) a high solubility for actinides and rare earths (10 to 20 wt%); (2) high chemical durability in nature; (3) an apparent resistance to radiation damage as natural monazites are seldom found in the metamict state, despite very high alpha-decay event is induced (Boatner and Sales 1988).¹⁷ There have been extensive studies of monazite and apatite as potential wastes from phases, and a considerable amount of work on a number of synthetic phosphate phases has been completed.

1-4. REFERENCES

- 1) J. V. Smith, *Mineral Soc. Am. Spec. Paper*, 1, 281(1963).
- 2) G. O. Brunner and W. M. Meier, *Nature*, 337, 146 (1989).
- 3) C. B. Murphy, O. Hrycyk, W. T. Gleason In *Natural Zeolite: Occurrence, Properties, Use*; L. B. Sand, and F. A. Mumpton, Eds. Pergamon Press, New York, 471(1978).
- 4) Y. Tarasevich *Khim. Teknol. Vody* 16, 626(1994).
- 5) D. Kallo, In *Natural Zeolite*; D. W. Ming, and F. A. Mumpton, Eds. Pergamon Press, New York, 341(1995).
- 6) E. R. Kreidler and F. A. Hummel, *Am. Mineral* 55, 170 (1970).
- 7) D. McConnell *Springer*, New York (1973).
- 8) D. M. Roy, L. E. Drafall and R. Roy, In *Phase Diagrams*. Eds. Academic Press, New York, 186 (1978).
- 9) J. C. Elliott, Elsevier Amsterdam (1994).
- 10) R. F. Dymek and B. E. Owens, *Econ. Geol.* 96, 797 (2001).
- 11) B. Bunker, J. Virden, B. Kurn, and R. Kuinn In *Encycropedia of energy technology and the environment*. Eds John Wiley & Sons, New York, 2023 (1995) .
- 12) S. L. Lambert and D. S. Kim, Westinghouse Hanford Company, WHC-SP-1143, UC-811 (1994).
- 13) L. A. Boatner, Division of Materials Sciences, Washington, DC, 28 (1978).
- 14) L. A. Boatner, G. W. Beall, M. M. Abraham, C. B. Finch, P. G. Huray and M. Rappaz,

In Scientific Basis for Nuclear Waste management, Vol. 2, Northrup, CJM Jr. Eds.

Plenum Press, New York, 289(1980)

15) G. J. McCarthy *Mater. Res. Bull.* 13 1239 (1978).

16) G. J. McCarthy, J. P. Pepin and D. D. Davis In Scientific Basis for Nuclear Waste management, Vol. 2, Northrup, CJM Jr. Eds. Plenum Press, New York, 289(1980).

17) L. A. Boatner and B. C. Sales, In Radioactive Waste Forms for the Future. Eds. North-Holland, Amsterdam, 495(1988).

CHAPTER 2

ION EXCHANGE BEHAVIOR OF NATURAL ZEOLITES

Natural zeolites from Shimane, Japan

2-1. INTRODUCTION

In recent years, wastewaters are discharged after the primary process of flocculation and the sedimentation, and secondary process of biological treatment. Increasing levels of ammonium and phosphate are the main factors of eutrophication in river or lakes. These levels are now being controlled by legislation on discharge limits in many countries. The increase in ammonium and phosphate levels causes increases in BOD (biochemical oxygen demand) and COD (chemical oxygen demand) in many rivers and lakes. Therefore a process to further reduce the quantity of ammonium and phosphate levels is needed. To achieve better wastewater treatment, the use of activated carbon, which is comparatively expensive, is proposed.

Natural zeolites have been proposed as an alternative to activated carbon, and can also be used as a pretreatment material prior to biological processing to ensure a constant concentration feed to a biological treatment plant. Clinoptilolite and mordenite are the main minerals of natural zeolites found in abundance in many locations.¹⁻² These minerals consist of three-dimensional open-framework structures consisting of AlO_4 and SiO_4 tetrahedra linked together by oxygen sharing and contain channels and cavities in which cations and water molecules can diffuse, as well as ion-exchange sites. These are widely used as low-cost ion exchangers.³⁻⁴

The chemical behavior of natural zeolites in aqueous solutions has been investigated.

⁵⁻⁶ The use of natural zeolites for removal of ammonium in wastewater treatment has also been reviewed by a number of researchers.⁷⁻¹² The method of regeneration of zeolites has also been discussed.³ Zeolites saturated with ammoniacal nitrogen have been continuously regenerated in biological processes without the use of chemical regenerants such as NaCl.⁹ The adsorption behavior of treated zeolites has also been described.¹³⁻¹⁶ For example, it has been shown that ammonium ions can be stripped from zeolite using 2 M sodium chloride solution.¹⁷ The ion exchange selectivity of zeolite is related to its ionic charge and ion radius. Zeolites also have the ability to absorb ammonium ions in the low-concentration range that is often observed in rivers or lakes.¹⁸

In the present study, the chemical behavior of three natural zeolites from Shimane, Japan was investigated in distilled water and hydrochloric acid. Ammonium adsorption by these zeolites in ammonium chloride solution was also investigated and the results obtained were compared with published adsorption values for other zeolites.

2-2. EXPERIMENTAL METHOD

2-2-1. Materials

Three types of natural zeolites mined from Shimane, Japan were used in this study. Two of the three natural zeolites (CLI1 and CLI2) consisted mainly of clinoptilolite, and the remaining one (MOR3) consisted mainly of mordenite. They were all sieved to below 50 μm particle size before use.

2-2-2. Characterization

Mineral identification was carried out by the powder X-ray diffraction (XRD) with CuK α radiation (RIGAKU RINT 2200). The zeolites were characterized by scanning electron microscopy (SEM) (JEOL S-5500). The chemical compositions of the zeolites were determined by inductively coupled plasma spectroscopy (ICP) (SEIKO HVR 1700).

A photomultiplier tube was used as the detector for ICP. The operating conditions for ICP are given in Table 2.1. The solutions for ICP were prepared as follows: For Si and Al, 50 mg of sample was mixed with Na₂CO₃ and H₃BO₃ powders. The mixture was dissolved by addition of HCl solution, and pure water was added to the solution to a final volume of 100 ml. For Na, K, Ca and Mg, 50 mg of sample was dissolved in HF and H₂SO₄ solutions. After the solution was evaporated, the dried residue was dissolved in HCl solution with heating, and pure water was added to the solution to a final volume of 100 ml. The detection limits of ICP were 0.002 ppm for Na and Si, 0.004 ppm for Al, 0.00004 ppm for Ca and Mg, and 0.030 ppm for K.

2-2-3. Adsorption Experiment

For ammonium adsorption experiments, 30.0 ml of each solution containing different proportions of NH₄Cl (10⁻⁴-10⁻¹M) was added to 0.1 g of air-dried zeolite samples in stoppered polyethylene tubes. The tubes were shaken at 25°C for 7 days. The mixture was separated by centrifugation at 15000 rpm for 30 minutes and then filtered with a 0.45 μ m membrane filter (Millipore, 0.45 μ m HA-type).

The ion concentration of the filtered solution was determined by ICP (SEIKO-SPS4000). pH was determined using a pH meter (Toa Dempa Kogyo HM-60V). Adsorption experiments in distilled water and hydrochloric acid (10^{-5} - 10^{-1} M) were also carried out using the same experimental method. The ammonium concentration of the filtered solution was determined using an ammonium ion-specific electrode (Toa Dempa Kogyo IM-20B, ammonia electrode Ae-235). After the adsorption experiments, XRD using $\text{CuK}\alpha$ radiation was used to examine the crystal structure.

2-3. RESULTS and DISCUSSION

2-3-1. Identification by XRD

The XRD patterns of the three zeolite powders are shown in Fig. 2.1. CLI1 and CLI2 consisted mainly of clinoptilolite with traces of quartz, feldspar and layered silicate (Figs 2.1a and 2.1b). CLI2 was richer in clinoptilolite than CLI1. MOR3 consisted mainly of mordenite with quartz and layered silicate (Fig. 2.1c).

2-3-2. SEM

SEM photographs showed that the main mineral in CLI1 is clinoptilolite (Fig. 2.2) and that in MOR3 is mordenite (Fig. 2.3). Clinoptilolite in CLI1 was crystalline, submicron in size, and assumes a sharp similar to the coffin -shape of heulandite.¹⁹ Mordenite in MOR3 was fibrous and ranged from 0.05 to 0.1 μm in diameter and from 1 to 5 μm in length.

2-3-3. Chemical Composition by ICP

The chemical compositions of the zeolites determined by ICP are shown in Table 2.2. The Si/Al ratios of the three samples were constant, in the range of 4.8 to 5.0. The total amount of Na^+ , K^+ , Mg^{2+} and Ca^{2+} in ion-exchange sites on the zeolites was about 5 wt%.

Hydrogen Adsorption Behavior

The concentrations of cations, silica and alumina in solution, initial pH and equilibrium pH in distilled water are shown in Table 2.3. The concentrations of all species in the blank solution, that is, distilled water without zeolite, were below the detection limit of ICP. The equilibrium pH increased from the initial pH in distilled water due to exchange of hydrogen ions from the solution with the other cations in the zeolite matrix. The amount of exchanged cations was less than 0.1wt% in all of the samples. The amount of exchanged cations for MOR3 was the smallest of three samples, and the equilibrium pH was also the smallest in this sample. This may be explained by considering the exchange of cations Na^+ , K^+ , Mg^{2+} and Ca^{2+} in ion-exchange sites on zeolites with H^+ ions in distilled water. For each type of zeolite, the exchange of Na^+ in the zeolite structure is the easiest and thus has the largest effect. The results of H^+ ion exchange for MOR3 in hydrochloric acid are shown in Table 2.4. The increase in the equilibrium pH was due to the increase in cation concentration. This phenomenon was also observed for the other cations Na^+ , K^+ , Mg^{2+} and Ca^{2+} in ion-exchange sites on zeolites which exchanged with H^+ ions in hydrochloric acid as well as in distilled water. Sodium was observed to be more easily exchanged than the other cations in the zeolites. By decreasing the equilibrium pH, dissolved silica and

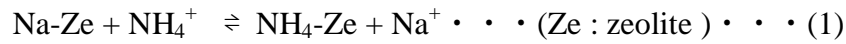
alumina concentrations increased. This result indicates that the structures of silica and alumina are destroyed at low pH.

Ammonium Adsorption Behavior

The ammonium adsorption isotherm of the three natural zeolites in ammonium chloride solution is shown in Fig. 2.4. CLI2 shows the highest ammonium capacity among the three natural zeolites, with a capacity of 1.28 mmol/g. This phenomenon can be explained by the difference in mineral compositions among the three zeolites. CLI2 was shown to be nearly pure clinoptilolite using XRD m (Fig. 2.1.) and to have the highest exchange capacity. The ammonium adsorption capacity of the three zeolites was compared with other published data on zeolites in Table 2.5.³ The results indicate that the three samples have similar but slightly higher exchange capacities than other previously reported zeolites.

The pH of the solution before/after adsorption, the concentration of silica, alumina and cations in ion-exchange sites on zeolites in solution, and the theoretical and experimental ammonium adsorption levels in $3 \times 10^{-3} \sim 1 \times 10^{-4}$ M ammonium chloride solutions are shown in Table 2.6. By increasing the initial concentration of ammonium chloride solution, the concentration of silica and alumina decreased. This result indicates that the framework structures of the zeolites are stable in high-ammonium-concentration solution. This was also confirmed by the unchanged crystal structures of the zeolites after ammonium adsorption, as determined by XRD. The order of ammonium ion exchange selectivity for cations on zeolites is $\text{Na}^+ \gg \text{K}^+ > \text{Ca}^{2+} > \text{Mg}^{2+}$, i.e., the exchange of Na^+ on zeolites is the

largest. This also indicates that Na^+ exchange on zeolites occurs by the following ion-exchange reaction (Eqn. 1).



It is apparent that Na^+ are very weakly bound in the structures of these zeolites. Other ions are strongly held in the structure of all zeolite samples compared with Na^+ . The theoretical amounts of various cations exchanged with zeolites are calculated using the formula below (Eqn. 2), the assumption that a charge balance on the zeolites with an equivalent number of charged ions are exchanged with ammonium ions, i.e., one Na^+ or K^+ with one NH_4^+ , one-half Ca^{2+} or Mg^{2+} with one NH_4^+ .²⁰ The concentration of the cations released in distilled water (Table 2.3) was deducted from the above concentrations.

$$[\text{Total NH}_4^+] = [\text{Na}^+] + [\text{K}^+] + 1/2[\text{Mg}^{2+}] + 1/2[\text{Ca}^{2+}] \cdot \cdot \cdot (2)$$

The amount of adsorbed ammonium ions determined experimentally is quantitatively in agreement with the amount determined using the above approach at high ammonium concentrations. This result indicates that ammonium adsorption occurs by ion exchange involving Na^+ , K^+ , Mg^{2+} and Ca^{2+} in cation exchange sites on zeolites.

2-4. CONCLUSION

Three natural zeolites mined from Shimane, Japan have been shown to have a high ammonium adsorption capacity. Of these three zeolites, CLI2, which is rich in clinoptilolite, was shown to have the highest ammonium adsorption capacity of 1.28 mmol/g. The amount of cation released from this zeolite was less than 0.1 wt% of the initial amount in the sample in distilled water. The lowest ammonium adsorption capacity was observed in MOR3. This indicates that the cations Na^+ , K^+ , Mg^{2+} and Ca^{2+} in ion-exchange sites on zeolites exchanged with H^+ ions in distilled water and hydrochloric acid. With decreasing equilibrium pH, silica and alumina concentrations increase. This indicates that the structures of silica and alumina are destroyed under these conditions. Regarding ion exchange of the Na^+ on natural zeolite were used as an alternative to ammonium ion in ammonium chloride solution and H^+ ions in distilled water and hydrochloric acid.

The order of ammonium ion exchange selectivity for cations on zeolite is $\text{Na}^+ \gg \text{K}^+ > \text{Ca}^{2+} > \text{Mg}^{2+}$. The amount of ammonium ions adsorbed in this experiment quantitatively corresponded to the theoretically expected amount of adsorbed ions given a mole balance on the zeolite at high ammonium concentrations. This result indicates that ammonium adsorption occurs by ion exchange with Na^+ , K^+ , Mg^{2+} and Ca^{2+} in cation-exchange sites on zeolites.

Table 2.1. Operating Conditions for ICP.

Frequency	27.12 MHz	
RF power	1.3 kW	
Plasma gas	16 l min ⁻¹	
Auxiliary gas	0.5 l min ⁻¹	
Carrier gas	1.0 l min ⁻¹	
Observation height in plasma	13.0 mm	
Analytical lines :		
Si : 251.611 nm	Al : 396.152 nm	
Na : 588.955 nm	K : 766.490 nm	
Ca : 393.366 nm	Mg : 279.553 nm	

Table 2.2. Chemical composition of natural zeolites CLI1, CLI2, and MOR3 (wt%).

	CLI1	CLI2	MOR3
Si	29.3	29.3	30.8
Al	5.93	5.93	6.35
Fe	0.76	0.49	0.49
Na	2.57	2.43	1.88
K	1.19	1.42	1.53
Ca	1.40	1.21	0.91
Mg	0.44	0.40	0.40
Si/Al	4.94	4.94	4.85

Table 2.3. The concentration of dissolved cations, silica and alumina from zeolites in distilled water (mol/L).

	CLI1	CLI2	MOR3
pH ₀	5.45	5.45	5.45
pHeq	9.31	6.87	6.59
SiO ₂	0.098	0.035	ND
Al ₂ O ₃	0.051	0.035	ND
Na	0.459	0.093	0.056
K	0.019	0.037	0.017
Ca	0.011	0.007	ND
Mg	0.008	0.001	ND

pH₀ = initial pH values. pHeq = equilibrium pH values after reaction.
 ND = not detected

Table 2.4. The concentration of dissolved cations, silica and alumina from zeolites in distilled water (mol/L).

pH ₀	pHeq	SiO ₂	Al ₂ O ₃	Na	K	Ca	Mg
1.33	1.33	0.363	-	1.516	-	-	-
1.78	1.89	0.208	-	1.381	-	-	-
2.17	2.29	0.104	0.104	1.121	0.091	0.242	0.121
2.55	2.87	0.053	0.020	0.800	0.075	0.175	0.122
2.92	3.55	0.034	0.001	0.485	0.031	0.055	0.086
3.34	6.01	0.025	ND	0.290	0.018	0.011	0.013
3.79	6.54	0.021	ND	0.139	0.015	0.004	0.002
4.34	6.69	0.018	ND	0.088	0.013	0.005	0.002

pH₀ = initial pH values. pHeq = equilibrium pH values after reaction.
 "—" = not determined. ND = not detected.

Table 2.5. Exchange capacities of various zeolites in 1 mol/L (NH₄⁺).

Zeolite Origin	Ammonium Exchange Capacity meq NH ₃ (N)/g	Ref
CLI1	0.336	
CLI2	0.359	
MOR3	0.351	
Grant Co., NM	0.288	(3)
Owyhee Co., ID	0.247	(3)
Fremont Co., WY	0.187	(3)
Lander Co., NV	0.255	(3)
Washoe Co.,NV	0.140	(3)
Malheur Co.,OR	0.377	(3)
Maricopa Co.,AZ	0.139	(3)
Hector Clinoptilolite	0.286	(3)

Table 2.6. The concentration of dissolved cations, silica, and alumina from zeolite (mmol/L) and the amount of adsorbed ammonium (mmol/g) in ammonium chloride solution (mmol/L).

	C ₀ (NH ₄ ⁺)	pH ₀	pH _{eq}	SiO ₂	Al ₂ O ₃	Na ⁺	K ⁺	Ca ²⁺	Mg ²⁺	C ₁ (NH ₄ ⁺ ads)	C ₂ (NH ₄ ⁺ ads)
CLI1	3.0	5.42	8.14	0.072	0.001	1.330	0.187	0.150	0.027	0.544	0.583
	1.0	5.30	8.77	0.086	0.003	0.760	0.065	0.025	0.012	0.252	0.252
	0.3	5.52	9.00	0.116	0.005	0.230	0.026	0.011	0.010	0.072	0.081
	0.1	5.70	9.27	0.114	0.005	0.160	0.020	0.010	0.009	0.048	0.255
CLI2	3.0	5.42	6.34	0.023	ND	1.760	0.140	0.010	0.010	0.631	0.655
	1.0	5.30	6.40	0.022	ND	0.920	0.036	0.006	0.008	0.285	0.279
	0.3	5.52	6.53	0.068	0.006	0.340	0.017	0.007	0.009	0.108	0.086
	0.1	5.70	6.76	0.069	0.007	0.220	0.010	0.006	0.009	0.072	0.026
MOR3	3.0	5.42	5.59	0.017	ND	1.340	0.143	0.086	0.063	0.514	0.568
	1.0	5.30	6.02	0.018	ND	0.700	0.050	0.021	0.022	0.231	0.270
	0.3	5.52	6.17	0.024	0.001	0.210	0.018	0.004	0.002	0.051	0.084
	0.1	5.70	6.43	0.023	0.001	0.130	0.014	0.009	0.003	0.029	0.027

C₀(NH₄⁺) = initial concentration of ammonium chloride solution. pH₀ = initial pH values.

pH_{eq} = equilibrium pH values after ammonium removal.

C₁(NH₄⁺ads) = calculated values of ammonium adsorption.

C₂(NH₄⁺ads) = experimental values of ammonium adsorption.

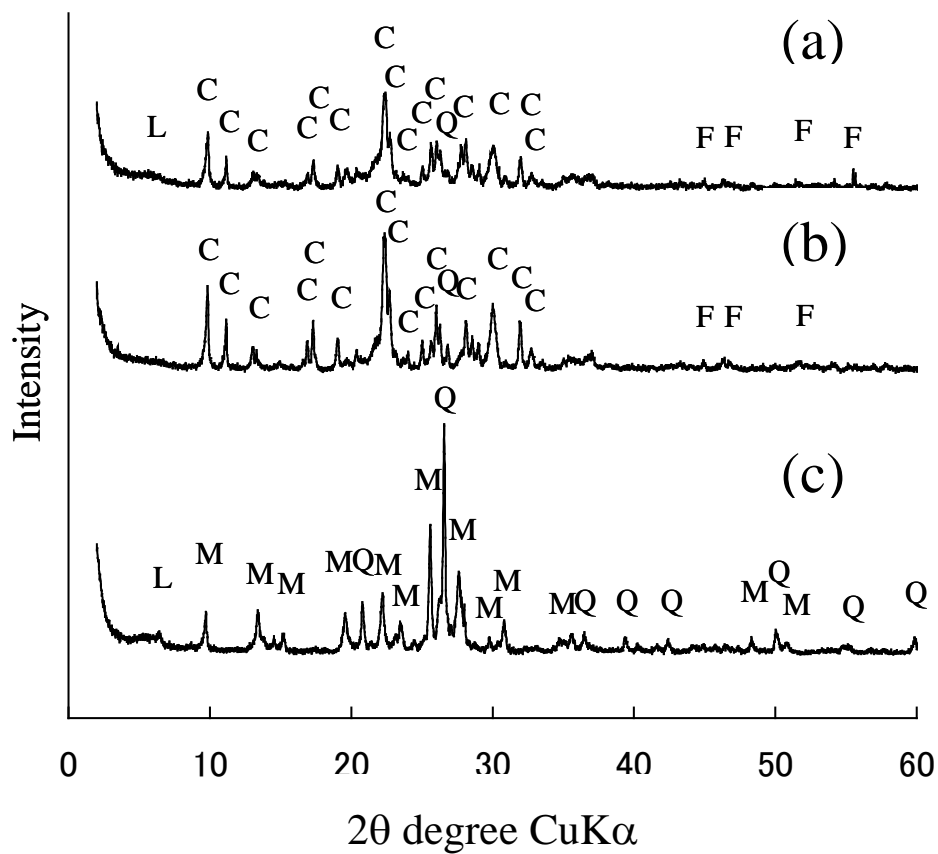


Fig. 2.1. X-ray powder diffraction patterns of natural zeolites. (a) CLI1, (b) CLI2, (c) MOR3. C, clinoptilolite, M: mordenite, Q: quartz, F: feldspar, L: layered silicate.

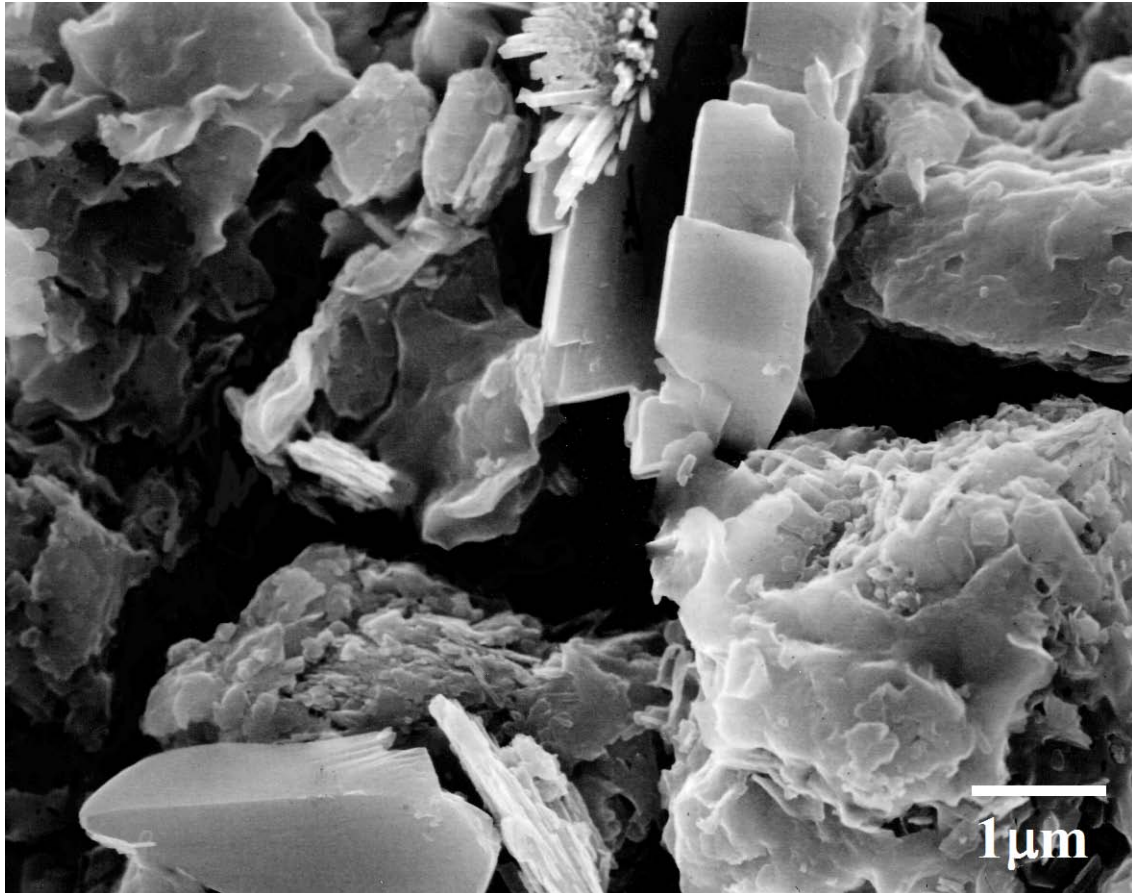


Fig. 2.2. SEM photograph of clinoptilolite in CLI1.

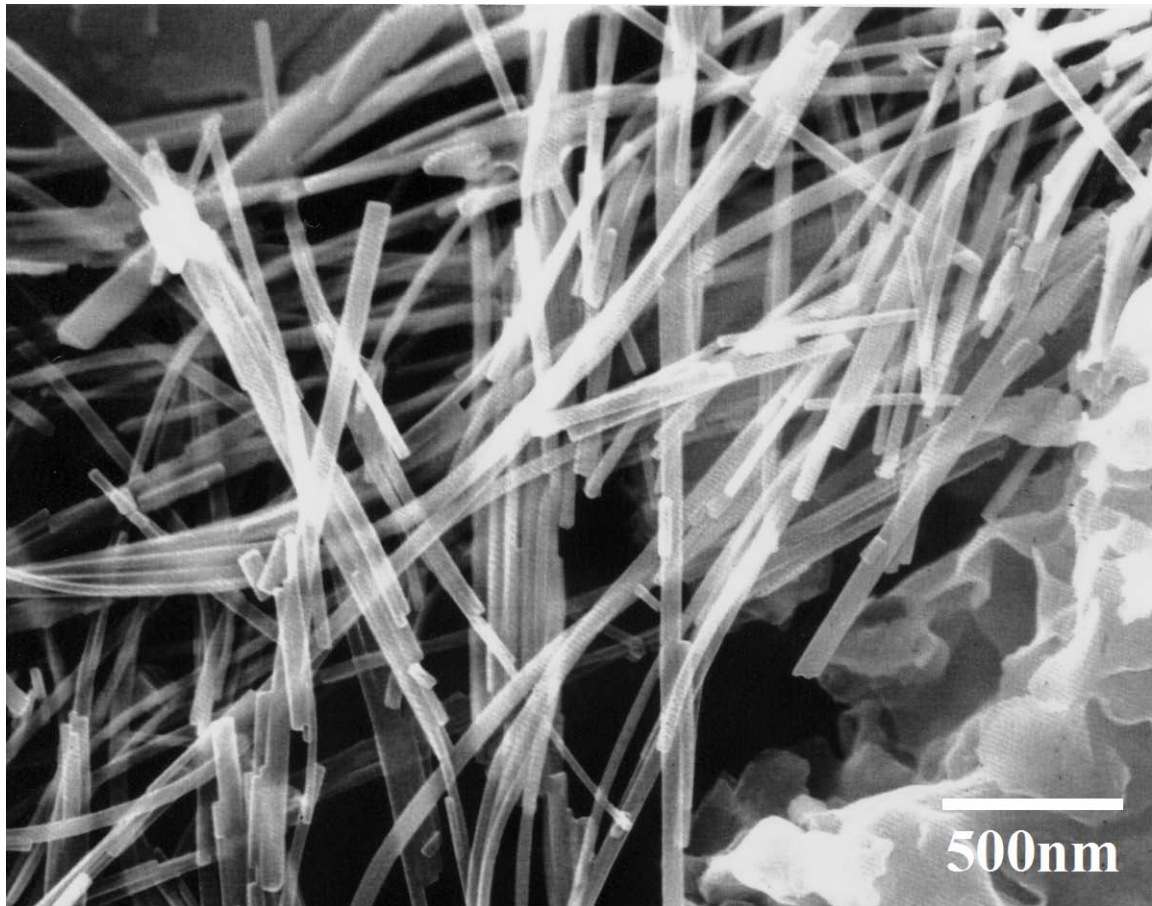


Fig. 2.3. SEM photograph of mordenite in MOR3.

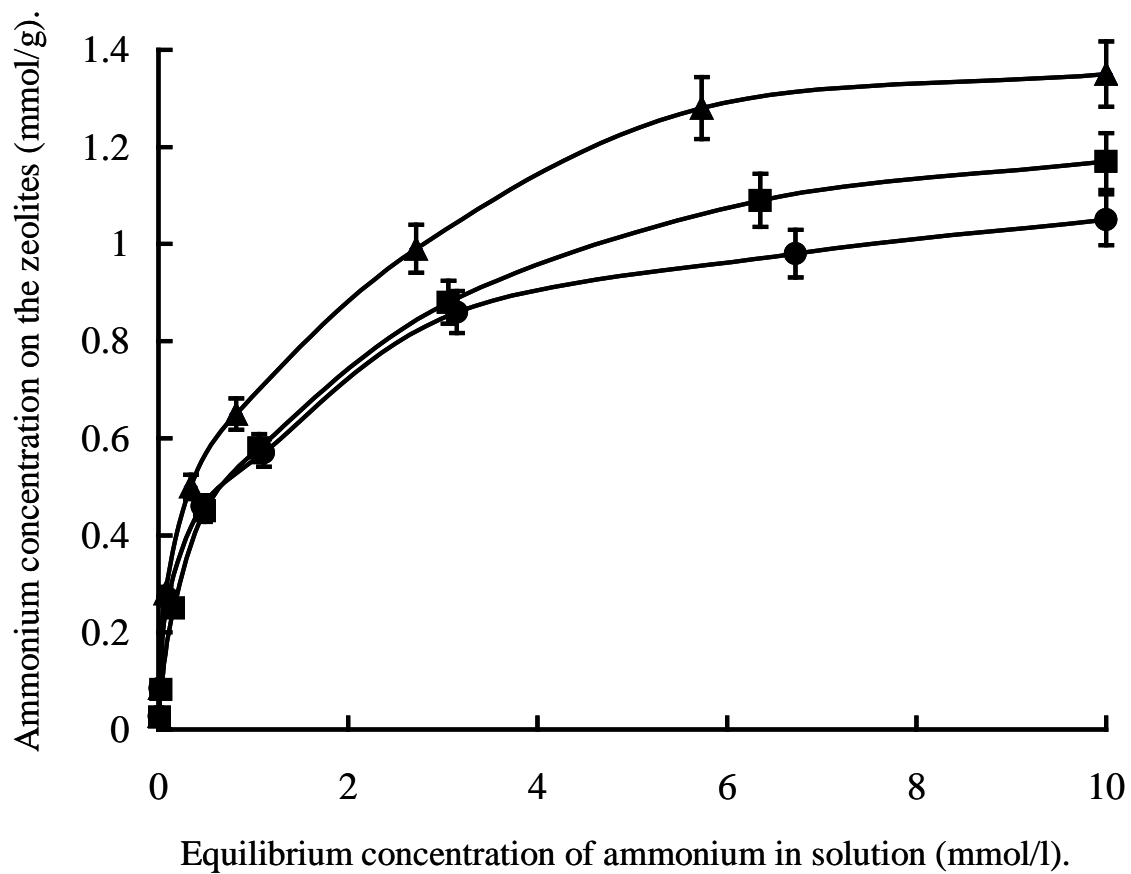


Fig. 2.4. The ammonium adsorption isotherm of three natural zeolites. ■: CLI1, ▲: CLI2. ●: MOR3.

Natural zeolites from Akita, Japan and Australia

2-5. INTRODUCTION

Clinoptilolite is an abundant zeolite found in nature with high cation-exchange capacity, ion adsorption and high ammonium-selective properties. Its chemical composition is $(\text{Ex})^{8+}(\text{Al}_8\text{Si}_{40})\text{O}_{96} \cdot 24\text{H}_2\text{O}$, where Ex denotes exchangeable cation. The exchangeable cations are required for preserving electrical neutrality in aluminosilicate framework, because the charge imbalance in framework is occurred from the substitution of aluminum atoms for silicon atoms. In natural zeolite, these cations are typically Na^+ , K^+ , Ca^{2+} , Mg^{2+} , or other alkali earth elements. The use of zeolite for removal of ammonium ion in wastewater treatment has been reported by a number of researchers.^{13-18, 21} In the 1960s, Ames found that the ion selectivity for clinoptilolite as $\text{K}^+ > \text{NH}_4^+ > \text{Na}^+ > \text{Ca}^{2+} > \text{Mg}^{2+}$. They revealed that highest ammonium removal efficiency was achieved when the cation-exchange sites were converted to the sodium form. In chapter from 2-1 to 2-4, we reported that the order of selectivity of ammonium ions for cations on the zeolites was $\text{Na}^+ \gg \text{K}^+ > \text{Ca}^{2+} > \text{Mg}^{2+}$.²³ The natural zeolite with various combinations of cations would be expected to show the different ammonium ion exchange behavior.

In this study, the ammonium exchange behavior of two natural clinoptilolites from Akita Prefecture, Japan and Mount Gipps, Australia with several cations were investigated in ammonium chloride solution with different concentration. The results obtained were compared with the published ones for other clinoptilolite.

2-6. EXPERIMENTAL METHOD

Two natural zeolites mined from Akita Prefecture, Japan and Mount Gipps, Australia were used in this study. These zeolites were abbreviated to AKI and AUS, respectively. They were all sieved to below 50 μm particle size before use. Mineral identification was carried out by the powder X-ray diffraction (XRD) with $\text{CuK}\alpha$ radiation (RIGAKU RINT 2200). In order to determine the chemical compositions of the natural clinoptilolites, the inductively coupled plasma spectroscopy (ICP) (SEIKO HVR 1700) was used. The solutions for ICP were prepared as follows: For Si and Al, 50.0 mg of the AKI and AUS zeolites was melted with Na_2CO_3 and H_3BO_3 at 1000 $^\circ\text{C}$. The mixture obtained after cooling was dissolved into HCl solution, and distilled water was added to the solution to a final volume of 100.0 ml. For Na, K, Ca and Mg, 50.0 mg of the AKI and AUS samples was dissolved in HF and H_2SO_4 solutions. After the solution was evaporated, the dried residue was dissolved into HCl solution at 60 $^\circ\text{C}$, and distilled water was added to the solution to a final volume of 100.0 ml. A photomultiplier tube was used as the detector for ICP. The detection limits of ICP were 2×10^{-3} ppm for Na and Si, 4×10^{-3} ppm for Al, 4×10^{-5} ppm for Ca and Mg, and 3×10^{-2} ppm for K.

For ammonium ion exchange experiment, 30.0 ml of each solution containing four different concentrations of NH_4Cl (0.1-10.0 mM: $\text{M}=\text{mol dm}^{-3}$) was added to 0.1 g of air-dried zeolites in stoppered polyethylene tubes. The tubes were shaken at 25 $^\circ\text{C}$ for 7 days. The mixture was separated by centrifugation at 15000 rpm for 30 minutes and then

filtered with a 0.45 μm membrane filter (Millipore, 0.45 μm HA-type). The ammonium ion concentration of the filtered solution was determined using an ammonium ion-specific electrode (Toa Dempa Kogyo IM-20B, ammonia electrode Ae-235). The other ions concentration of the filtered solution was determined by ICP (SEIKO-SPS4000). The structural change was not detected for the zeolites before and after the ion exchange experiments through the powder XRD method.

2-7. RESULTS and DISCUSSION

The XRD patterns of the two zeolites powders, AKI and AUS, are shown in Fig.2.5. They were identified to be clinoptilolite with quartz (Fig.2.5a and 5b). AKI was nearly pure clinoptilolite. The peak intensities of clinoptilolite of AKI were higher than these of AUS. The chemical composition of AKI and AUS shown in Table 2.7 together with those of the clinoptilolite from Shimane prefecture, Japan, which is abbreviated to SHI.²³ The Si/Al ratios of the three samples are similar, in the range of 4.9 to 5.2. One can see in the Table 2.7, the AKI contains more Na^+ and K^+ than the AUS by about twice although amount of Na^+ in AKI samples is about half of SHI.

Table 2.8 shows the concentration of silica, alumina and cations in ion exchange sites on zeolites in solution, and the theoretical and experimental ammonium exchange amount vs. the ammonium chloride solutions in the range of 0.3-10 mM. The theoretical values²³ are calculated through the eq.(1):

$$[\text{Total NH}_4^+] = [\text{Na}^+] + [\text{K}^+] + 1/2[\text{Mg}^{2+}] + 1/2[\text{Ca}^{2+}] \cdot \cdot \cdot \quad (1)$$

The concentration of Na^+ in three samples was higher than other cations in the low ammonium concentration (0.3-1.0 mM) solutions. In high ammonium concentration solutions (3.0-10.0 mM), the concentration of K^+ and Ca^{2+} was higher than those values in the low ammonium concentration solutions. It is apparent that Na^+ are very weakly bound in the structures and other ions are strongly held in the structure of all zeolite samples compared with Na^+ . The ammonium ion is exchanged with dominantly Na^+ on clinoptilolite. These results agreed with ammonium ion exchange selectivity reported by Watanabe et al.²³ The relationship between equilibrium concentration of ammonium ion in solution and ammonium concentration on zeolites is shown in Fig.2.6. AKI shows the highest ammonium capacity among the three natural zeolites of 1.318 mmol/g. With increasing the initial concentration of ammonium chloride solution, the concentration of silica and alumina in solution decreased given in Table 2.8. This result indicates that the framework structures of the clinoptilolites were stable even in higher ammonium concentrations. No change of the XRD pattern after ammonium ion exchange also confirmed the stability of clinoptilolite in ammonium solution. It is noted that the ion-exchange capacity of clinoptilolite for ammonium ion was dependent on mainly both the species of exchangeable cation and purity because natural zeolites studied contain many other impurity ions. The previous studies (Cooney et al.¹¹ Watanabe et al.²³) showed that the Na-formed clinoptilolite indicated the highest ammonium removal efficiency.

But the exchanged amount of ammonium ion on Na-rich SHI was slightly smaller than that of K-rich AKI. This discrepancy can be mainly explained by the amount of impurities. SHI contained the small amount of quartz and feldspar, but AKI was almost pure clinoptilolite as shown in Fig.2.5. For the case of AUS, the lower amount of exchanged ammonium ion was explained by mainly the larger amounts of calcium ion. The presence of calcium ion reduced the amount of exchanged ammonium ion in zeolite.¹¹ Furthermore the selectivity of ammonium ion for Ca^{2+} in clinoptilolite was worse than that for Na^+ and K^+ .^{11, 23}

Ammonium ion exchange behavior on clinoptilolites clarified in this study will be useful as a basic research for the removal of ammonium ion from municipal wastewater.

2-8. CONCLUSION

The amounts of ammonium ion exchange on natural clinoptilolites were investigated in ammonium chloride solution for the samples from Akita, Japan and Mount Gipps, Australia together with that from Shimane, Japan reported previously. The exchange capacity for the natural clinoptilolite from Akita, which consists of almost pure clinoptilolite, showed the highest ammonium ion exchange value of 1.318 mmol/g. The measured amount of ammonium ions exchanged quantitatively agreed well with the theoretical values of exchanged ions calculated by an equation between the concentration of ammonium ion and that of the exchanged ions on the zeolites in ammonium chloride

solution. The ammonium ion was mainly exchanged with Na^+ , K^+ and Ca^{2+} ions on these clinoptilolites. By changing the concentration of the ammonium chloride solution, the dissolved Na^+ amount was the largest among these three ions. This showed that the ammonium ion was dominantly exchanged with Na^+ ion. The exchange capacity of Na-rich Shimane clinoptilolite was smaller than that of the K-rich Akita sample. This indicated that the ion-exchange was depend not only the ion species on the natural clinoptilolites but also contained impurities such as quartz and feldspar.

Table 2.7. Chemical composition of natural zeolites. AKI, AUS and SHI (wt%)

	AKI	AUS	*SHI
Si	31.5	30.8	29.3
Al	6.10	6.10	5.93
Fe	0.45	0.77	0.76
Na	1.52	0.62	2.57
K	2.66	1.10	1.19
Ca	0.69	1.98	1.40
Mg	0.42	0.63	0.44
Si/Al	5.20	5.00	4.94

* Watanabe et al.(2003).²³

Table 2.8. The concentration of dissolved cations, silica and alumina from zeolites (mmol/L) and amounts of exchanged ammonium ion (mmol/g) in ammonium chloride solution.

	$C_0(\text{NH}_4^+)$	SiO_2	Al_2O_3	Na^+	K^+	Ca^{2+}	Mg^{2+}	$C_1(\text{NH}_4^+\text{exc})$	$C_2(\text{NH}_4^+\text{exc})$
AKI	10.0	0.006	ND	1.847	1.429	0.208	0.111	1.150	1.318
	3.0	0.006	ND	1.505	0.088	0.028	0.042	0.724	0.618
	1.0	0.006	ND	0.363	0.021	ND	0.007	0.344	0.269
	0.3	0.011	ND	0.286	0.019	ND	ND	0.115	0.087
AUS	10.0	0.024	ND	0.522	0.075	0.755	0.194	0.749	0.738
	3.0	0.029	ND	0.456	0.040	0.156	0.053	0.274	0.267
	1.0	0.030	ND	0.352	0.018	0.051	0.022	0.155	0.169
	0.3	0.034	ND	0.286	0.008	0.017	0.008	0.103	0.071
SHI*	10.0	0.072	ND	1.556	0.385	0.266	0.062	0.976	1.094
	3.0	0.086	0.001	1.330	0.187	0.150	0.027	0.544	0.583
	1.0	0.116	0.003	0.760	0.065	0.025	0.012	0.252	0.252
	0.3	0.114	0.005	0.230	0.026	0.011	0.010	0.072	0.081

$C_0(\text{NH}_4^+)$ = initial concentration of ammonium chloride solution.

$C_1(\text{NH}_4^+\text{exc})$ = calculated values of ammonium ion exchange.

$C_2(\text{NH}_4^+\text{exc})$ = experimental values of ammonium ion exchange.

ND = not detected. *Watanabe et al.(2003)²³.

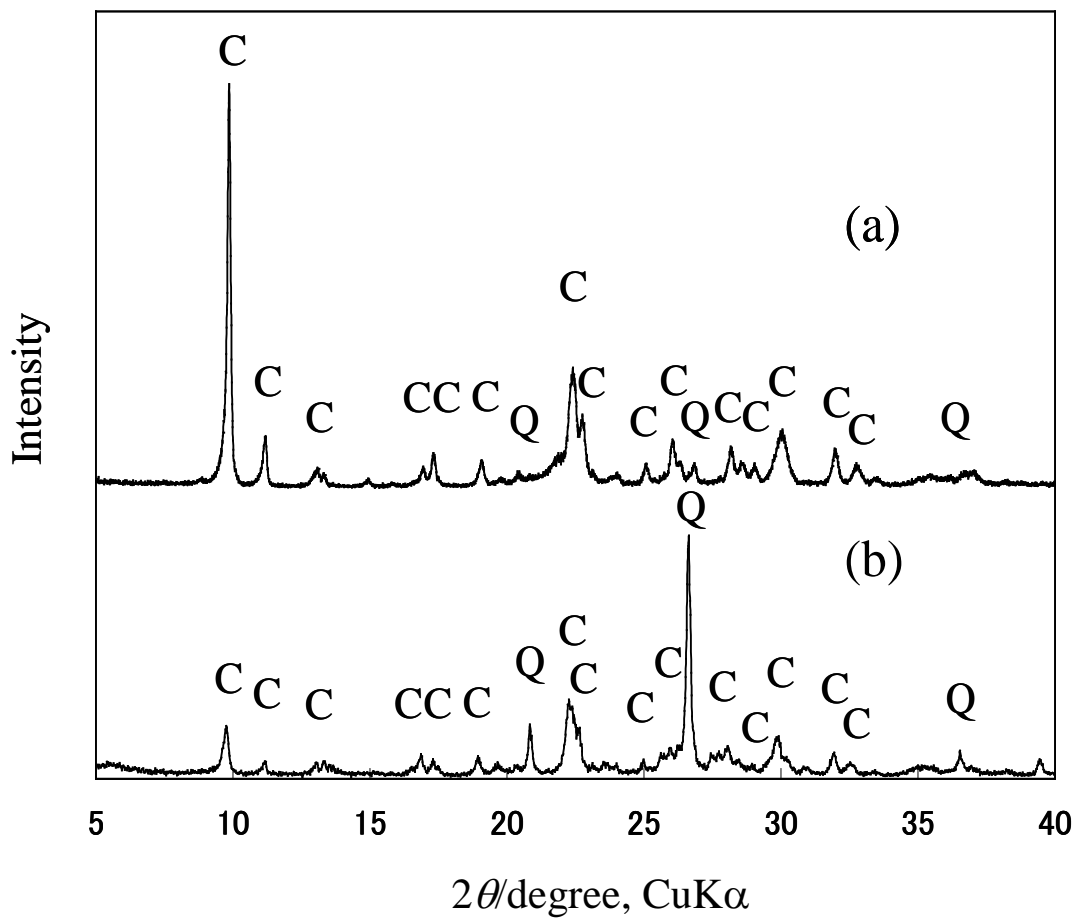


Fig. 2.5. X-ray diffraction patterns of zeolites (a) AKI, (b) AUS C: cinoptilolite, Q: quartz

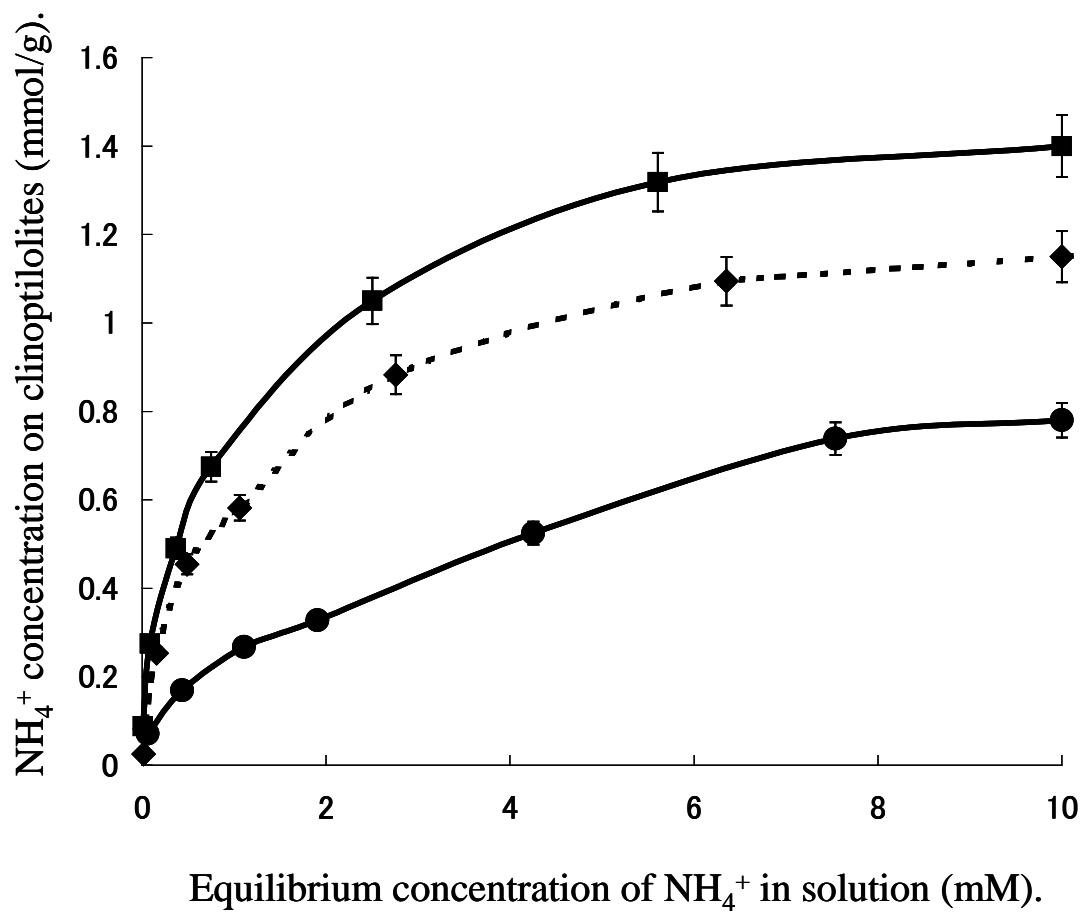


Fig. 2.6. The relationship between equilibrium concentration of NH_4^+ in solutions and NH_4^+ concentration on zeolites. ■:AKI, ●:AUS, ◆:SHI (Watanabe et al.²³).

2-9 REFERENCES

- 1) R. L. Hay, In *Natural Zeolites: Occurrence, Properties, Use*; L. B. Sand and F. A. Mumpton, Eds. Pergamon Press, New York, 135(1976).
- 2) A. Iijima, and M. A. Utada, *Jpn. J. Geol. Geogr.*, 42, 61(1972).
- 3) C. B. Murphy, O. Hrycyk, and W. T. Gleason, In *Natural Zeolite: Occurrence, Properties, Use*; L. B. Sand, and F. A. Mumpton, Eds. Pergamon Press, New York, 471(1978).
- 4) B. W. Mercer and L. L. Ames, In *Natural Zeolite: Occurrence, Properties, Use*; L. B. Sand, and F. A. Mumpton, Eds. Pergamon Press, New York, 451(1978).
- 5) C. B. Murphy, O. Hrycyk, and W. T. Gleason In *Natural Zeolite: Occurrence, Properties, Use*; L. B. Sand, and F. A. Mumpton, Eds. Pergamon Press, New York, 353(1978).
- 6) D. W. Breck, *Zeolite Molecular Sieves*. Eds. Wiley: New York, 498(1974).
- 7) F. A. Mumpton, In *Natural Zeolite: Occurrence, Properties, Use*; L. B. Sand, and F. A. Mumpton, Eds. Pergamon Press, New York, 3(1978).
- 8) K. Torii, In *Natural Zeolite: Occurrence, Properties, Use*; L. B. Sand, and F. A. Mumpton, Eds. Pergamon Press, New York, 441(1978).
- 9) C. Y. Chang, D. H. Son, and D. H. Ahn, *Water Sci. Technol.*, 42 (5-6), 127(2000).
- 10) N. A. Booker, E. L. Cooney, and A. J. Priestley, *Water Sci. Technol.*, 34 (9), 17(1996).
- 11) E. L. Cooney, N. A. Booker, D. C. Shallcross and G. W. Stevens, *Sep. Sci. Technol.*, 34

- (12), 2307(1999).
- 12) E. L. Cooney, N. A. Booker, D. C. Shallcross and G. W. Stevens, *Sep. Sci. Technol.*, 34 (14), 2741(1999).
- 13) A. Rivera, G. R. Fuentes, and E. Altshuler, *Microporous Mesoporous. Mat.*, 40, 173(2000).
- 14) G. R. Fuentes, A. R. Ruiz, M. Mir, O. Picazo, G. Quitana and M. Delgado, *Microporous Mesoporous Mat.*, 20, 269(1998).
- 15) M. A. Jama, and H. Yucel, *Sep. Sci. Technol.*, 24 (15), 1393(1989).
- 16) W. E. Wright, W. N. Rom and F. Moatamed, *Arch. Environ. Health.*, 2, 99(1983).
- 17) Z. Hagiwara and M. Uchida In *Natural Zeolite: Occurrence, Properties, Use*; L. B. Sand, and F. A. Mumpton, Eds. Pergamon Press, New York, 463(1978).
- 18) N. Aral, A. Gunay, O. Sevimoglu, M. Cali, and E. Debik, *Fresen. Environ. Bull.*, 8 (5-6), 344(1999).
- 19) F. A. Mumpton, In *Natural Zeolite: Occurrence, Properties, Use*; L. B. Sand, and F. A. Mumpton, Eds. Pergamon Press, New York, 113(1978).
- 20) M. Rozic, S. C. Stefanovic, S. Kurajica, V. Vancina and E. Hodzic, *Water Res.*, 34(14), 3675 (2000).
- 21) L. L. Ames, *Am. Mineral.*, 45 689 (1960).
- 22) Y. Watanabe, H. Yamada, H. Kokusen, J. Tanaka, Y. Moriyoshi and Y. Komatsu, *Sep. Sci. Technol.*, 38(7), 1519(2003).

CHAPTER 3

AMMONIUM ION EXCHANGE OF SYNTHETIC ZEOLITES

3-1. INTRODUCTION

Municipal wastewater often contains a considerable amount of ammonium ions, which causes an environmental problem. The ions are discharged after the primary process of flocculation and sedimentation, and the secondary process of biological treatment. The increase in an ammonium level causes increases in BOD (biochemical oxygen demand) and COD (chemical oxygen demand) in rivers and lakes. Therefore, the establishment of a process to reduce the quantity of ammonium ions is needed. The use of activated carbon has been proposed for this purpose¹, but this is comparatively expensive.

Zeolites are crystallites composed of hydrated aluminosilicates with exchangeable cations. The aluminosilicate portion of the structure is a 3-dimensional open framework consisting of a network of AlO_4 and SiO_4 tetrahedra linked each other by sharing all the oxygen molecules. Zeolites have periodic and molecular-sized pores, and channels in their unique structure. Therefore, they have high cation exchange capacity, high ion adsorption capacity, and high ammonium ion selectivity.² The high affinity of zeolites for ammonium ions and the slow release of ammonium ions from them are of special interest for minimizing environmental pollution in municipal and industrial wastewater.

Natural zeolites such as clinoptilolite and mordenite are found in abundance in many locations. These are widely used as a low-cost ion exchanger. The use of zeolites for the removal of ammonium ions from wastewater has been reviewed by a number of researchers.³⁻⁸ Furthermore, zeolites have been proposed as an alternative to activated

carbon, and can also be used as a pretreatment material prior to biological processing to ensure a constant concentration feed to a biological treatment plant. In Chapter 2, the ammonium ion exchange behavior of natural clinoptilolite and mordenite that have similar pore sizes and cation exchange capacities (CEC) was investigated with an ammonium chloride solution. Natural zeolites are rich in clinoptilolite having the highest ammonium ion exchange capacity of 1.318 mmol/g.^{3,8}

More than 100 different species of synthetic zeolites have been identified.⁹ Among them, Linde Type A (LTA) zeolite with α -cages and β -cages, and faujasite (FAU) zeolite with β -cages and super cages are the 2 most important zeolites that have been extensively used in industries for ion exchange, adsorption, catalysis, and other aspects. Studies of ammonium ion exchange with a sodium form of synthetic LTA and FAU have been carried out by various researchers till now.^{2,10-14} Sodalite (SOD) and rho zeolite (RHO) are known as a zeolite with only β -cages¹⁴⁻¹⁵ and a zeolite with α -cages,¹⁶ respectively. These have been studied for applications ranging from catalysis to adsorption and ion exchange.¹⁴⁻¹⁹

In the present study, the behavior of ammonium ions in ion exchange on synthetic zeolites such as SOD with Na^+ ions (Na-SOD), RHO with Na^+ ions and Cs^+ ions (NaCs-RHO), LTA with Na^+ ions (Na-LTA), and FAU with Na^+ ions (Na-FAU) was investigated. In particular, the effects of the cage sizes, open-window sizes, pore structures, and CEC of the zeolites on ammonium ion exchange were examined in order to find the best candidate for ammonium adsorption from wastewater.

3-2. EXPERIMENTAL METHOD

3-2-1. Preparation of Zeolites

The synthesis of Na-SOD was performed under hydrothermal conditions by a modified procedure derived from the pioneering work of Barrer and coworkers.¹⁴⁻¹⁵ A mixture of 1.802 g of SiO₂ (High Pure Chemical Co., Ltd., Japan), 1.529 g of Al₂O₃ (High Pure Chemical Co., Ltd., Japan), and 24.0 g of NaOH (Wako Pure Chemical Industries, Ltd., Japan) (the molar ratio, SiO₂:Al₂O₃:NaOH = 2:1:40) was dissolved in 50 mL of distilled water contained in a 100 mL Teflon cup fitted into a stainless steel pressure vessel, and heated at 150°C under autogenous pressure for 7 days.

NaCs-RHO was prepared using a method similar to that of Robson et al.¹⁵ Twelve g of NaOH (Wako Pure Chemical Industries, Ltd., Japan) were dissolved in 19.4 mL of distilled water, and 9.33 g of aluminum hydroxide hydrate (Al(OH)₃·xH₂O) (Aldrich Chemical Co., Inc.) were added to this solution with warming at 80°C. The solution was then cooled down, and mixed with 12 mL of 50wt% CsOH (the purity 99.9%, Aldrich Chemical Co., Inc.) solution. Finally, the resulting solution was blended with 100 g of 30wt% colloidal silica (Ludox HS-30) by vigorous mixing to make the colloid homogeneous sol. During incubation of the sol at room temperature for 7 days, it turned to gel, and the gel in a sealed Teflon container was then heated at 85°C for 7 days. The molar ratio of the compositions of the gel was Na₂O: Cs₂O: Al₂O₃: SiO₂: H₂O = 3: 0.4: 1: 10: 110.

Na-LTA and Na-FAU were supplied in a powder form by Wako Pure Chemical Industries, Ltd., Japan. The zeolites described above were characterized by a powder X-ray diffraction (XRD) method with Cu K α radiation (RIGAKU: RINT2200) and by scanning electron microscopy (SEM) (HITACHI: S-5500). Their chemical compositions were determined by inductively coupled plasma spectroscopy (ICP) (SEIKO: HVR1700). The solutions for ICP were prepared as follows: on Si and Al, 50.0 mg of the synthetic zeolites were melted with Na₂CO₃ and H₃BO₃ at 1000°C. The mixtures were dissolved in a HCl solution after cooling, and distilled water was added to the solutions to the final volume of 100.0 mL. On Na⁺, K⁺, Ca²⁺, and Mg²⁺, 50.0 mg of the synthetic zeolites were dissolved in HF and H₂SO₄ solutions. After the solutions were evaporated, the dried residues were dissolved in a HCl solution at 60°C, and distilled water was added to the solutions to a final volume of 100.0 mL. A photomultiplier tube was used as a detector for ICP. The detection limits of ICP were 2 \times 10⁻³ ppm of Na⁺ and Si⁴⁺, 4 \times 10⁻³ ppm of Al³⁺, 4 \times 10⁻⁵ ppm of Ca²⁺ and Mg²⁺, and 3 \times 10⁻² ppm of K⁺.

3-2-1. Ammonium Ion Exchange

The experiments of ammonium ion exchange were carried out with 2 stages. Firstly, the effect of reaction time on ammonium ion exchange was examined. Thirty mL of a 10⁻² M ammonium chloride solution were added to 0.1 g of synthetic zeolites in polyethylene tubes. The tubes were then shaken at 30 rpm by an end-over-end shaker (Towa Labo

RKVSD 10101) at 25°C for 1 min to 7 days. The resultant suspensions were filtered with 0.45 µm membrane filters (Millipore, HA-type) at various reaction times. The ammonium concentrations of the filtered solutions were determined using an ammonium ion-specific electrode (Toa Denpa Kogyo IM-20B, Ammonia Electrode Ae-235). The amounts of exchanged ammonium ions were calculated from differences between the concentrations of ammonium ions in the filtered solutions and that in the initial solution.

Secondly, the effect of the initial concentration of ammonium ions on ion exchange was examined. Thirty mL of ammonium chloride solutions whose ammonium concentrations ranging from 10^{-4} to 3×10^{-2} M were added to 0.1 g of synthetic zeolites in polyethylene tubes. The tubes were shaken at 30 rpm by an end-over-end shaker (Towa Labo RKVSD 10101) at 25°C for 7 days. The suspensions were filtered with 0.45µm membrane filters (Millipore, HA-type). The ammonium concentrations of the filtered solutions were determined using an ammonium ion-specific electrode (Toa Denpa Kogyo IM-20B, Ammonia Electrode Ae-235). The amounts of exchanged ammonium ions were calculated from differences between the concentrations of ammonium ions in the filtered solutions and those in the initial solutions.

3-3. RESULTS and DISCUSSION

3-3-1. Structures and Compositions of Synthetic Zeolites

The powder XRD patterns and SEM images of the zeolites obtained are shown in Fig.

3.1 and 2, respectively.

The powder XRD pattern in Fig. 3.1a demonstrated for Na-SOD having no impurity and high crystallinity as reported previously.¹⁴ The grain size of Na-SOD was about a few hundred nm (Fig. 3.2a). The chemical formula determined by ICP was the same as that of reported sodalite with Na⁺ ions, Na₈(AlSiO₄)₆(OH)₂·nH₂O.^{9,14}

The XRD pattern of NaCs-RHO in Fig. 1b agreed well with that of NaCs-RHO shown in a previous study.¹⁶ NaCs-RHO obtained in the present study had high crystallinity with no impurity. Morphologically, NaCs-RHO zeolite formed 0.5-1 μm rhombododecahedral crystals (Fig. 3.2b). The chemical formula determined by ICP was Na₇Cs₄(AlO₂)₁₁(SiO₂)₃₇·nH₂O per unit cell. This result shows slightly silica rich compared to the chemical formula reported by previous studies.^{9,16}

The powder XRD patterns of Na-LTA (Fig. 3.1c) and Na-FAU (Fig. 3.1d) were the same as those of LTA and FAU with Na⁺ ions, respectively, reported previously.² The chemical compositions of Na-LTA and Na-FAU determined by ICP were (Na₁₂)(Si₁₂Al₁₂O₄₈)·nH₂O and Na₈₄(Al₈₄Si₁₀₈O₃₈₄)·nH₂O, respectively, which were the same as those expected for LTA with Na⁺ ions⁹ and FAU with Na⁺ ions (Na_xAl_xSi_{192-x}O₃₈₄·nH₂O; x = 77–96).² Na-LTA was found to be the intergrowth of typical cubic crystallites of micrometer size (Fig. 3.2c), and Na-FAU was found to be the aggregate or intergrowth of fine octahedral crystallites of submicrometer size (Fig. 3.2d).

3-3-2. Ammonium Ion Exchange on Synthetic Zeolites

The relationship between the amounts of ammonium ions exchanged on the zeolite and the reaction times is shown in Fig. 3.3. Initial ammonium concentration was 10^{-2} M. The amounts of synthetic zeolites were 0.1 g. The amounts of ammonium ions exchanged on the samples were calculated from differences between the concentrations of ammonium ions in the filtered solutions and that in the initial solution. Regarding Na-SOD, a small amount of ammonium ions, 0.60 mmol/g (about 20% of the original amount) was exchanged at the initial stage, but the amount of exchanged ammonium ions decreased with reaction time. After 7 days, about 10,000 min, no ion exchange was observed. Regarding NaCs-RHO, the amount of exchanged ammonium ions, 1.37 mmol/g (about 46% of the original amount) increased at 1-10 min, but after that the amount of the ions became changeless. Regarding Na-LTA, the amount of exchanged ammonium ions increased at the initial stage and decreased at 1-10 min, and after that the amount of the ions became changeless. The value of the equilibrium state was 1.77 mmol/g (about 52% of the original amount). There was no such dependence on reaction time in Na-FAU. The value of the equilibrium state was 2.00 mmol/g (about 60% of the original amount). After the ammonium ion exchange, the crystal structure of these zeolites was confirmed as unchanged by the XRD patterns.

The framework structures of zeolites are schematically shown in Fig. 3.4. The structure of SOD is formed by placing β -cages (sodalite cages) on the body-centered cubic lattice

(Fig. 3.4a). There are relatively small windows of 2.2 Å in free diameter, which are smaller than the diameter of ammonium ions (2.9 Å). The framework of RHO consists of α -cages joined together by double 8-membered rings (Fig. 3.4b), and the size of the open-window is 3.6 Å, which is slightly larger than that of ammonium ions. In LTA, large cages (α -cages) with an inner diameter of about 11 Å are surrounded by 8 β -cages linked by double 4-membered rings (Fig. 3.4c). The α -cages are arrayed in a simple cubic structure, and are connected by shared windows with an inner diameter of about 5 Å. The size of the open-window is dependent on the type of exchangeable cations in the cages. The open-window size of Na-LTA is about 4 Å. The framework of FAU consists of β -cages linked by double 6-membered rings (Fig. 3.4d). In the FAU structure, the SOD cages stack in the same way, same as carbon atoms in diamond. The pore opening of Na-FAU is about 7.4 Å, which is largest among the presently studied zeolites.

Regarding the β -cages of Na-SOD, physical adsorption probably occurred at the initial stage but no ion exchange was observed at the equilibrium state. This conclusion is supported by the open-windows size of the β -cages of Na-SOD, which is smaller than that of ammonium ions.

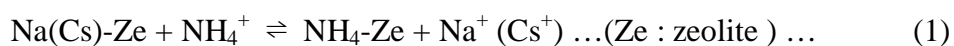
The open-windows of the other 3 zeolites are larger than ammonium ions, which makes ammonium ion exchange possible. Regarding RHO, the size of the open-windows in the α -cages is barely larger than ammonium ions. Furthermore, large cations, Cs⁺ ions, in the α -cages make the actual size of the open windows smaller. Therefore, the ion exchange of

ammonium ions was more or less blocked in RHO in the present study. A similar behavior has been observed in previous studies of the ion exchange of Ag^+ ions.¹⁹ Because of these reasons, the amount of exchanged ammonium ions probably increased with increasing of reaction time at the initial stage, and then the equilibrium state was reached in RHO. Regarding LTA, the amount of exchanged ammonium ions decreased with increasing of reaction time, and then reached plateau. It indicates that both the ion exchange on the α -cages and the physical adsorption on the β -cages occurred at the initial stage, which was followed by the equilibrium state of ion exchange on the α -cages. Regarding Na-FAU, no dependence on reaction time was observed, because the size of the open-windows is largest among the zeolites and large enough for ion exchange of ammonium ions. The result of Na-FAU is also supported by a “case” for ammonium ions to move inward. Therefore, instantaneous equilibrium was not achieved in ion exchange of Na-FAU.

Fig. 3.5 shows the relationship between the exchanged amounts of ammonium ions and the concentrations of ammonium ions. The exchange capacities of Na-SOD, NaCs-RHO, Na-LTA, and Na-FAU calculated from their chemical formulas in this study as well as published data of other zeolites are shown in Table 3.1. Regarding Na-SOD, ammonium ion exchange was expected to happen in the various concentrations of ammonium ions at the equilibrium state, because the CEC of Na-SOD calculated from the chemical formula was 6.4 mmol/g, which is higher than those of clinoptilolite and mordenite (Table 3.1). But ammonium ion exchange didn't completely occur at the

equilibrium state (Fig. 3.5) because the open-window size is smaller than the diameter of ammonium ions.

Ammonium ion exchange occurred in other 3 synthetic zeolites, because their open-window sizes are larger than the diameter of ammonium ions. The type of isotherm curves was corresponded with Langmuir type. The curve occurs in probably majority of cases of adsorption from dilute solution. The initial curvature shows that as more sites in the zeolites are filled it became increasingly difficult for a bombarding solute molecule to find a vacant site available.^{20,21} Regarding NaCs-RHO, the ammonium ion exchange was higher than that of Na-LTA and Na-FAU at low ammonium concentrations. These results are not easy to explain precisely for complex reaction, but the effect of Cs⁺ ions on RHO is one probable factor. The maximum capacity was 1.65 mmol/g of ammonium. The value was lower than those of Na-LTA (2.56 mmol/g) and Na-FAU (3.20 mmol/g). The ammonium ion exchange mechanism is probably explained by Na⁺ (Cs⁺) exchange on zeolites occurring by the following ion exchange reaction (Eq. 1).



It is apparent that Na⁺ ions bind very weakly to the structure of zeolites, because the hydration energy of Na⁺ ions is lower than other cations.²

Based on this reaction, the main factor influenced the results is explained that the

CEC of NaCs-RHO (3.1 mmol/g) calculated from the chemical formula is smaller than those of Na-LTA (7.0 mmol/g) and Na-FAU (6.4 mmol/g) (Table.3.1). But this explanation is not applied when the CEC of Na-LTA is compared with that of Na-FAU. The latter is better explained by ammonium ion selectivity of these zeolites. The selectivity is Na-FAU > Na-LTA when the percentages of ammonium ion exchange on these zeolites is higher than 10 %.² Also added to the explanation is that the size of the open-windows of Na-FAU (7.4 Å) is not only larger than that of Na-LTA but also considerably larger than the diameter of ammonium ions (2.9 Å), therefore, physical ammonium adsorption was maintained at the equilibrium state. Na-FAU showed the highest exchange capacity for ammonium ions among the synthetic zeolites tested in the present study as well as other zeolites reported previously (Table. 3.1).^{3,11} The maximum amount of ammonium ion exchange was 3.20 mmol/g. From these results and discussion, we conclude that the factors influencing ammonium ion exchange are ammonium ion concentration, reaction time of zeolite with ammonium ions, the open-window size and pore structure of zeolite, and cation exchange capacity of zeolite.

3-4. CONCLUSION

The behavior of synthetic zeolites, i.e. Na-SOD, NaCs-RHO, Na-LTA, and Na-FAU, in ammonium ion exchange was investigated at 25°C. The ammonium ion exchange activity of these zeolites was dependent on their open-window sizes, pore structures, and

cation exchange capacities. The Na-FAU, which has the largest open-windows among these zeolites, showed the highest exchange capacity of ammonium ions, and ,therefore, we conclude that this zeolite is an ideal candidate for the removal of ammonium ions from municipal wastewater.

Table 3.1. Exchange capacities of various zeolites

Zeolite	CEC (mmol/g) calculated from chemical formula, Anhydrous	Maximum Ammonium Exchange Capacity (mmol/g)	Ref.
Na-SOD	6.4	0	
NaCs-RHO	3.1	1.65	
Na-LTA	7.0	2.56	
Na-FAU(X)	6.4	3.20	
Clinoptilolite	2.6	1.35	(3)
Mordenite	2.6	1.05	(3)
Na-FAU(Y)	4.3	3.04	(10)

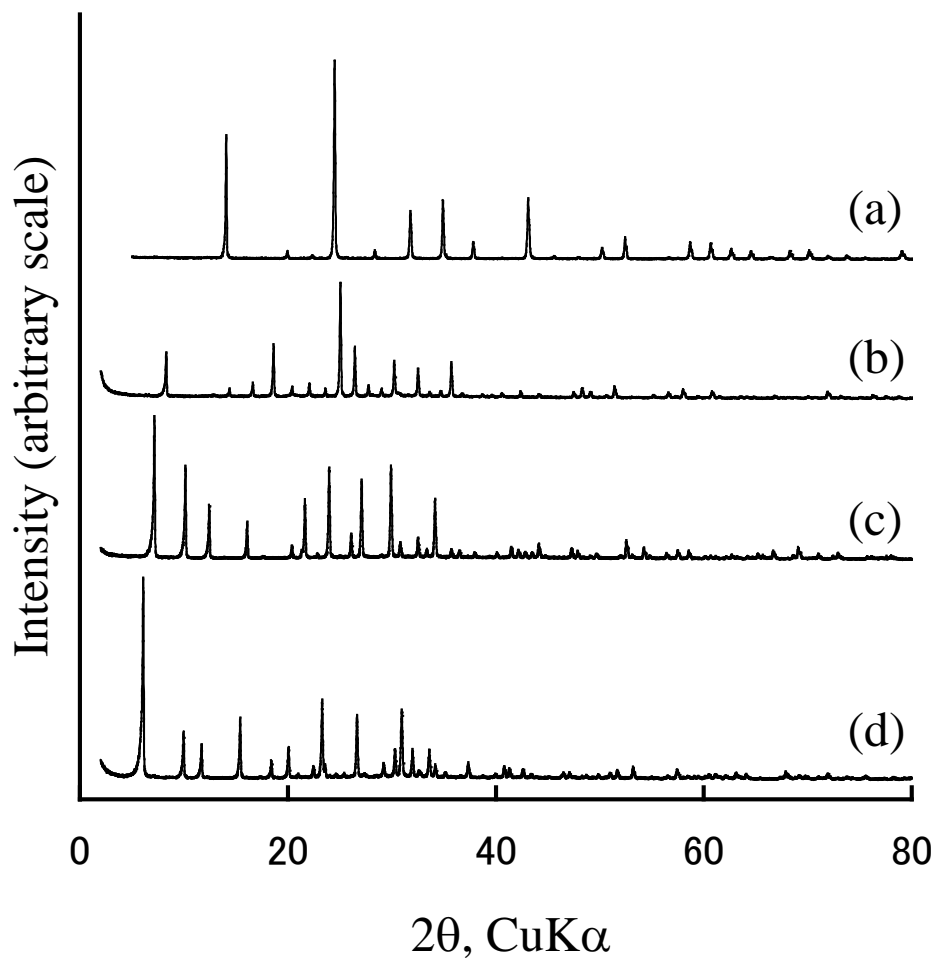
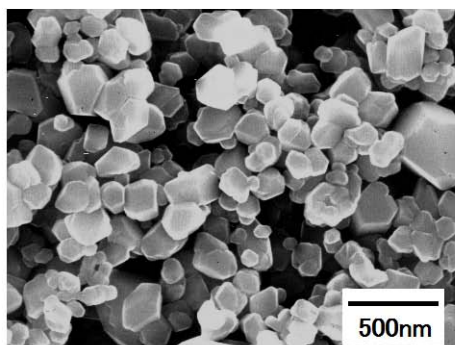
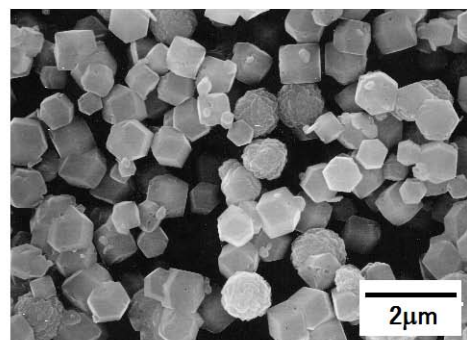


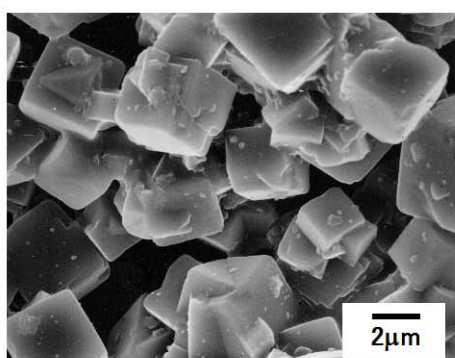
Fig.3.1. XRD patterns of the synthetic zeolites. (a) Na-SOD (b) NaCs-RHO (c) Na-LTA (d) Na-FAU.



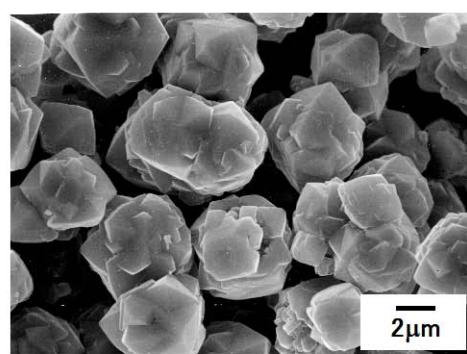
(a)



(b)



(c)



(d)

Fig.3.2. SEM photographs of the synthetic zeolites. (a) Na-SOD. (b) NaCs-RHO. (c) Na-LTA. (d) Na-FAU.

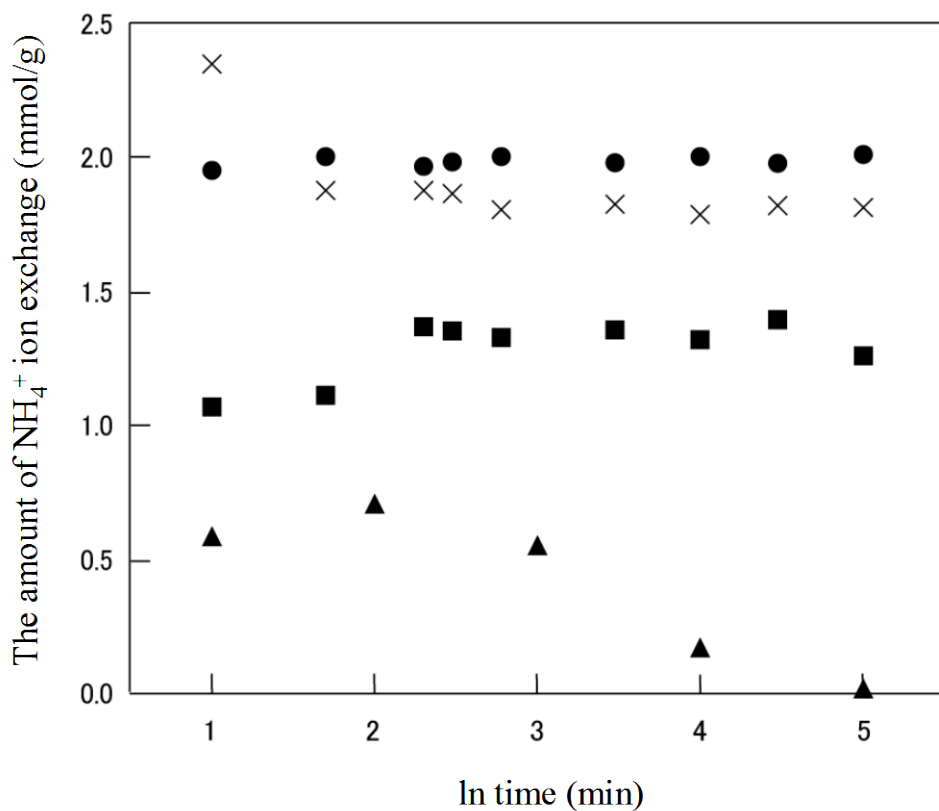


Fig. 3.3. The relationship between the ion exchange amount of ammonium ion and the reaction time. Initial ammonium concentration: 10^{-2} M, Amount of zeolite: 0.1g ▲: Na-SOD. ■: NaCs-RHO. ×: Na-LTA. ●: Na-FAU.

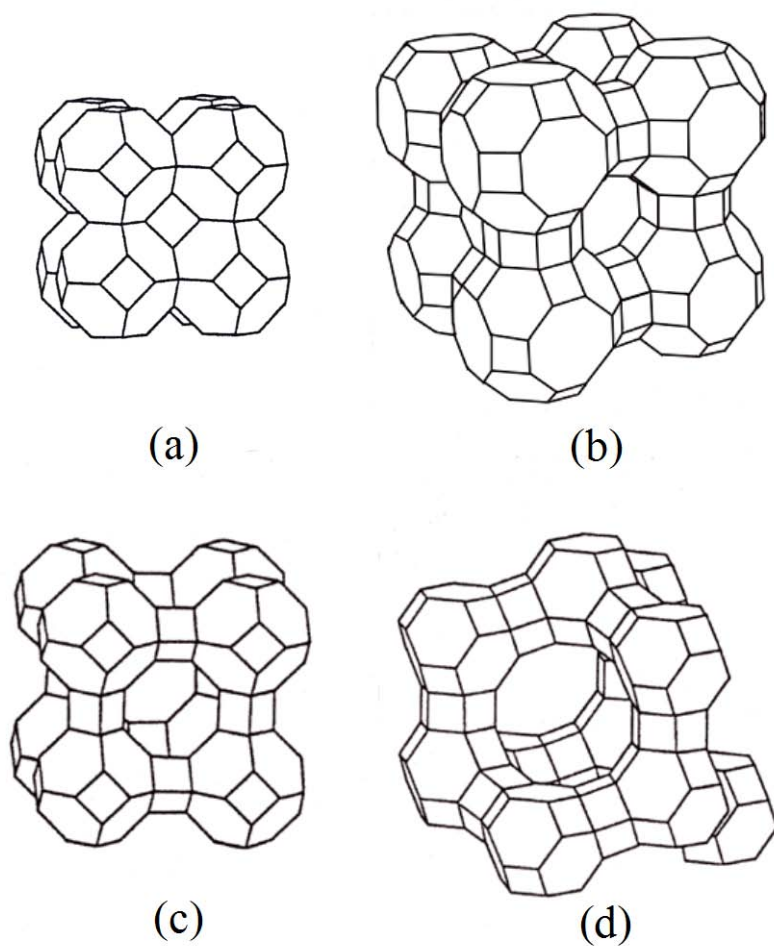


Fig.3.4. The schematic representation of the framework structure of zeolites. (a) SOD. (b) RHO. (c) LTA. (d) FAU.

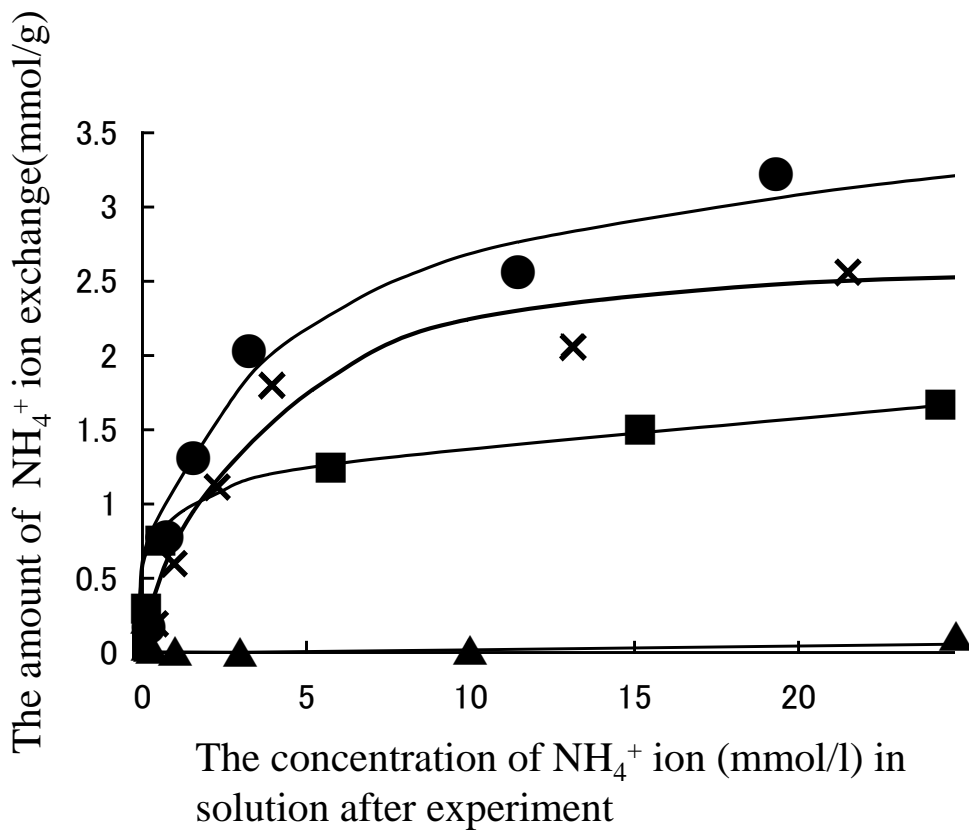


Fig.3.5. The relationship between the ion exchange amount of ammonium ion and the concentration of ammonium solution.

▲: Na-SOD. ■: NaCs-RHO. ×: Na-LTA. ●: Na-FAU.

3-5 REFERENCES

- 1) R. Abdul-Rahman, H. Tsuno, and N. Zainol, *Water Sci. Technol.*, 45(12),197(2002).
- 2) D. W. Breck, *Zeolite Molecular Sieves*. Eds. John Wiley & Sons, Inc. New York, (1974).
- 3) Y. Watanabe, H. Yamada, H. Kokusen, J. Tanaka, Y. Moriyoshi and Y. Komatsu, *Sep. Sci. Technol.*, 38(7), 1519(2003).
- 4) C. Y. Chang, D. H. Son, and D. H. Ahn, *Water Sci. Technol.*, 42 (5-6), 127(2000).
- 5) N. A. Booker, E. L. Cooney, and A. J. Priestley, *Water Sci. Technol.*, 34 (9), 17(1996).
- 6) E. L. Cooney, N. A. Booker, D. C. Shallcross and G. W. Stevens, *Sep. Sci. Technol.*, 34 (12), 2307(1999).
- 7) E. L. Cooney, N. A. Booker, D. C. Shallcross and G. W. Stevens, *Sep. Sci. Technol.*, 34 (14), 2741(1999).
- 8) Y. Watanabe, Y. Moriyoshi, H. Yamada, J. Minato, M. Sekita, J. Tanaka, Y. Komatsu, and G. W. Stevens, *J. Ion Exchange*, 14, 217(2003).
- 9) W. Meier, D. Olson, and C. Baerlocher, *Zeolites*, 17(1-2), 1(1996).
- 10) H. S. Sherry, *J. Phys. Chem.*, 70(4), 1158(1966).
- 11) B. K. G. Theng, E. Vansant and J. B. Uytterhoeven, *Trans. Faraday. Soc.*, 64, 3370(1968).
- 12) P. P. Lai and L. V. C. Rees, *J. Chem. Soc., Faraday Trans. I*, 72, 1809(1976).
- 13) P. Fletcher and R. P. Townsend, *J. Chem. Soc., Faraday Trans. I*, 78, 1741(1982).

- 14) R. M. Barrer, J. F. Cole and H. Sticher, *J. Chem. Soc.*, 2475(1968).
- 15) R. M. Barrer and J. F. Cole, *J. Chem. Soc.*, 1516(1970).
- 16) H. E. Robson, D. P. Shoemaker, R. E. Ogilvie and P. C. Manor, *Adv. Chem. Ser.*, 121, 106(1973).
- 17) M. Erdmann and D. Stachel, *Glass Science and Technology*, 76(4), 195(2003).
- 18) S. M. Kuznicki, V. A. Bell, S. Nair, H. W. Hillhouse, R. M. Jacobinas, C. M. Braunbarth, B. H. Toby and M. Tsapatsis, *Nature*, 412(6848), 720(2001).
- 19) B. Xu, and L. Kevan, *J. Phys. Chem.*, 95, 1147(1991).
- 20) C. H. Giles, T. H. Macewan and S. N. Nakhwa, *J. Chem. Soc.*, 111, 3973(1960).
- 21) C. H. Giles, Smith, D. and A. Huitson, *J. Colloid Interface Sci.*, 47, 755 (1974).

CHAPTER 4

AMMONIUM IONS EXCHANGE OF SYNTHETIC ZEOLITES OBTAINED FROM HYDROTHERMAL MODIFICATION OF NATURAL ZEOLITES

4-1. INTRODUCTION

Clinoptilolite and mordenite are the main natural zeolite minerals found in abundance in many locations.¹⁻² They have high cation exchange capacity (CEC) and ion adsorption capacity with remarkably high ammonium ion selective properties.³ They are widely used as low cost ion-exchangers and especially used for the removal of ammonium ions in wastewater treatment.⁴⁻⁶

Synthesis of high-quality zeolites by hydrothermal treatment of various materials, such as fly ash,⁷⁻⁹ kaolinite,¹⁰ smectite,¹¹⁻¹² bentonite¹³ and natural zeolite,¹⁴⁻¹⁵ has been reported. Kang et al. have synthesized sodium phillipsite (Na-P) with a trace of feldspar from natural clinoptilolite and mordenite by hydrothermal treatment with 2 M NaOH for 16 hours at 103°C.¹⁴ They have found that the natural clinoptilolite treated hydrothermally changes to Na-P, sodium faujasite (Na-X) and hydroxy-sodalite depending on the reaction conditions.¹⁵ The CEC of the synthesized Na-P is higher than those of Na-X, hydroxy-sodalite and the starting materials. The improvement of CECs of natural homoionic zeolites by Na⁺ exchange has also been reported by many researchers¹⁶⁻¹⁸.

In the present study, natural zeolites originated in Japan, such as mordenite and clinoptilolite, with traces of quartz and feldspar were treated hydrothermally with 0.1, 0.3, 1.0 and 3.0 M NaOH solutions at temperatures in the range of 25-150°C for 7 days. The amounts of ammonium ions up-taken by the hydrothermally treated zeolites were compared with those of untreated zeolites. The up-take mechanism of ammonium ions was confirmed

by investigation of the modified material with the highest CEC for ammonium ions.

4-2. EXPERIMENTAL METHODS

Two natural zeolitic rocks mined in Shimane Prefecture, located in the South-West of Japan, were used as starting materials. The mineral composition and morphology of this zeolite have been reported by Watanabe et al.¹⁹ The first sample (CLI1) was clinoptilolite with traces of quartz, feldspar and layered silicate. The clinoptilolite in CLI1 was a coffin-shaped crystallite in a submicron size. The Si/Al molar ratio of CLI1 was 4.94, which is similar to that of published natural clinoptilolites^{18,22}, the surface area was 91.8 m²/g, and the pore volume was 0.144 mm³/g. The second one (MOR3) consisted mainly of mordenite with quartz and a trace of layered silicate. The mordenite in MOR3 had fibrous morphology with the length of 1 to 5 μm and the diameters of 0.05 to 0.1 μm. The Si/Al molar ratio of MOR3 was 4.85, which is similar to that of published natural mordenite²², the surface area was 129.6 m²/g, and the pore volume was 0.143 mm³/g. They were sieved and only particles with the sizes below 50 μm were used as starting materials.

The mixtures of 2.0 g of a starting material and 30 ml of 0.1, 0.3, 1.0 and 3.0 M NaOH solutions were placed in Teflon cups fitted into stainless steel pressure vessels and heated in an oven at 25, 50, 100 and 150°C under autogenous pressure for 7 days. The modification of natural zeolites is to be performed under an alkaline condition because this reaction is for recrystallization. The hydrothermal treatment was carried out for 7 days in

order to remove impurities as much as possible. After the hydrothermal treatment, the resultant products were filtered through membrane filters of 0.45 μm in pore size and washed several times with distilled water. Then they were freeze-dried for 24 hours.

Identification of minerals was carried out by the powder X-ray diffraction (XRD) method with monochromatized $\text{CuK}\alpha$ radiation at 40 kV and 40 mA using RIGAKU RINT2200 diffractometer. Morphological changes of the crystallites were observed by scanning electron microscopy (SEM) using Hitachi S-5000 electron microscope. The chemical composition of the sample obtained was determined by inductively coupled plasma spectroscopy (ICP) (Seiko HVR 1700) with a photomultiplier tube as a detector. The test solutions were prepared as follows. For the measurement of Si and Al, 50 mg of a sample were mixed with Na_2CO_3 and H_3BO_3 powders and then dissolved in HCl solution. The volume of the solution was increased up to 100 ml with pure water. For the measurement of Na, K, Ca and Mg, 50 mg of a sample were dissolved in a mixture of HF and H_2SO_4 solutions and evaporated. The dried residue was then dissolved in HCl solution with heating, and the volume was increased up to 100 ml with water. The specific surface areas were measured by the multipoint Brunauer-Emmet-Teller (BET) method using a Beckman Coulter SA3100 instrument with N_2 gas as an adsorbent after degassed at 200°C for 3 hrs in vacuum.

For ammonium ions up take experiments, 30.0 ml of solutions containing different concentrations of NH_4Cl (10^{-3} - 10^{-2} M, the initial pH= 5.1-5.4) were added to 0.1 g of each

product in stoppered polyethylene tubes. The tubes were shaken at 30 rpm by an end-over-end shaker (Towa Labo RKVSD 10101) for 7 days at 25°C, and then the solids phase were separated by centrifugation at 15000 rpm for 30 minutes and filtration using membrane filters of 0.45 µm in pore size.

The concentrations of ammonium ions in the filtrated solutions were determined with an ammonium specific ion electrode (Toa Dempa Kogyo IM-20B, Ammonia Electrode Ae-235). The amounts of ammonium ions up-take were calculated from differences between the concentrations of ammonium ions in the filtrated solutions and those in the initial solutions. The values were the averages of three samples. The concentrations of Na⁺ K⁺ Ca²⁺ and Mg²⁺ in the filtrated solutions were determined by ICP analysis (Seiko SPS4000). Before and after the up-take experiments, the separated solids were examined for the confirmation of the changes of zeolite structures by the powder XRD method. The CECs of the samples were determined by extracting ammonium with 1 M KCl solution (pH=7) from the ammonium-saturated samples obtained by repeating centrifugal washing with 1 M CH₃COONH₄ solution (pH=7).¹⁴ The amounts of ammonium ions were determined with an ammonium specific ion electrode.

4-3. RESULTS and DISCUSSION

4-3-1 Characterization of hydrothermally modified products

Changes of the phases of the natural zeolites, CLI1 and MOR3, by hydrothermal

treatment are shown in Table 4.1. The transformation of the natural zeolites to phillipsite, hydroxy-sodalite and analcime depended on types of the zeolitic rocks, and the reaction conditions such as hydrothermal temperature and NaOH concentration.

The structure of CLI1 was not changed after treatment with 0.1 M NaOH solution at temperatures below 150°C. The CLI1 samples treated with 0.3 M NaOH solution at 25, 50 and 100°C also didn't show any change of XRD patterns. But after treatment at 150°C, the amount of clinoptilolite, which is the major zeolite species in CLI1, decreased, and analcime was formed. CLI1 treated with 1 M NaOH solution at 25°C didn't show any phase change, but at 50°C, the low intensity pattern of phillipsite was identified. Treatment at 100°C transformed CLI1 mainly to phillipsite with a trace of feldspar, and at 150°C, analcime with a cubo-octahedral shape of 10-30 μm in diameter was formed. The CLI1 treated with 3 M NaOH solution at 25°C didn't show any phase change. At 50°C, the phase consisted mainly of phillipsite with traces of clinoptilolite and feldspar. The treatment at 100°C led to phillipsite and hydroxy-sodalite with a trace of feldspar, and that at 150°C led to sodalite with layered silicate.

On the other hand, MOR3 treated with 0.1 M NaOH solution at temperatures below 150°C and with 0.3 M NaOH or 1 M NaOH solution at below 50°C didn't show the structural changes. After treatment with 0.3 M NaOH solution at 100 and 150°C, phillipsite started appearing. After treatment with 1 M NaOH solution at 100°C, the main phase became phillipsite with traces of quartz and feldspar, whereas at 150°C MOR3 was mainly

transformed to analcime with traces of quartz and feldspar. The MOR3 in 3 M NaOH solution was transformed to phillipsite or hydroxy-sodalite depending on treatment temperature.

The chemical composition of MOR3 obtained after treatment with 3 M NaOH solution at 100°C as determined by ICP analysis showed that the Si/Al molar ratio was about 1.64, and the amount of Na⁺ ions was 13.0 wt%, which is nearly equal with the Si/Al molar ratio and CEC of synthetic PHL.³ K⁺, Ca²⁺ and Mg²⁺ were not detected by ICP analysis.

The SEM image of the phillipsite showed aggregates or intergrown fine rosette crystallites submicrons in size (Fig. 4.1). These results indicate that the phase transformation of natural zeolites as the result of hydrothermal treatment depends on the compositions of starting zeolite materials, hydrothermal temperature and NaOH concentration.

4-3-2 Ammonium up-take

Ammonium up-take experiments were carried out with the samples modified by hydrothermal treatment with 1 and 3 M NaOH solutions at 100°C. The relationship between the amounts of ammonium up-taken by the modified samples of CLI1 and MOR3, and the equilibrium concentrations of ammonium chloride is shown in Figs. 4.2 and 4.3, respectively.

Phillipsite obtained from MOR3 treated at 100°C in 3 M NaOH solution has a greater ammonium up-take capacity than the untreated sample as reported by Watanabe et al.¹⁹ In the present study, the amount of ion-exchanged ammonium by phillipsite (1.92 mmol/g in 10 mM NH₄Cl) was about twofold larger than that obtained by MOR3. The surface area of phillipsite was 31.4 m²/g, which is lower than that obtained from MOR3 (129.6 m²/g), and the pore volume was 0.119 mm³/g. These results indicate that the surface area is not related to ammonium up-take.

Similar results were obtained from CLI1 treated with 1 M NaOH solution at 100°C. When CLI1 was transformed to phillipsite, the up-take of ammonium ions increased. The increase of the amount of up-taken ammonium ions by phillipsite is related to a larger number of ion-exchange sites in phillipsite framework rather than those in mordenite and clinoptilolite lattices.²² The real CECs of CLI1, MOR3 and the treated zeolites are shown in Table 4.2. The CECs of phillipsite obtained from CLI1 and MOR3 treated with 3 M NaOH at 100°C were 2.88 and 3.13 meq/g, respectively, but the values were nearly two time larger than those of CLI1 (1.40 meq/g) and MOR3 (1.12 meq/g). From these results we conclude that the change of clinoptilolite and mordenite to phillipsite improves CEC and ammonium up-take.

The CECs of the zeolites used in this study are compared with other published data on zeolites in Table 4.3. This comparison indicates that the treated zeolites composed of mainly phillipsite have similar but slightly higher exchange capacities than other

previously reported zeolites.^{15, 17, 20, 21}

4-3-3 Ion-exchange mechanism of Ammonium ions

Phillipsite modified from MOR3 at 100°C in 3 M NaOH solution, with the highest ion-exchange capacity for ammonium ions, was used to investigate the up-take mechanism of ammonium ions. Fig. 4.4 shows the relationship between the amounts of ammonium ions up-taken by phillipsite and the amounts of the Na⁺ released from phillipsite. The amounts of ammonium ions up-taken by phillipsite were equal to those of Na⁺ released from phillipsite. The amounts of K⁺, Ca²⁺ and Mg²⁺ were not detected. These results indicate that the up-take of ammonium ions proceeds by an ion-exchange mechanism. X-ray diffraction patterns did not show any structural change of phillipsite after ion-exchange, which proves that the framework structure is stable under this condition.

4-4. CONCLUSION

Natural zeolitic rocks, such as mordenite and clinoptilolite with traces of quartz and feldspar, were treated hydrothermally with 0.1, 0.3, 1.0 and 3.0 M NaOH solutions at temperatures below 150°C. The phase changes of these zeolites depended on reaction conditions such as hydrothermal temperature and NaOH concentration, as well as the chemical compositions of the starting materials.

The amount of ammonium ions up-taken by the product modified from MOR3 at 100°C in 3 M NaOH solution, which contained mainly phillipsite, was twofold larger

(1.92 mmol/g) than that up-taken by the starting material. This result is explained by higher CEC of phillipsite framework in comparison to mordenite and clinoptilolite. The mechanism of ammonium up-take by phillipsite involved ion-exchange of Na^+ ions with ammonium ions. The framework structure of phillipsite was stable in ammonium ion solutions, and therefore we conclude that phillipsite is ideal for an industrial ion-exchanger to remove ammonium ions from wastewater.

Table 4.1. The hydrothermal modifications of natural zeolites, CLI1 and MOR3.

Starting Materials	T(°C)	C _{NaOH} (N)	products
CLI1	25	0.1	Cli, Feld, Qtz, LS
		0.3	Cli, Feld, Qtz, LS
		1.0	Cli, Feld, Qtz, LS
		3.0	Cli, Feld, Qtz, LS
	50	0.1	Cli, Feld, Qtz, LS
		0.3	Cli, Feld, Qtz, LS
		1.0	Cli, Feld, Qtz, LS, Phi
		3.0	Phi, Cli, Feld, Qtz, LS
	100	0.1	Cli, Feld, Qtz, LS
		0.3	Cli, Feld, Qtz, LS
		1.0	Phi, Feld
		3.0	Phi, Sod, Feld
	150	0.1	Cli, Feld, Qtz, LS
		0.3	Cli, Ana, Feld, Qtz, LS
		1.0	Ana
		3.0	Sod, LS
MOR3	25	0.1	Mor, Qtz, LS
		0.3	Mor, Qtz, LS
		1.0	Mor, Qtz, LS
		3.0	Mor, Qtz, LS
	50	0.1	Mor, Qtz, LS
		0.3	Mor, Qtz, LS
		1.0	Mor, Qtz, LS
		3.0	Phi, Mor, Qtz, LS
	100	0.1	Mor, Qtz, LS
		0.3	Mor, Phi, Qtz, LS
		1.0	Phi, Qtz, LS
		3.0	Phi
	150	0.1	Mor, Qtz, LS
		0.3	Mor, Phi, Qtz, LS
		1.0	Ana, Qtz, Fed
		3.0	Phi, Sod

C_{NaOH}(N): NaOH concentration in normality

Cli: clinoptilolite. Mor: mordenite. Phi: phillipsite. Ana: analcime. Sod: sodalite.

Qtz: quartz. Feld: feldspar. LS: layered silicate.

Table 4.2. Cation exchange capacities of CLI1, MOR3 and treated zeolite.

Starting Materials	T(°C)	C _{NaOH} (N)	CEC (meq/g)
CLI1	-	-	1.40
	100	1.0	2.76
	100	3.0	2.88
MOR3	-	-	1.12
	100	1.0	2.30
	100	3.0	3.13

Table 4.3. Cation exchange capacities of various zeolites.

Zeolite Origin	Cation Exchange Capacity meq /g	Ref
CLI1	1.40	
MOR3	1.12	
CLI1 treated 3N at 100 °C	2.88	
MOR3 treated 3N at 100 °C	3.13	
Natural clinoptilolite	1.75	(15)
Na-P	4.18	(15)
Natural clinoptilolite (Na type)	0.44	(17)
Faujasite (Na type)	3.20	(20)
Natural clinoptilolite (Na type)	2.05	(21)

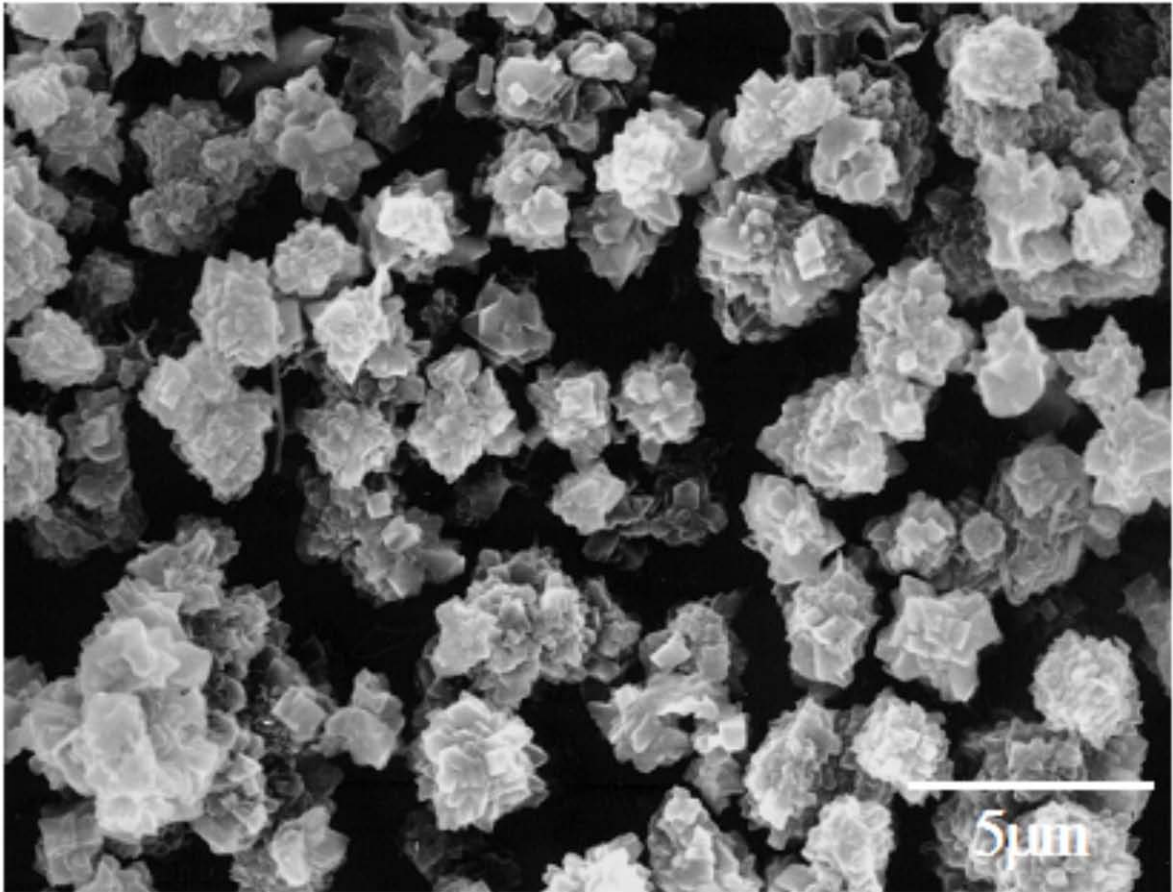


Fig. 4.1. The SEM image of phillipsite obtained after treatment of natural mordenite. (MOR3) with 3 M NaOH solution at 100°C.

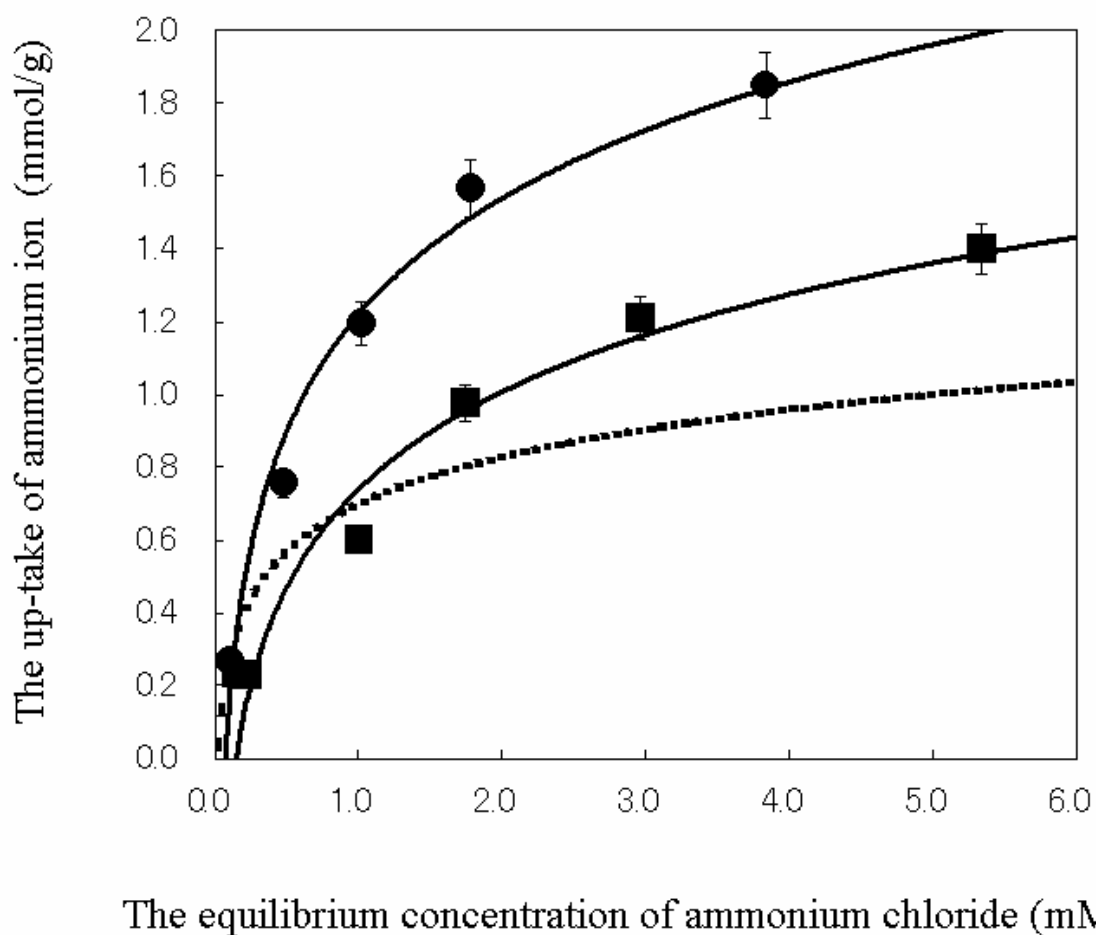


Fig. 4.2. The adsorption isotherms for modified clinoptilolite. Solid circles: phillipsite with trace of feldspar (1 M NaOH, 100°C). Solid squares: phillipsite with trace of hydroxy-sodalite and feldspar (3 M NaOH, 100°C). Dotted line: starting material (CLI1).¹⁹

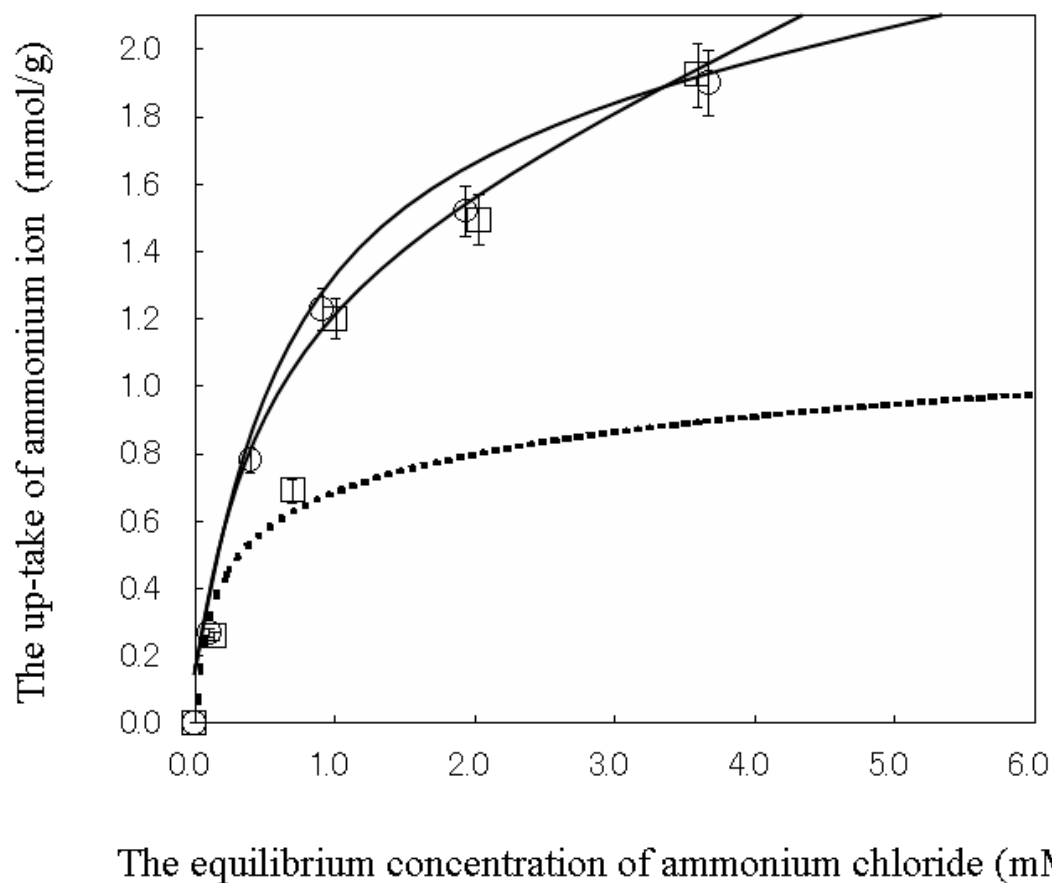


Fig. 4.3. The adsorption isotherms for modified mordenite. Circles: phillipsite with trace of feldspar (1 M NaOH 100°C). Squares: phillipsite (3 M NaOH, 100°C). Dotted line: starting material (MOR3).¹⁹

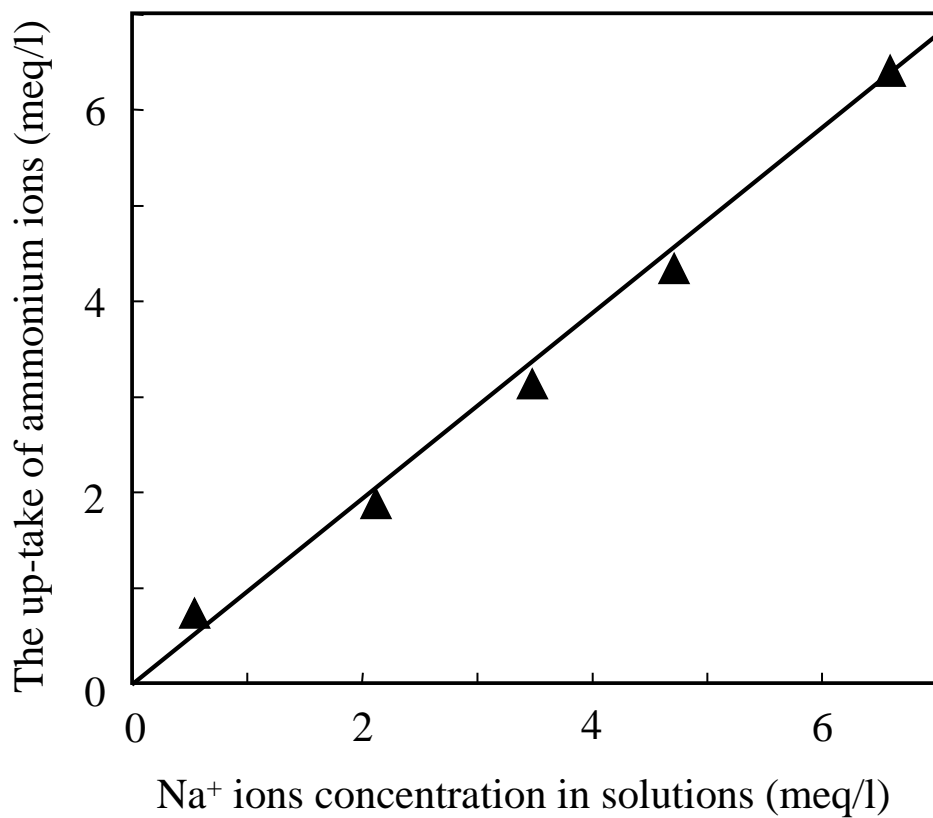


Fig. 4.4. The relationship between the released amounts of Na⁺ ions and the amounts of ammonium ions up-taken by phillipsite (3 M NaOH, 100°C).

4-5. REFERENCES

- 1) R. L. Hay, In *Natural Zeolites: Occurrence, Properties, Use*; L. B. Sand and F. A. Mumpton, Eds. Pergamon Press, New York, 135(1976).
- 2) A. Iijima, and M. A. Utada, *Jpn. J. Geol. Geogr.*, 42, 61(1972).
- 3) D. W. Breck, *Zeolite Molecular Sieves*. Eds. Wiley: New York, 498(1974).
- 4) C. Y. Chang, D. H. Son, and D. H. Ahn, *Water Sci. Technol.*, 42 (5-6), 127(2000).
- 5) N. A. Booker, E. L. Cooney, and A. J. Priestley, *Water Sci. Technol.*, 34 (9), 17(1996).
- 6) E. L. Cooney, N. A. Booker, D. C. Shallcross and G. W. Stevens, *Sep. Sci. Technol.*, 34 (14), 2741(1999).
- 7) T. Henmi, *Soil Sci. Plant Nutr.* 33, 517 (1987).
- 8) Y. Okada, *Jpn. J. Soil Sci. Plant Nutr.* **62**, 1(1991).
- 9) X. Querol, F. Plana, A. Alastuey, and A. Lopez, *Fuel.* **8**, 793(1997).
- 10) M. Murat, A. Amokrane, J. P. Bastide and L. Montanarro, *Clay Miner.* 27, 119(1992).
- 11) K. Abdmezien and B. Siffert, *Appl. Clay Sci.* 4, 1(1989).
- 12) K. Abdmezien and B. Siffert, *Appl. Clay Sci.* **8**, 437(1994).
- 13) R. Ruiz, C. Blanco, C. Pesquera, F. Gonzalez, I. Benito and J. L. Lopez, *Appl. Clay Sci.* 12, 3(1997).
- 14) S. J. Kang and K. Egashira, *Appl. Clay Sci.* 12, 131(1997).
- 15) S. J. Kang, K. Egashira and A. Yoshida, *Appl. Clay Sci.* 13, 117(1998).
- 16) J. D. Sherman, in *Zeolite*, Eds. Martinus Nijhoff Publishers, pp. 584(1984).

- 17) M. J. Semmens and W. P. Martin, *Water Res.* **22**, 537(1988).
- 18) L. Curkovic, S. CerjanStefanovic and T. Filipan, *Water Res.* 31, 1379(1997).
- 19) Y. Watanabe, H. Yamada, H. Kokusen, J. Tanaka, Y. Moriyoshi and Y. Komatsu, *Sep. Sci. Technol.*, 38(7), 1519(2003).
- 20) Y. Watanabe, H. Yamada, J. Tanaka, Y. Komatsu and Y. Moriyoshi, *Sep. Sci. Technol.* 39, 2091(2004).
- 21) A. Dyer, S. Amini, H. Enamy, H. A. Elnaggar and M. W. Anderson, *Zeolite* 13, 281(1993).
- 22) F. A. Mumpton, *Mineralogy and geology of natural zeolite*, Eds. Mineralogical society of America, Washington, 1(1981).

CHAPTER 5

HYDROTHERMAL FORMATION OF HYDROXYAPATITE LAYERS ON THE SURFACE OF TYPE-A ZEOLITE

Preparation of a novel type-A zeolite with hydroxyapatite layers on its surface by a hydrothermal method

5-1. INTRODUCTION

Increased levels of ammonium, heavy metals and radioactive elements result in serious environmental pollution problems. These levels have been controlled by legislation on discharge limits in many countries. It is thus important to develop new materials for removing harmful ions such as NH_4^+ , Cd^{2+} and Pb^{2+} and for fixing radioactive ions such as Cs^+ , Sr^{2+} and I^- for long terms. Zeolite, hydrated aluminosilicate, has a high cation exchange and ion adsorption capacities with characteristic nanopores, which is extensively used as an adsorbent for NH_4^+ , Cs^+ , Sr^{2+} and I^- .¹⁻³ We focused on the high cation exchange ability to prepare multi-functional ceramic composites with the adsorption properties. Hydroxyapatite [$\text{Ca}_{10}(\text{PO}_4)_6(\text{OH})_2$] has also a high cation exchange capacity for Cd^{2+} and very low solubility product of under 1×10^{-100} , and shows particularly high stability at alkaline solutions.⁴ Several studies have succeeded in growing apatite crystals on the surface of wollastonite and alite for biological and medical applications.⁵⁻⁷ However, in these studies, the substances were rather self-destroyed in coating hydroxyapatite on its surfaces. We prepared a novel type-A zeolite with hydroxyapatite layers on its surface by a hydrothermal method on the basis of the cation exchange of Ca^{2+} in zeolite for NH_4^+ in solution and discussed the formation mechanism of hydroxyapatite on the surface.

5-2. EXPERIMENTAL METHODS

Type-A zeolite with Ca^{2+} (Ca-LTA) as a starting substance for hydrothermal treatment was prepared as follows. Type-A zeolite powder (200 meshes under) with Na^+ as an exchangeable cation was purchased from Wako Pure Chemicals Industries, Ltd., Japan. The exchange of Na^+ for Ca^{2+} was carried out by washing 5.0g of zeolite three times in 500 ml of 0.5 M CaCl_2 solution. The resultant sample was filtered with a membrane filter 0.45 μm in pore size and washed in distilled water to remove excess cations. The Ca-LTA was obtained after dried at 100°C for 24 hours. The hydrothermal treatments were conducted as follows. 0.3 g of the Ca-LTA powder was immersed in 20 ml of 1 M ammonium phosphate $[(\text{NH}_4)_3\text{PO}_4]$ solution in a 100ml teflon cup fitted into a stainless steel pressure vessel. The pH value of the solution was controlled to 9 by addition of an ammonium solution and heated at 120°C for 8 hours. The sample was quenched and washed three times in distilled water and dried at 100°C for 24 hours. The Ca-LTA and the resultant sample of the hydrothermal treatment were characterized by powder X-ray diffraction (XRD), scanning electron microscopy (SEM) and Fourier transform-infrared spectroscopy (FT-IR), and transmission electron microscopy (TEM) equipped with an energy dispersive X-ray spectrometer (EDS).

5-3. RESULTS AND DISCUSSION

The SEM images in Figs. 5.1a and c showed that the Ca-LTA had a cubic automorphism with smooth surface. Figs. 5.1b and d showed the resultant LTA after

hydrothermal treatment. The hydrothermal treatment was not destroyed the cubic automorphism but changed its surface morphology with complete covering of scaly particles. The scaly particles were aggregated with needle-like crystals of 100-200 nm in diameter and 30 nm in thickness. The crystal morphology was very similar to that of hydroxyapatite obtained under hydrothermal treatment.⁸

The XRD pattern of the Ca-LTA indicated the complete exchange of Na^+ for Ca^{2+} in zeolite and showed typical Ca-type zeolite with high crystallinity (Fig. 2a) from the change of diffraction intensities and the appearance of a new diffraction at 25.1 degree.⁹ After the hydrothermal treatment of Ca-LTA, broad peaks were observed as indicated arrows in Fig. 2b. The broad peaks corresponded closely to those of apatite although the positions of the broad peaks were difficult to determine exactly because these extremely broad peaks overlapped with those due to the zeolite structure. The other sharp peaks in Fig 2b agreed with those of LTA replaced Ca^{2+} by NH_4^+ , indicating that the most cation sites in the Ca-LTA were occupied by NH_4^+ during the hydrothermal treatment as described previously by Matsumoto et al.¹⁰ The XRD patterns demonstrated that there was no significant difference in the FWHM before and after the hydrothermal treatment (Fig. 2). From the results of SEM and XRD, the LTA structure is stable in the 1 M ammonium phosphate solution heated at 120°C for 8 hours.

Fig. 3 shows FT-IR spectra of Ca-LTA (a) and Ca-LTA after hydrothermal treatment (b). The absorption bands at 542 and 460 cm^{-1} were attributed to double rings and Si,

Al-O bend in the LTA structure, and those at 1130/1055/998 and 742/705/665 cm^{-1} were judged due to asymmetric and symmetric stretches of the framework aluminosilicate in the LTA, respectively (Figs. 3a and b).¹¹ These results indicated that the framework of LTA was not affected by the hydrothermal process, which was comparable to the results obtained by XRD. After the hydrothermal treatment, absorption bands due to ν_2 , ν_3 and ν_4 vibration of PO_4^{3-} (474 cm^{-1} , 1092/1045 cm^{-1} and 602/572 cm^{-1} , respectively) and OH^- (632 cm^{-1}) were observed and corresponded to the characteristic absorption bands of hydroxyapatite.¹² Absorption bands due to CO_3^{2-} ions (875 cm^{-1} and 1450 cm^{-1}) that could replace PO_4^{3-} sites (B sites) in hydroxyapatite were observed. An absorption band at 1400 cm^{-1} was attributed to NH_4^+ present in the exchangeable cation sites of the LTA structure. Thus, the hydrothermal treatment caused the cation exchange of Ca^{2+} for NH_4^+ which was agreed with the results of XRD.

A TEM image and selected-area electron diffraction (SAED) pattern of the scaly particles present on the surface of the LTA after hydrothermal treatment are shown in Fig. 4. The SAED and EDS revealed that the scaly particles growing in the direction roughly perpendicular to the surface were hydroxyapatite since the SAED pattern of the scaly particles corresponded to that of apatite and the scaly particles had only the components of Ca, P and O. The hydroxyapatite had about 30 nm in thickness and a sharp interface with the LTA, indicating that the hydroxyapatite grew toward the outside solution without the marked dissolution of LTA. In the SAED pattern, the Debye ring of the 002

reflection had a crescent-like form. The crescent-like Debye ring is known to decide the preferential orientation of hydroxyapatite crystals.¹³ The TEM image corresponded to the SAED pattern, indicating that the *c*-axes of the hydroxyapatite crystals preferentially oriented along the direction perpendicular to the LTA surface. It has already known this orientation of hydroxyapatite depends strongly on a substratum^{8,13}.

Therefore, the orientation of hydroxyapatite is possibly controlled by the surface porous structure of LTA. The SAED pattern showed the sharp Debye rings and some spots, suggesting that the broad peaks in the XRD pattern were formed by the fine crystallites but not the defective structure.

The hydroxyapatite prepared had a similar shape to those formed on the surfaces of alite and wollastonite particles.^{5,7} Moriyoshi et al. have discussed a formation mechanism of hydroxyapatite.⁷ According to their reports, Ca^{2+} in alite released in an ammonium phosphate solution reacts very rapidly with PO_4^{3-} to form hydroxyapatite at the interface between the hydrated alite and hydroxyapatite particles. Liu et al. have also reported a formation mechanism of hydroxyapatite on wollastonite in a simulated body fluid (SBF).⁵ They released discussed that Ca^{2+} released from wollastonite increases the ion activity of the apatite in SBF, and the hydrated silica on the surface of wollastonite provides sites favourable for apatite nucleation. Consequently, the apatite nuclei are rapidly formed on the surface of wollastonite. However, in our study, the reaction of Ca-LTA and ammonium phosphate is concluded to take place by a different mechanism.

The ion exchange of Ca^{2+} on LTA for NH_4^+ in an ammonium phosphate solution is a driving force of the formation of hydroxyapatite and then the discharged Ca^{2+} ions reacted with the phosphate ions on the surface of LTA due to Ca^{2+} supersaturation at the local area.

5-4. CONCLUSION

We successfully obtained the nanocomposite by a new concept which applied an ion exchange reaction. The thin layers of hydroxyapatite needle-like crystals with 100-200nm in diameter and 30nm in thickness were formed on the surface of type-A zeolite by a reaction between discharged Ca^{2+} ions from type-A zeolite and an ammonium phosphate solution in hydrothermal treatment. The *c*-axes of the hydroxyapatite crystals preferentially oriented along the direction perpendicular to the LTA surface. The ion exchange of Ca^{2+} on LTA for NH_4^+ in an ammonium phosphate solution is a driving force of the formation and the preferential orientation of hydroxyapatite. The nanocomposite obtained is a novel material for the simultaneous removal of both harmful and radioactive ions, which has the excellent characteristics of both zeolite and hydroxyapatite.

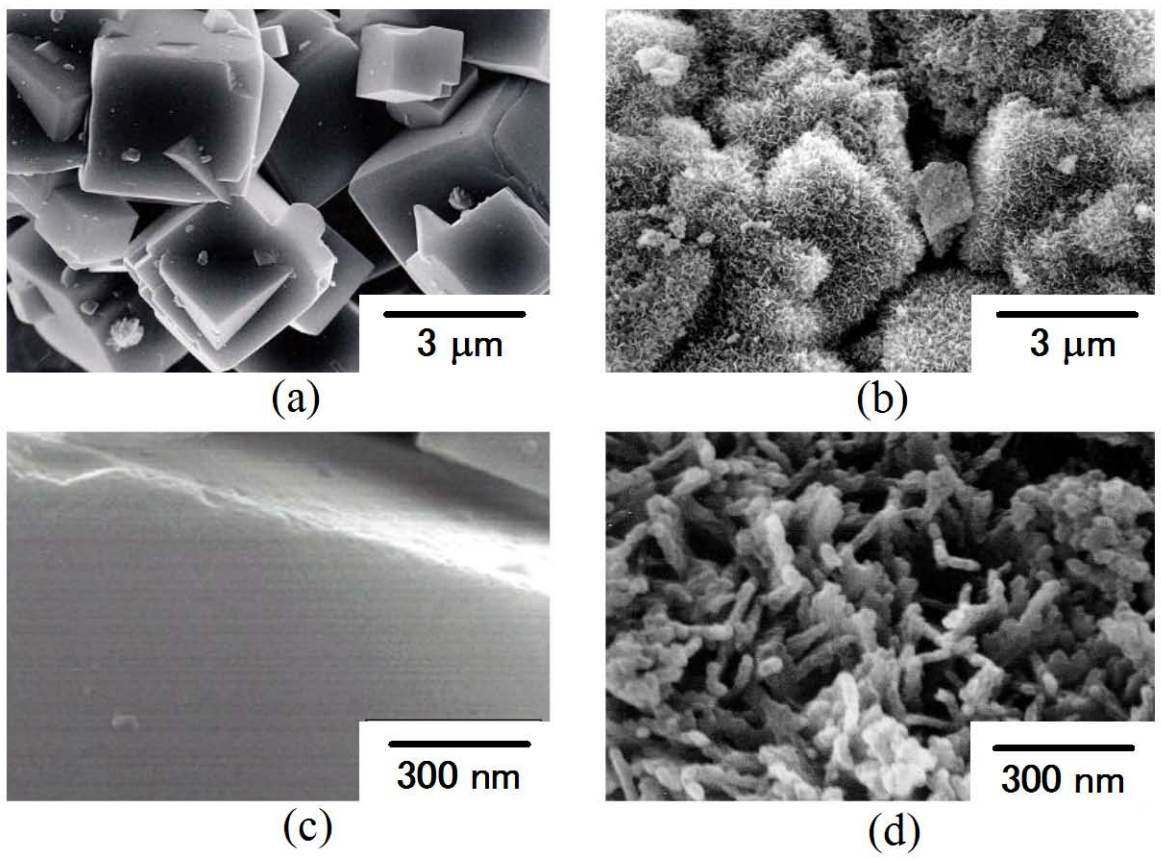


Fig. 5.1. SEM images of Ca-LTA (a, c) and LTA after hydrothermal treatment (b, d).

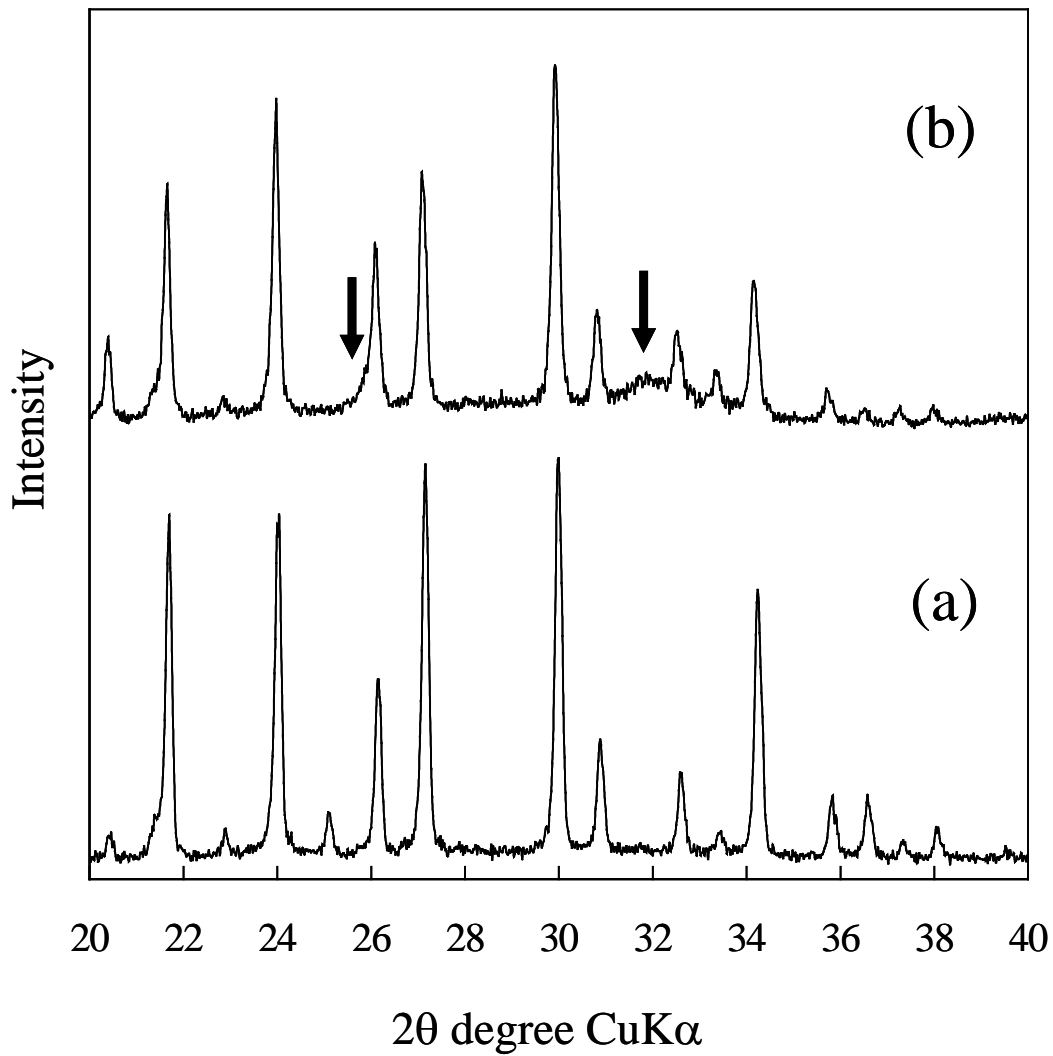


Fig. 5.2. XRD patterns of Ca-LTA (a) and LTA after hydrothermal treatment (b). All diffraction peaks in (a) are attributed to Ca-LTA. The arrows in (b) indicate the diffractions due to hydroxyapatite.

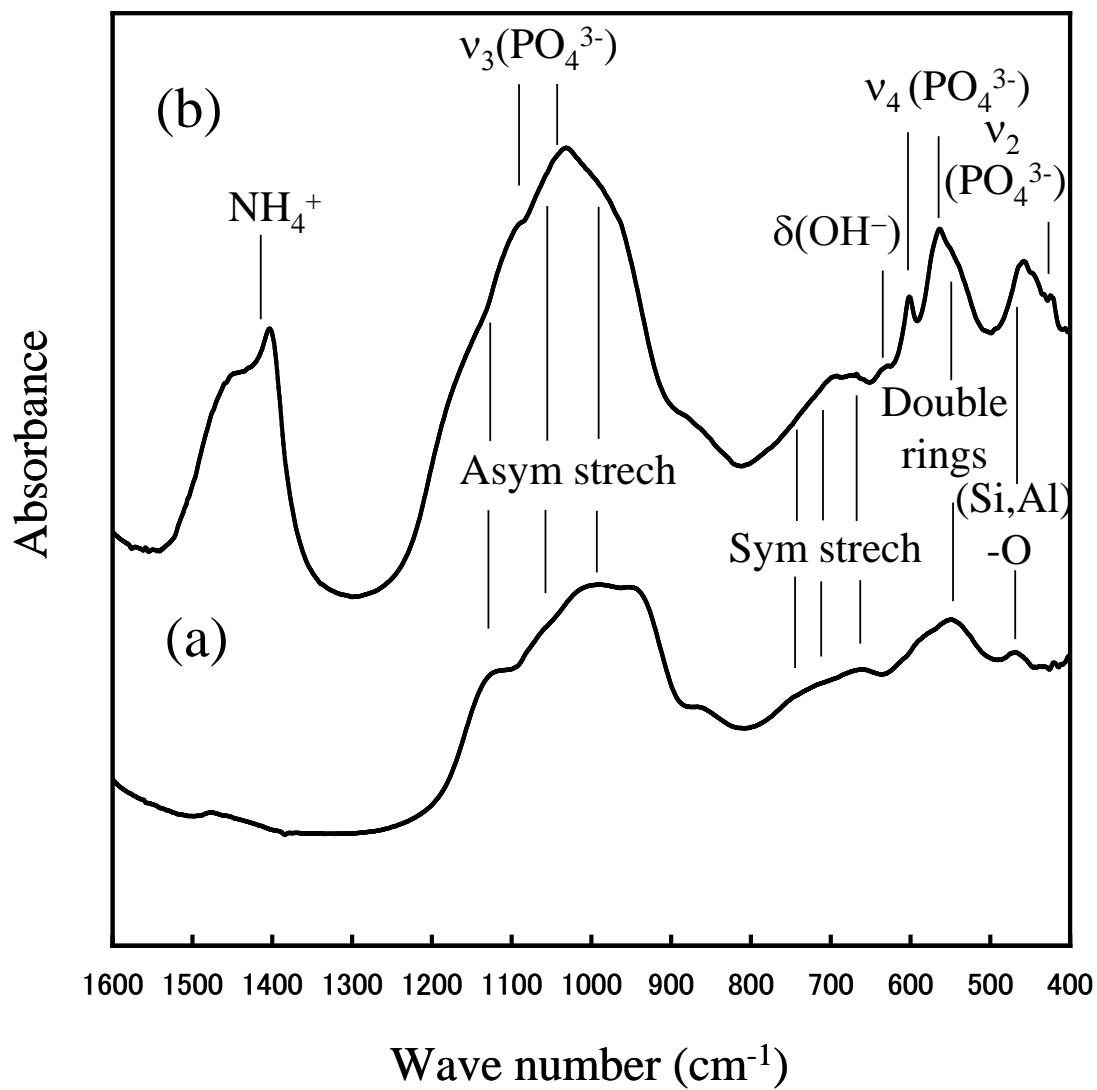


Fig. 5.3. FT-IR spectra of Ca-LTA (a) and LTA after hydrothermal treatment.

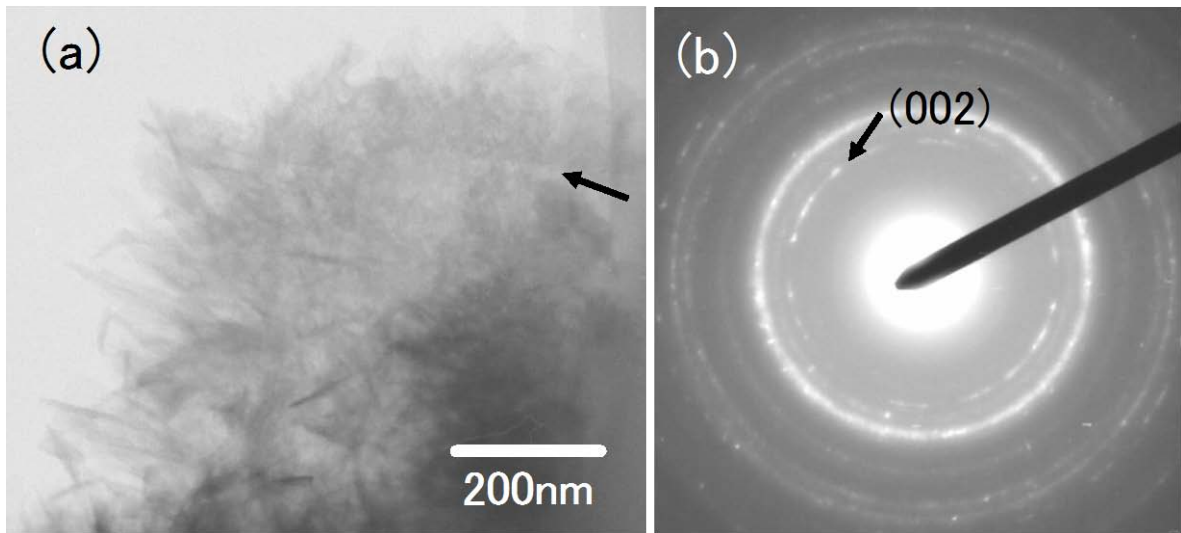


Fig. 5.4. TEM image (a) and SAED pattern (b) of LTA after hydrothermal treatment. The arrow in (a) indicate the interface between LTA and hydroxyapatite.

Ion exchange ability in NaCl solution and stability of its structure in the process of the ion exchange for the type-A zeolite with hydroxyapatite surface layers.

5-5. INTRODUCTION

Increased levels of harmful elements caused serious environmental pollutions. These levels have been controlled by legislation on discharge limits in many countries. It is thus important to develop new materials for removing harmful elements such as NH_4^+ , Cd^{2+} and Pb^{2+} ions. Zeolite, hydrated aluminosilicate with exchangeable cations has high cation exchange and ion adsorption capacities with characteristic nanopores, which is extensively used as an adsorbent for NH_4^+ ions in wastewater.² Hydroxyapatite [$\text{Ca}_{10}(\text{PO}_4)_6(\text{OH})_2$] (HAp) has also a high cation exchange capacity for Cd^{2+} and Pb^{2+} ions in wastewater. We prepared a novel type-A zeolite with hydroxyapatite layers on its surface by a hydrothermal method on the basis of the cation exchange of Ca^{2+} in zeolite for NH_4^+ .¹⁴ In this study, ion exchange ability in 0-10mM NaCl solution and stability of its structure in the process of the ion exchange were investigated for the type-A zeolite with hydroxyapatite surface layers.

5-6. EXPERIMENTAL METHODS

5-6-1. Preparation of type-A zeolite with hydroxyapatite surface layers

Type-A zeolite with Ca^{2+} ions (Ca-LTA) as a starting substance for the hydrothermal

treatment was prepared as follows. Type-A zeolite powder (200 meshes under) with Na⁺ ions as an exchangeable cation was purchased from Wako Pure Chemicals Industries, Ltd. The exchange of Na⁺ ions for Ca²⁺ ions was carried out by immersing 5.0 g of the zeolite in 1500 ml of 0.5 M CaCl₂ solution for 24 hours. The resultant sample was filtered with a membrane filter of 0.45 μm in pore size and rinsed with distilled water to remove excess cations. The Ca-LTA was dried at 100°C for 24 hours.

The hydrothermal treatment was conducted as follows. 0.3 g of the Ca-LTA powder was immersed in 30 ml of 1 N ammonium phosphate ((NH₄)₃PO₄) solution in a 100ml Teflon cup fitted into a stainless steel pressure vessel. The pH value of the solution was controlled to 9 by addition of an ammonium solution and heated at 120°C for 8 hours. The sample was rinsed in 1500 ml of distilled water and dried at 100°C for 24 hours. The Ca-LTA and the resultant sample of the hydrothermal treatment (HAp-LTA) were characterized by Fourier transform-infrared spectroscopy (FT-IR), scanning electron microscopy (SEM) and powder X-ray diffraction (XRD). The chemical compositions of these samples were determined by both inductively coupled plasma spectroscopy (ICP) and the KJELDAHL determination.¹⁵

5-6-2. Ion exchange ability of type-A zeolite with hydroxyapatite layers

0.1 g of HAp-LTA was immersed in 30.0 ml solutions containing different concentrations of NaCl (0-10mM) in polyethylene tubes. The tubes were shaken for 1 day at 25°C and the solid phases were separated by filtration using membrane filter of

0.45 μm . The concentration of NH_4^+ ions in filtrated solutions were determined by an ammonium specific ion electrode. The concentrations of cations in filtrated solutions were measured by inductively coupled plasma (ICP) analysis. After the ion exchange experiments, the separated solids were examined by the powder XRD method.

5-7. RESULTS AND DISCUSSION

The chemical compositions of Ca-LTA and HAp-LTA were shown in Table 5.1. The chemical formula of the Ca-LTA obtained was determined to be $(\text{Ca}_{5.45}\text{Na}_{0.55})(\text{Si}_{12}\text{Al}_{12.02}\text{O}_{47.7})\cdot n\text{H}_2\text{O}$. The Na^+ ions were almost exchanged for Ca^{2+} ions. After the hydrothermal treatment, the NH_4^+ ions were partially exchanged for the Ca^{2+} and Na^+ ions and the Si/Al molar ratio was near 1.0. Furthermore, the phosphate ions were detected due to the crystal growth of HAp on the surface of LTA. The exact chemical formula of the HAp-LTA was not determined from these experiments because the mechanism of HAp crystal growth was a complex manner. However, it was concluded that the ion exchange of Ca^{2+} ions for NH_4^+ ions was a driving force for the crystal growth of HAp on its surface.

Fig. 5.5 shows FT-IR spectra of Ca-LTA (a), HAp-LTA (b) and HAp-LTA after mixing it in 10mM NaCl solution (c). The absorption bands at 542 and 460 cm^{-1} were attributed to double rings and Si, Al-O bond, and those at 1130/1055/998 and 742/705/665 cm^{-1} were to asymmetric and symmetric stretches of the LTA framework.¹⁷ After the

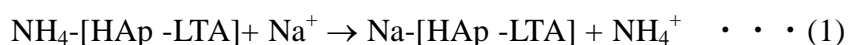
hydrothermal treatment, absorption bands due to ν_2 , ν_3 and ν_4 vibration of PO_4^{3-} (474 cm^{-1} , $1092/1045\text{ cm}^{-1}$ and $602/572\text{ cm}^{-1}$, respectively) and OH^- (632 cm^{-1}) were observed and corresponded to the characteristic absorption bands of HAp.¹² An absorption band at 1400 cm^{-1} was attributed to NH_4^+ present in the exchangeable cation sites of the HAp-LTA structure. After mixing HAp-LTA in 10mM NaCl solution, the absorption band at 1400 cm^{-1} for NH_4^+ was decreased in comparison with that of HAp-LTA. The characteristic bands of HAp were not diminished, which means that the crystal structure of HAp was stable in the process of the ion exchange experiments.

Fig. 5.6a and Fig. 5.6b shows the Ca-LTA and HAp-LTA with a cubic automorphism, respectively. The surface morphology of Ca-LTA with a smooth surface was completely different compared with that of HAp-LTA. The small crystals of needle-like HAp were aggregated to form the scaly particles on the surface of HAp-LTA. The hydrothermal treatment did not destroy the cubic automorphism but only changed its surface morphology. Furthermore, the HAp-LTA mixed in 10 mM NaCl solution had almost similar structure of HAp-LTA.

Table 5.2 shows the concentrations of cations, initial and equilibrium pH values after mixing HAp-LTA in various NaCl solutions. The amounts of Ca, P, Si and Al were less than 0.1 wt% for all samples. The increase in the equilibrium pH was observed due to the increases in the cation concentrations. The increase of initial concentration of NaCl caused the increase of NH_4^+ ion in the solutions. The Na^+ ion exchanged after the

reactions were almost equal to the amounts of NH_4^+ ions leached from HAp-LTA at these conditions, when the amount of NH_4^+ ions leached in distilled water was excluded.

The ion exchange ability in NaCl solutions was confirmed for type-A zeolite (NH_4^+ type) covered with hydroxyapatite layer on the surface prepared by hydrothermal treatment. The amounts of dissolved Si and Al were less than 0.1 wt%. The concentrations of the dissolved Ca and P from HAp-LTA were also negligible. These results indicate that the structures of HAp-LTA are stable in 0-10mM NaCl solutions. This was also confirmed by the unchanged crystal structures of the LTA and HAp from the results of XRD measurements. We already reported the ion exchange behavior of natural zeolites and ammonium adsorption was occurred by the ion exchange with cation on zeolites.² In this study, also sodium uptake on LTA occurred by ion exchange. The sodium ion-exchange proceeds by the following ion-exchange reaction (Eqn. 1).



This was also confirmed by the decrease of absorption band at 1400 cm^{-1} which was attributed to NH_4^+ ions in the LTA structure after the reactions as compared with that of before reactions (Fig. 5.5). The amount of Na^+ ions exchanged in the HAp-LTA is almost equal to the amount of NH_4^+ ions leached from HAp-LTA. This result indicates that the type-A zeolite with HAp surface layers maintains ion-exchange ability and is a novel material for the simultaneous removal of harmful elements such as NH_4^+ , Cd^{2+} and Pb^{2+} ions. The complex composites with the excellent characteristics of both zeolite and HAp

will be applicable to the environmental purification material.

5-8. CONCLUSION

The ion exchange ability in 0-10mM NaCl solutions was investigated for a novel type-A zeolite (NH_4^+ type) covered with hydroxyapatite layer on the surface prepared by hydrothermal treatment. The silicon and aluminum ions dissolved from the zeolite framework were less than 0.1 wt% and the structure was not collapsed. The Na^+ ions in the solutions were exchanged for NH_4^+ ions in cation exchange sites on the type-A zeolite since the exchanged amount of Na^+ ions for NH_4^+ ions was almost coincident. This result indicates that the type-A zeolite with hydroxyapatite layers maintains ion-exchange ability.

Table. 5.1 Chemical composition of Ca-LTA and HAp-LTA (wt%).

	Ca-LTA	HAp-LTA
Si	15.40	13.60
Al	14.80	12.80
Na	0.58	0.22
Ca	10.40	7.24
NH ₃	ND	5.10
P	ND	3.32

ND = not detected.

Table. 5.2 The concentration of dissolved cations from HAp-LTA (mmol/l) and the amount of adsorbed sodium (mmol/l) in NaCl solutions.

C ₀ (Na ⁺)	pH ₀	pHeq	Si	Al	Ca	P	NH ₄	Na _{ads}
10.0	6.78	8.23	0.133	0.013	0.002	0.016	5.851	4.061
7.0	6.61	8.30	0.137	0.018	0.002	0.012	5.075	3.121
5.0	6.42	8.32	0.142	0.022	0.001	0.011	4.415	2.449
3.0	6.35	7.82	0.154	0.033	ND	0.011	3.506	1.655
1.0	6.26	6.90	0.172	0.068	ND	0.008	2.320	0.574
0.0	6.24	7.48	0.056	ND	0.001	0.015	1.820	ND

C₀ (Na⁺) = initial concentration of NaCl solution. Na_{ads}= The values of sodium adsorption
 ND = not detected. pH₀ = initial pH values. pHeq = equilibrium pH values.

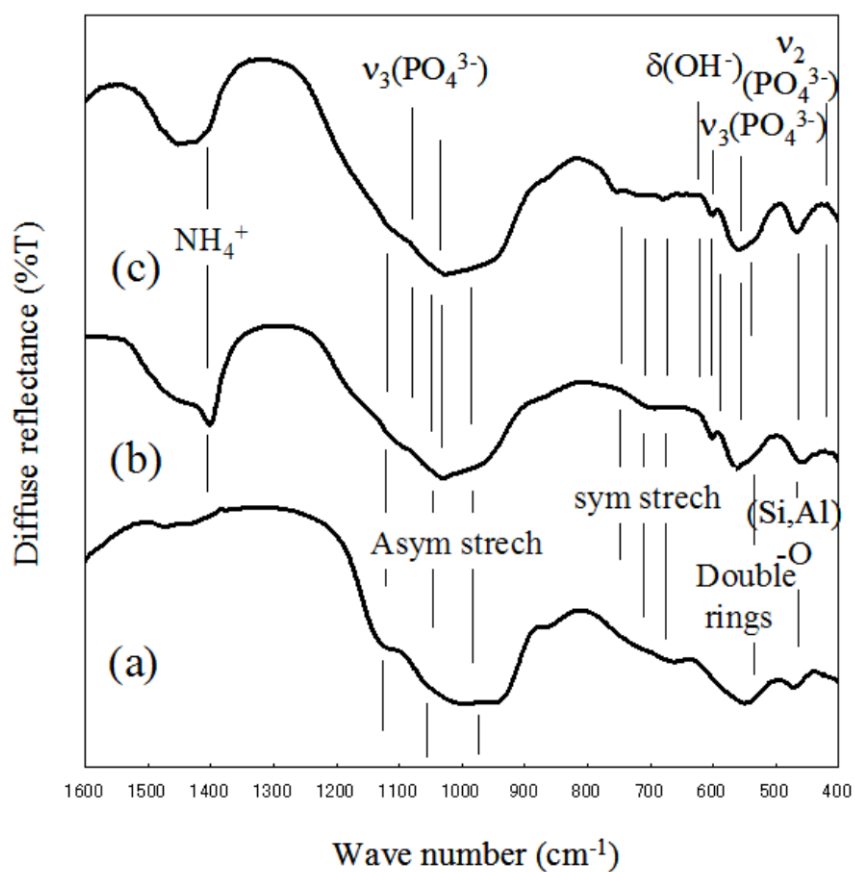


Fig. 5.5. FT-IR spectra of Ca-LTA (a), HAp-LTA (b) and HAp-LTA after mixing it in 10mM NaCl solution (c).

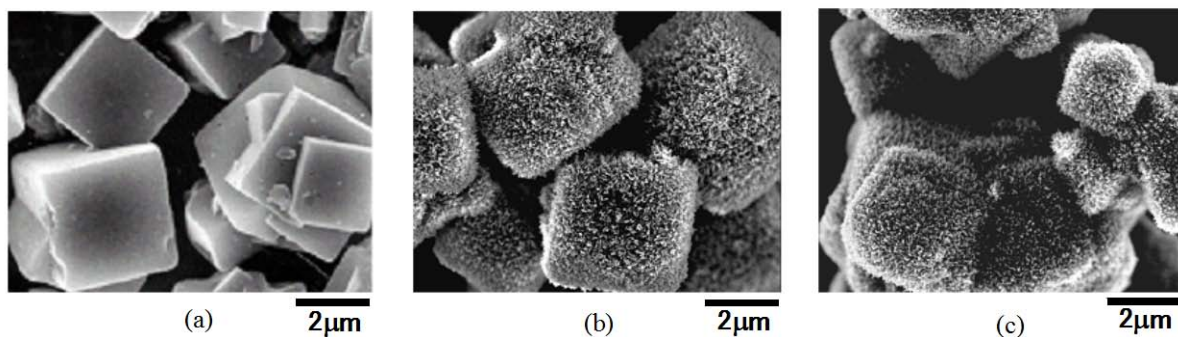


Fig. 5.6. SEM images of Ca-LTA (a), HAp-LTA (b) and HAp-LTA after mixing it in 10mM NaCl solution (c).

HAp thin layers synthesized on the LTA surface by hydrothermal treatments at different temperatures and durations in the reactions

5-9. INTRODUCTION

Zeolites consist of a three-dimensional open-framework structure composed of AlO_4 and SiO_4 tetrahedra linked together by oxygen sharing, and contain channels and cavities into which cations and water molecules diffuse, as well as functioning as ion-exchange sites.¹⁷ More than 100 different species of synthetic zeolites have been identified.¹⁸ Linde type A zeolite ($(\text{X}_{12/m})(\text{Si}_{12}\text{Al}_{12}\text{O}_{48})\cdot n\text{H}_2\text{O}$, X=cation, m=charge number, LTA) is the most useful among the zeolites due to highest cation exchange capacity (CEC).¹⁷ LTAs are widely used as an ion exchanger for ammonium and cadmium,^{2-3,19-20} and are considered to utilize them for the adsorption of radioactive elements, such as cesium and iodine.¹ Hydroxyapatite [$\text{Ca}_{10}(\text{PO}_4)_6(\text{OH})_2$, HAp] has a high CEC for cadmium and lead, and shows the high stability in an alkaline solution.⁴ These properties are suitable for adsorbents or materials to fix harmful elements by controlling the morphology and the amount of HAp on the LTA surface.

Several studies have succeeded in growing apatite crystals on the surfaces of wollastonite and alite for biological and medical applications.⁵⁻⁷ However, in these studies, the substances are self-destroyed in coating their surfaces with HAp. We have been focused on the preparation of multi-functional ceramic composites with the adsorption and/or fixation properties. In our previous studies, LTA with HAp thin layers were prepared by a hydrothermal treatment at 120°C for 8 hrs based on the basis of a cation exchange^{14,22}. The hydrothermal treatment did not destroy the cubic automorphism but changed its surface morphology by covering evenly with needle crystals of nano-HAp.

In this study, HAp thin layers were synthesized on the LTA surface by hydrothermal treatments at different temperatures and durations in the reactions. The crystal phases and morphologies of HAp grown on the LTA surface were evaluated by the powder X-ray diffraction method (XRD), scanning electron microscopy (SEM) and transmission electron microscopy (TEM). The yield was calculated from the weight changes of samples before and after the reactions. The specific surface areas and pore diameters were evaluated by the Brunauer-Emmet-Teller (BET) method.

5-10. EXPERIMENTAL

5-10-1. Preparation of LTA with Ca²⁺

LTA with Ca²⁺ (Ca-LTA) as a starting substance for hydrothermal treatments was prepared as follows. LTA with Na⁺ (Na-LTA) was purchased from Wako Pure Chemicals Industries, Ltd. The exchange of Na⁺ for Ca²⁺ was carried out by immersing 5.0 g of the Na-LTA in 1500 ml of a 0.5 M CaCl₂ solution for 24 hrs. The resultant sample was filtered with a membrane filter of 0.45 μm in pore size and rinsed with distilled water to remove excess cations. The Ca-LTA was then dried at 100°C for 24 hrs.

5-10-2. Synthesis of HAp crystals on the LTA surface

Hydrothermal treatments were conducted as follows. 0.3 g of the Ca-LTA powder was immersed in 20 ml of a 1 M (NH₄)₃PO₄ solution in a 100 ml Teflon cup fitted into a stainless steel pressure vessel. The pH value was controlled to 9 by the addition of an ammonium solution. The suspension was heated at different temperatures ranging from 25 to 200°C and duration ranging from 1 to 168 hrs. The samples were quenched and washed 3 times with distilled water, and dried at 100°C for 24 hrs. The Ca-LTA and the resultant samples after the hydrothermal treatments were investigated by XRD (Rigaku,

RINT2200) with monochromatized CuK α radiation at 40 kV and 40 mA. The morphology was observed by SEM (Hitachi S-5500) and TEM (Hitachi H-9500 operated at 300 kV). The yield was calculated from the weight changes of samples before and after the reactions.

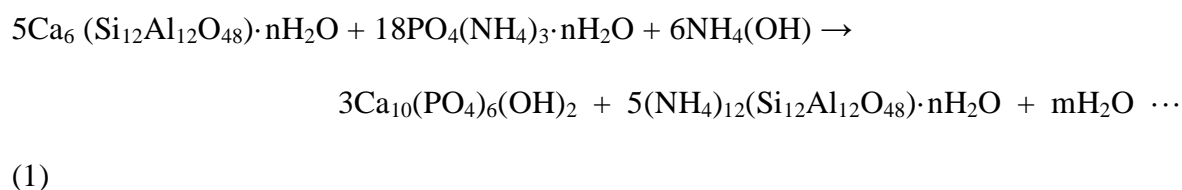
5-10-3. Specific surface areas measurement of LTA with HAp layers

The samples after the hydrothermal treatments were immersed in 1500 ml of a 0.5 M CaCl₂ solution for 24 hrs for the ion exchange of NH₄⁺ for Ca²⁺. The resultant samples were filtered with a membrane filter of 0.45 μ m in pore size and rinsed with distilled water to remove excess cations. The samples obtained were dried at 100°C for 24 hrs. 0.05 g of the samples and Ca-LTA obtained in the section 1.1 were degassed at 200°C for 3 hrs in vacuum. The specific surface areas and pore diameters were measured by the multipoint Brunauer-Emmet-Teller (BET) method using a Beckman Coulter SA3100 instrument with N₂ gas as an adsorbent.

5-11. RESULTS AND DISCUSSION

Fig. 5.7 shows the XRD patterns of Ca-LTA before and after the hydrothermal treatment at 120°C for the durations of 1-168 hrs. The Ca-LTA exhibited the complete exchange of Na⁺ for Ca²⁺ in LTA, which was judged from the change of diffraction intensities and the appearance of a new diffraction at 25.1 degrees in 2θ (Fig. 5.7a).⁹ After the hydrothermal treatment of Ca-LTA at 120°C for 4-168 hrs, broad diffractions at about 26° and 32° in 2θ were observed as indicated by solid circles, which corresponded to the diffractions from HAp. The other sharp diffractions in Fig 5.7b-f agreed with those of LTA replaced Ca²⁺ by NH₄⁺, indicating that the cation sites in the Ca-LTA were occupied by NH₄⁺ during the hydrothermal treatments as described by Matsumoto *et al.*¹⁰

The XRD patterns demonstrated that there was no significant difference in the full-width at half maximum intensity (FWHM) before and after the hydrothermal treatments until 72 hrs (Fig. 5.7c-e), but the shift of the diffractions of LTA with NH_4^+ ($\text{NH}_4\text{-LTA}$) and the increases of the FWHM were found at 168 hrs. The results of XRD indicate that the LTA structure is stable in a 1 M $(\text{NH}_4)_3\text{PO}_4$ solution heated at 120°C until 72 hrs, however the LTA structure starts to deteriorate at 168 hrs. The HAp thin layers were formed on the LTA surface after 4 hrs. The cation exchange model of Ca-LTA in the $(\text{NH}_4)_3\text{PO}_4$ solution can be described as the equation (1) and the yield of HAp after the hydrothermal treatments described as the equation (2):



$$\alpha = X/0.324W \dots (2)$$

If weight (W) g of LTA reacts perfectly in the $(\text{NH}_4)_3\text{PO}_4$ solution, the theoretical increase of the weight is 0.324 Wg. Therefore, the yield, α , can be calculated by the equation (2) using experimental data, where X is the weight increase of the formation of HAp at nominated durations and temperatures. Fig. 5.8 shows the change of the HAp yields after hydrothermal treatments of Ca-LTA at 120°C against various durations. The increase of α at 4hrs indicates the formation of HAp on the LTA surface, which was matched to the results of XRD measurements. The maximum value of α is 0.82 at 8 hrs, which is twentyfold larger than the value in the formation of HAp on alite.⁷ On the contrary, at 168 hrs, the α value was decreased because the dissolution of cations caused the destruction of the LTA structure.

Fig. 5.9 shows the XRD patterns of Ca-LTA before and after the hydrothermal

treatments at 25 to 200°C for 8 hrs. After the hydrothermal treatments, broad diffractions at about 26° and 32° in 2θ were observed as indicated by solid circles, which corresponded to the diffractions of HAp. The HAp crystals were grown at any synthetic temperatures. The other sharp diffractions in Fig 5.9b-f coincided with those of NH₄-LTA. These XRD patterns demonstrated that there was no significant difference in FWHM before and after the hydrothermal treatment at 25-160°C, but a decrease of the diffraction intensity and an increase in FWHM were found at 200°C. We thus conclude that the LTA structure is stable in the 1 M (NH₄)₃PO₄ solution heated at 25-160°C for 8 hrs but the structure starts to deteriorate at 200°C.

Fig. 5.10 shows the change of the HAp yields after the hydrothermal treatments of Ca-LTA for 8hrs against the various temperatures. The α values increased against the temperature range of 25-120°C but decrease against 160-200°C. The increase of α values was attributed to the formation of HAp and the decrease was corresponded to the destruction of LTA structures. The maximum α value at 120°C showed the homogeneous covering of HAp on the surface of LTA as shown in the next SEM image.

Fig. 5.11 shows the SEM images of Ca-LTA and those after the hydrothermal treatments at 25 to 200°C for 8 hrs. The morphology of the Ca-LTA before the treatments exhibited a cubic automorphism with smooth surface. The surface of the Ca-LTA heated at 25°C was covered by tiny ball-like HAp particles with the sizes of about 30 nm in diameter (Fig. 5.11b and g). This morphology was very similar to that of HAp formed in SBF.^{5-6, 21} The morphology of the Ca-LTA at 40°C showed tiny scaly HAp particles of about 80 nm in diameter (Fig. 5.11c and h). The Ca-LTA surface at 120°C was covered by needle-like HAp crystals of 100-200 nm in diameter (Fig. 5.11d and i). The morphology was very similar to that of HAp formed under same hydrothermal treatment.⁸ At 200°C

the amorphous-like particles were covered with the destroyed LTA (Fig. 5.11e and j), which corresponded with the XRD patterns shown in Fig. 5.9g.

TEM was applied to the observation of the interface between HAp and LTA. The TEM images as shown in Fig. 5.10 clearly indicated the HAp crystals of 30 nm in length grown on the LTA surface in the treatment at 40°C, and the complete covering of needle-like HAp crystals of up to 100 nm in length in the treatment at 120°C. In our previous study, the needle-like HAp crystals grew roughly perpendicular to the LTA surface from the SAED pattern.¹⁴

Moriyoshi *et al.* have discussed a formation mechanism of HAp on alite.⁷ According to their report, Ca^{2+} in the structure of alite released into a $(\text{NH}_4)_3\text{PO}_4$ solution reacts very rapidly with PO_4^{3-} to form further HAp crystals. Liu *et al.* have also reported a formation mechanism of HAp on wollastonite in a simulated body fluid (SBF).⁶ They discussed that Ca^{2+} released from wollastonite increase the ion activity of apatite in SBF, and hydrate silica on the surface of wollasonite provides the sites favorable for apatite nucleation. Consequently, the apatite nuclei are rapidly formed on the surface of wollastonite. The release of the Ca^{2+} was dependent on its solubility. However, in our study, the reaction of Ca-LTA with ammonium phosphate is the ion exchange model shown in equation (1). The exchange of Ca^{2+} on LTA for NH_4^+ in a $(\text{NH}_4)_3\text{PO}_4$ solution is a driving force of the formation of HAp, and then the discharged Ca^{2+} react with phosphate ions on the surface of LTA due to Ca supersaturation at local area. The reaction of HAp formation in the previous study was related to the number of calcium dissolution from alite. For this reason, the yield (maximum $\alpha=0.04$) for HAp formation are smaller than that (maximum $\alpha=0.82$) of LTA in this study. Furthermore, these substrates were self-destroyed in the reactions to form HAp. But in this study, the reaction of HAp formation was occurred by

ion exchange reaction in the equation (1). In particular, this reaction was considerably occurred in ammonium phosphate solution for high NH_4^+ selectivity of LTA. The Ca^{2+} ions in Ca-LTA were almost involved in the formation of HAp crystals on the surface of LTA.

The specific surface areas of Ca-LTA and samples synthesized from 25 to 200°C were shown in Table.5.3. The specific surface areas of samples synthesized at 25 and 40°C for 8 hrs were almost same as compared with that of Ca-LTA, and the pore diameter (0.88nm) also were almost constant. These results mean that pores in LTA are completely maintained at the conditions. These nanocomposites obtained are useful for the simultaneous adsorbent that has characteristics of LTA and HAp. At hydrothermal treatment at over 80°C, the specific surface areas of samples decreased with increase of temperature. These results means that the pores in LTA are partially covered by HAp thin layers. The materials were promising as material for encapsulate harmful ions or radioactive ion absorbed in LTA.

5-12. CONCLUSIONS

We successfully obtained the nanocomposite, HAp coated LTA by a new concept which applied an ion exchange reaction. The ion exchange of Ca^{2+} on LTA for NH_4^+ in an ammonium phosphate solution is a driving force of the formation. The structure of LTA was not destroyed by the hydrothermal treatment at 25-160°C for 8 hrs and also at 120°C for 1 to 72 hrs. The yield of LTA with HAp thin layers synthesized at 120°C for 8hrs showed maximum value of 0.82. The specific surface area was maintained in the treatment at 25 and 40°C for 8 hrs as compared with that of Ca-LTA, but over 80°C, the value decreased with an increase of temperature. These nanocomposites obtained are

novel materials for the simultaneous adsorption and capsulation of both harmful and radioactive ions, which has the excellent characteristics of both zeolite and hydroxyapatite.

Table. 5.3 The concentration of dissolved cations from HAp-LTA (mmol/l) and the amount of adsorbed sodium (mmol/l) in NaCl solutions.

Samples	Specific surface area (m ² /g)
Ca-LTA	591.0
LTA25	548.6
LTA40	584.8
LTA80	223.5
LTA120	148.5
LTA160	128.9
LTA200	31.1

Ca-LTA treated at 25°C, 40°C, 80°C, 120°C, 160°C and 200°C are shown as LTA25, LTA40, LTA120, LTA160 and LTA200, respectively.

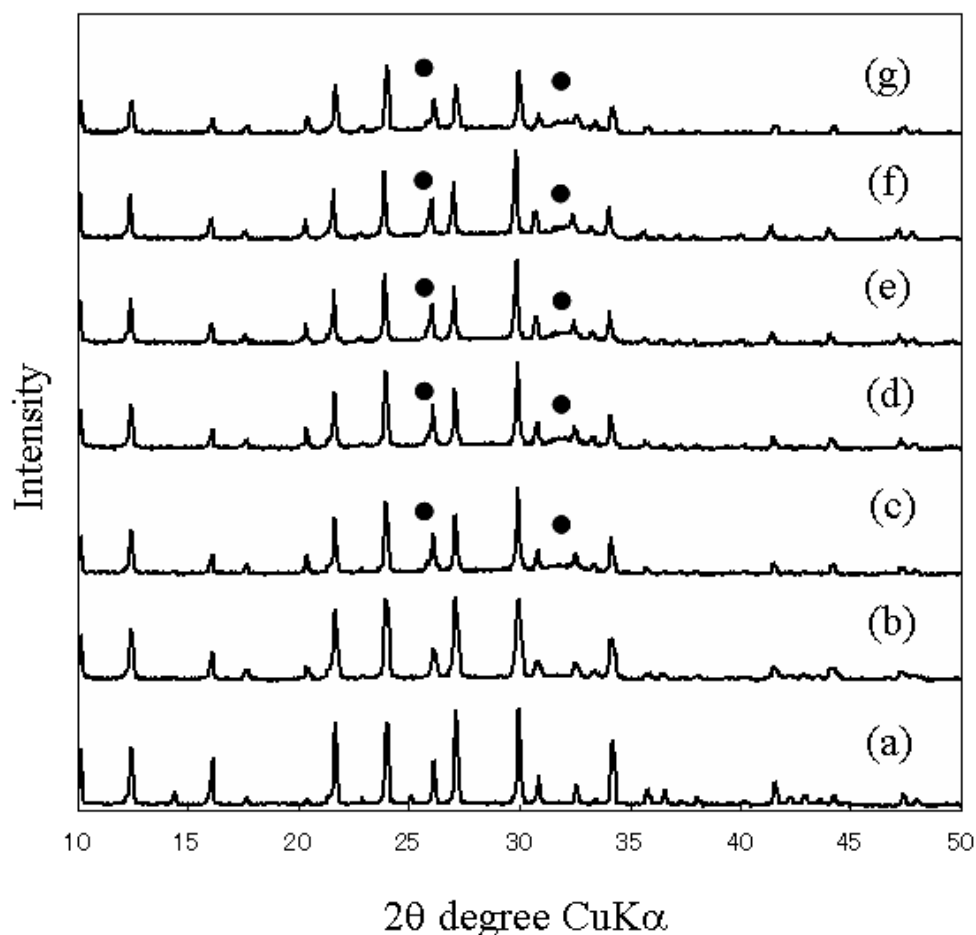


Fig. 5.7. XRD patterns of (a) Ca-LTA and LTAs after the hydrothermal treatments at 120 °C for (b) 1hrs, (c) 4 hrs, (d) 8hrs, (e) 24 hrs, (f) 72hrs and (g) 168 hrs. All diffractions in (a) are attributed to Ca-LTA. The solid circles indicate the diffractions from HAp. The other diffractions in (b-g) are attributed to NH_4 -LTA.

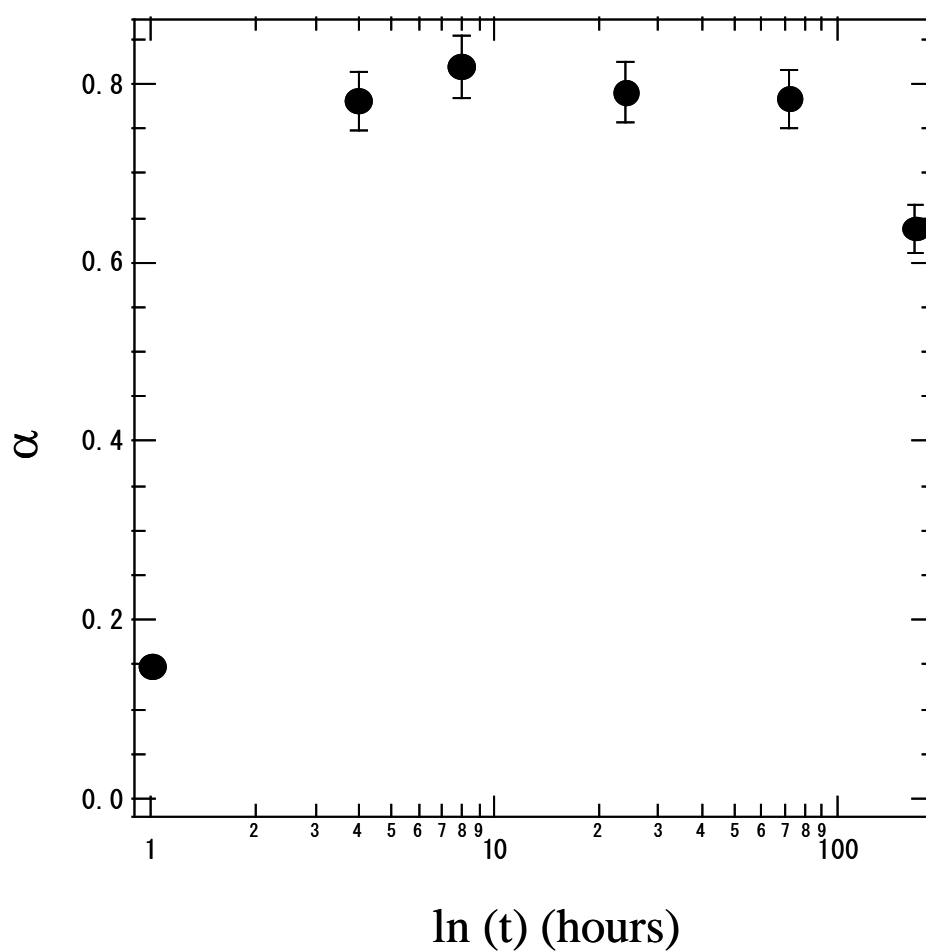


Fig. 5.8. The change of the HAp yields after hydrothermal treatments of Ca-LTA at 120°C against various durations.

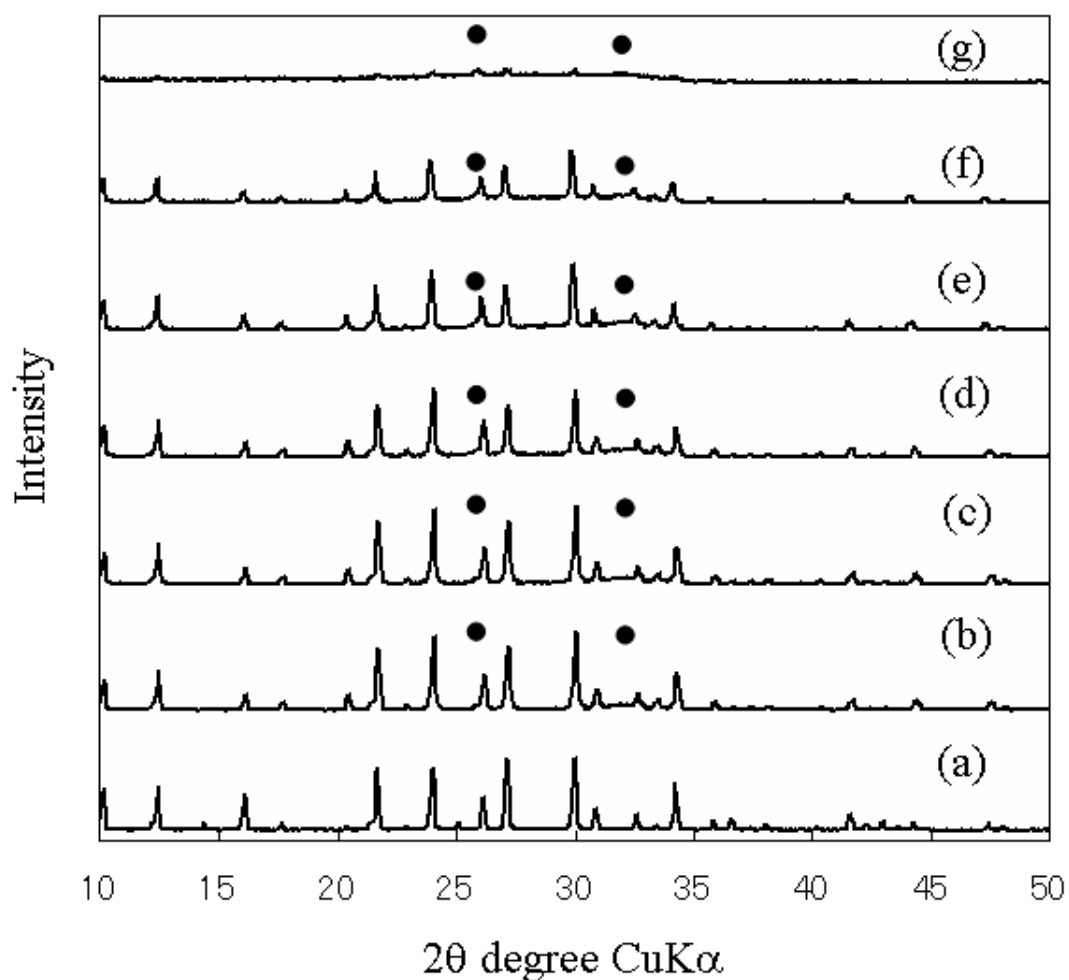


Fig. 5.9. XRD patterns of (a) Ca-LTA and LTAs after the hydrothermal treatments at (b) 25°C, (c) 40°C, (d) 80°C, (e) 120°C, (f) 160°C and (g) 200°C for 8 hrs. All diffractions in (a) are attributed to Ca-LTA. The black circles indicate the diffractions from HAp and the other diffractions in (b-g) are attributed to NH₄-LTA.

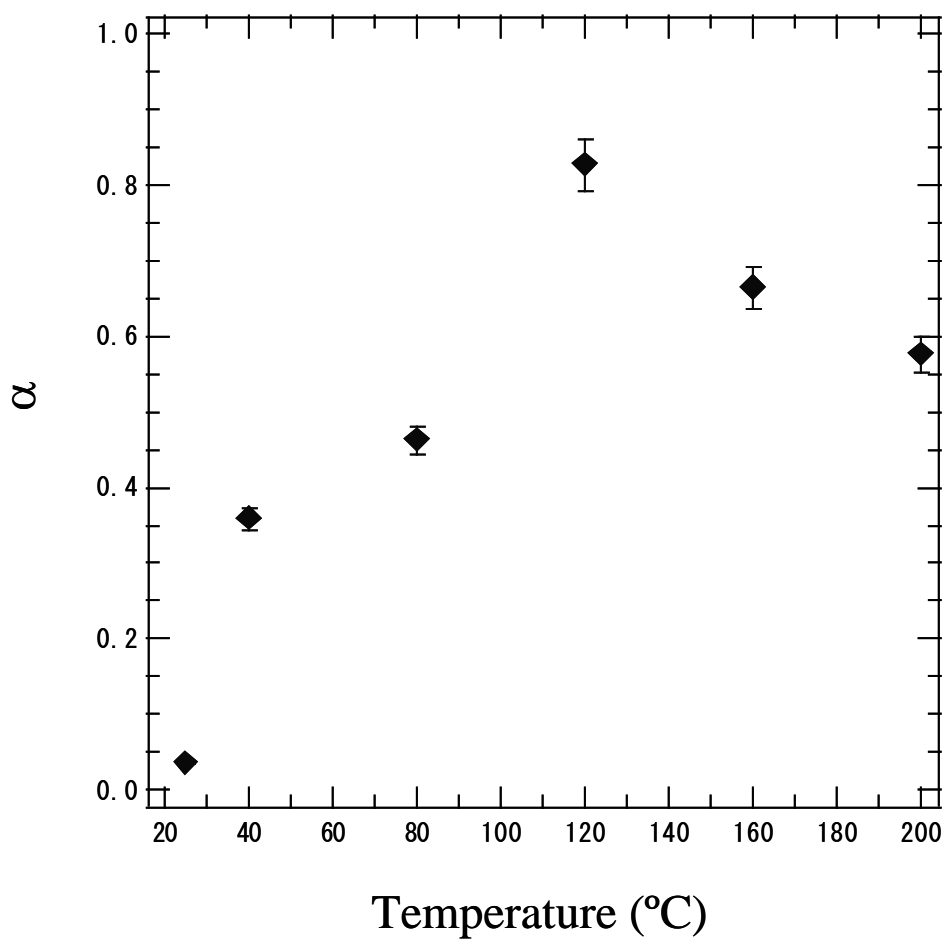


Fig. 5.10. The change of the HAp yields after the hydrothermal treatments of Ca-LTA for 8hrs against the various temperatures.

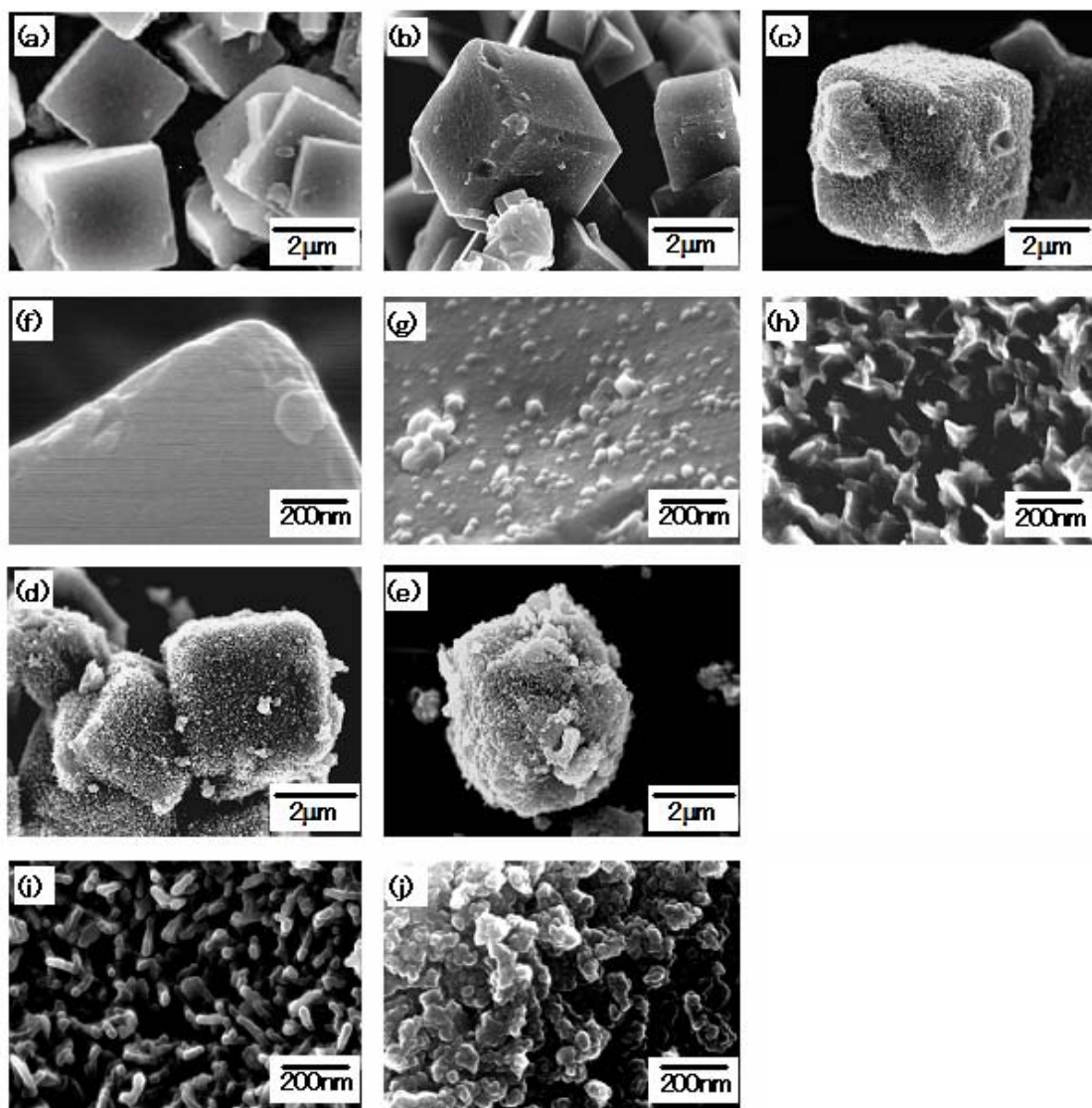


Fig. 5.11. SEM images of Ca-LTA (a, f) and LTAs after the hydrothermal treatments at various temperatures for 8 hrs; (b, g) 25°C, (c, h) 40°C, (c, h) 120°C, (d, i) 160°C and (e, j) 200°C.

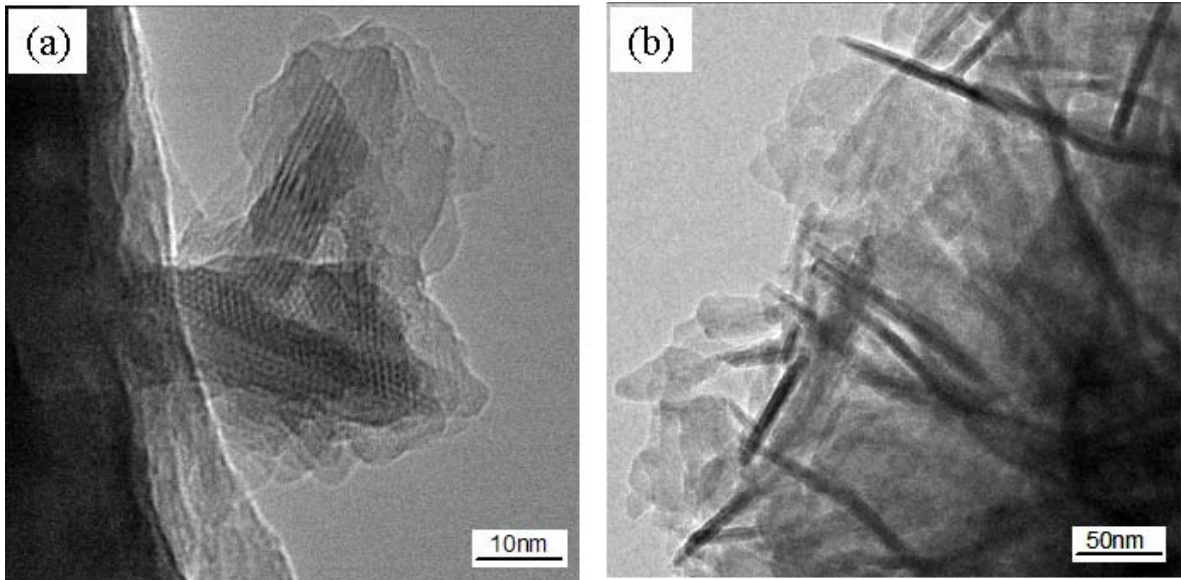


Fig. 5.12. The TEM images of Ca-LTA after the hydrothermal treatments at (a) 40 °C and (b) 120 °C for 8 hrs.

5-13. REFERENCES

- 1) K. C. Song, H. K. Lee, H. Moon and K. J. Lee, *Sep. Purif. Technol.*, 12[3], 215 (1997).
- 2) Y. Watanabe, H. Yamada, H. Kokusen, J. Tanaka, Y. Moriyoshi and Y Komatsu, *Sep. Sci. Technol.*, 38[7], 1519(2003).
- 3) H. Mimura and K. Akiba, *J. Nucl. Sci. Technol.*, 30[5], 436(1993).
- 4) E. C. Moreno, M. Kresak and R. T. Zaharadnik, *Nature*, 24[5435], 64(1974).
- 5) X. Y. Liu, and C. X. Ding, *Mater. Lett.*, 57[3], 652(2002).
- 6) X. Y. Liu, C. X. Ding, and Z. Y. Wang, *Biomaterials*, 22[14], 2007(2001).
- 7) Y. Moriyoshi, Y. Chiba, H. Monma and T. Ikegami, *Trans. Mater. Res. Soc. Jpn.*, 25[4], 1143(2000).
- 8) Y. Fujishiro, H. Yabuki, K. Kawamura, T. Sato and A. Okuwaki, *J. Chem. Technol. biotechnol.*, 57[4], 349(1993).
- 9) D. W. Breck, W. G. Eversole, R. M. Milton, T. B. Reed and T. L. Thomas, *J. Am. Chem. Soc.*, 78, 5963(1956).
- 10) T. Matsumoto, Y. Goto and K. Urabe, *J. Ceram. Soc. Jpn.*, 103[1], 93(1995).
- 11) D. W. Breck, in *Zeolite Molecular Sieves*. Eds. Wiley, New York, 352, 1958.
- 12) K. Sonoda, T. Furuzono, D. Walsh, K. Sato and J. Tanaka, *Solid State Ion.*, 151[1-4], 321(2002).
- 13) K. Sato, T. Kogure, Y. Kumagai, J. Tanaka, *J. Colloid Interface Sci.*, 240[1],

- 133(2001).
- 14) Y. Watanabe, Y. Moriyoshi, T. Hashimoto, Y. Suetsugu, T. Ikoma, T. Kasama, H. Yamada, and J. Tanaka, *J. Am. Ceram. Soc.*, 87, 1395(2004).
- 15) D. H. Bollman and D. M. Mortimore, *Anal. Chem.*, 43, 154(1971).
- 16) E. M. Flanigen, H. Khatami, and H. A. Szymanski, *Molecular Sieve Zeolite*, Eds. Advan. Chem. Ser., 101, American Chemical Society, Washington, D. C., 201(1971).
- 17) D. W. Breck, In *Zeolite Molecular Sieves*, Eds. D. W. Breck. Wiley, New York, 1(1974).
- 18) W. M. Meier, D. H. Olson, and C. Baerlocher, *Zeolites.*, 17, 1(1996).
- 19) Y. Watanabe, H. Yamada, J. Tanaka, Y. Komatsu and Y. Moriyoshi, *Sep. Sci. Technol.*, 39, 2091(2004).
- 20) Y. Watanabe, H. Yamada, H. Kokusen, J. Tanaka, Y. Moriyoshi, and Y. Komatsu, In *Proceedings of The 18th International Japan-Korea Seminar on Ceramics*, 543(2001).
- 21) P. Siriphannon, Y. Kameshima, A. Yasumori, K. Okada, and S. Hayashi, *J. Eur. Ceram. Soc.*, 22, 511(2002).
- 22) Y. Watanabe, Y. Moriyoshi, T. Hashimoto, T. Kasama, Y. Suetsugu, T. Ikoma, H. Yamada, and J. Tanaka, In *Proceedings of The 20th International Japan-Korea Seminar on Ceramics*, 213(2003).

CHAPTER 6

THE DENSIFICATION OF ZEOLITE/APATITE COMPOSITES USING A PULSE ELECTRIC CURRENT SINTERING METHOD

6-1. INTRODUCTION

High-level radioactive elements, such as cesium, strontium and iodine, are discharged in the processes of nuclear power generation and nuclear reprocessing. These levels are controlled by legislation on discharge limits in many countries. It is thus important to develop long-term assurance materials for adsorbing, fixing and preserving radioactive elements over a long period of time. More than 100 different species of synthetic zeolites have been identified.¹ Zeolites consist of a three-dimensional open-framework structure composed of AlO_4 and SiO_4 tetrahedra linked together by oxygen sharing with a three-dimensional open framework. The cations and water molecules diffuse through the channels and cavities as ion-exchange sites. Of the synthesized zeolites, Linde type-A zeolite ($(\text{X}_{12/n})(\text{Si}_{12}\text{Al}_{12}\text{O}_{48})\cdot 24\text{H}_2\text{O}$, X=cation, n=cation valence, LTA) with α - and β -cages has the highest cation exchange capacity (CEC).² Therefore, LTA is widely used as an adsorbent for harmful and radioactive elements.³⁻⁷ Hydroxyapatite ($\text{Ca}_{10}(\text{PO}_4)_6(\text{OH})_2$, HAp) has a very low solubility of 5.4×10^{-119} (K_{sp} ; $\text{mol}^{18}\text{l}^{-18}$) at a neutral pH solution, and shows high stability in an alkaline solution. Furthermore, the K_{sp} of fluorapatite ($\text{Ca}_{10}(\text{PO}_4)_6\text{F}_2$, FAp) is 8.1×10^{-121} , which is lower than that of HAp.⁸ The HAp and/or FAp sintered bodies have been studied as one of long-term assurance matrices for preserving the radioactive elements.⁹ Fabrication of dense HAp sintered bodies has been described by many researchers in which the spherical HAp particles improve sinterability.¹⁰⁻¹³

In our previous studies^{14, 15}, LTA with HAp thin layers was prepared by hydrothermal method in the cation exchange processes of Ca^{2+} to NH_4^+ . This treatment did not destroy the cubic automorphism but changed its surface morphology by covering completely with nano-HAp scaly particles. We expect that the HAp thin layers play an important role for improving the affinity between FAp as matrix and zeolite in a sintering process.

In this study, the sintered bodies of LTA with HAp thin layers and FAp were fabricated by using the pulse current sintering (PECS) method. The composites were characterized by XRD, SEM and STEM. The microstructure and mechanical properties of the sintered bodies were elucidated by using the dynamic-ultra-microhardness tester and universal tester.

6-2. EXPERIMENTAL METHODS

6-2-1. Preparation of LTA with Ca²⁺ and HAp thin layers on its surface

LTA powder (<200 meshes) with Na⁺ (Na-LTA) was purchased from Wako Pure Chemicals, Ltd., Japan. The complete cation exchange of Na⁺ for Ca²⁺ was carried out by reacting 5.0g of Na-LTA in 500ml of 0.5mol/l CaCl₂ solution for 1 hrs. This process was repeated three times. The resultant solid was isolated with a membrane filter of 0.45 μm in pore size, and washed with distilled water to remove excess cations. The LTA with Ca²⁺ (Ca-LTA) was obtained after dried at 100°C for 24 hrs. The Ca-LTA powder with the complete exchange of Na⁺ for Ca²⁺ in LTA was obtained, judged from the change of diffraction intensities and the appearance of a new diffraction at 25.1 degree in 2θ by XRD. The hydrothermal treatment was conducted as follows. 1.0 g of Ca-LTA powder was immersed in 20 ml of 1.0 mol/l ammonium phosphate ((NH₄)₃PO₄) solution in a 100 ml teflon cup fitted into a stainless-steel pressure vessel. The pH value of the solution was adjusted to 9 by adding an ammonium solution. The sample was heated at 120°C for 8 hrs and quenched, washed 3 times with distilled water and dried at 100°C for 24 hrs. The samples were characterized by X-ray diffractometer (XRD, Rigaku RINT2200, Japan) and scanning electron microscope (SEM, Jeol, JSM-5600LV, Japan).

6-2-2. Synthesis of spherical FAp powder

6.0 mol/l of H₃PO₄ solution and 2.0 mol/l of HF solution was mixed and aged for 1 day

in N₂ gas. The mixed solution was dropped slowly into 10.0 mol/l Ca(OH)₂ suspension with vigorous stirring at room temperature. The molar ratio of Ca²⁺, PO₄³⁻ and F⁻ was adjusted to 10, 6 and 2. The resultant mixture was then aged for 1 day, and the final pH was about 7.0. Spherical FAp powder was fabricated by a spray dryer (DL-41, YAMATO Sci. Co., Ltd, Japan(Fig.6.1)). The suspension was atomized under a pressure of 1.5 MPa at a flow rate of 500 ml/hrs, and inlet and outlet temperatures of a nozzle were adjusted to 180 and 80°C, respectively. The spray-dried FAp powder was calcined at 800°C for 3 hrs to increase the crystallinity. The resultant sample was characterized by XRD and SEM.

6-2-3. Fabrication of LTA with HAp thin layers/FAp sintered bodies

The LTA with HAp thin layers and the spherical FAp powder were mixed at a weight ratio of 3/7. The obtained powder was sintered by using a pulse electric current sintering method (PECS, Sumitomo Coal Mining, SPS-1030, Japan, (Fig.6.2)). The sample was pressed uniaxially at 50 MPa in the vacuum of 0.6×10^{-2} Pa throughout the sintering process. The temperature was increased to 900°C at a rate of 50°C/min. After keeping at 900°C for 10 min, the sample was slowly cooled to 600°C at a rate of 5°C/min. The sample was cooled further to room temperature after stopping the electric current and releasing the pressure. The sintered bodies with 20 mm in diameter and 4 mm in thickness were characterized by using XRD and SEM after polishing. The element mapping analyses were carried out with an energy dispersive X-ray spectrometer (EDX, Jeol, JRD2200, Japan) equipped with SEM.

The boundary structure in the sintered body with three different phases, i.e. LTA, HAp

and FAp, was observed by a scanning transmission electron microscope (STEM, Hitachi, HF2210, Japan). The element in the boundary structure was analyzed by an energy dispersive X-ray spectrometer (EDX, Genesis4000, USA). The specimen with 100 nm in thickness was prepared by a focused ion beam method (FIB, Noran Vantage: FB-2100, USA) and a pick-up method.

The microhardness of the sintered bodies was measured with a dynamic-ultra-microhardness tester (Shimadzu, DUH-W201, Japan). The three-point bending strength and Young's moduli were measured using a universal tester (Shimadzu, AGS-H, Japan) with a crosshead speed of 1mm/min. The size of the sample was 18×3×1 mm and the number of samples for bending strength and Young's moduli measurement was five. The measurements were conducted 3 times to give the average values.

6-3. RESULTS AND DISCUSSION

6-3-1. Characterization of Ca-LTAs and spherical FAp

The broad diffractions at about 26° and 32° in 2θ were found after the hydrothermal treatment of Ca-LTA, which were corresponded closely to the diffractions of HAp.¹⁴

Fig. 6.3 shows SEM image of the resultant LTA after the hydrothermal treatment. The hydrothermal treatment did not destroy the cubic automorphism but changed its surface morphology by complete covering with scaly particles. The scaly particles were aggregates of needle-like HAp crystals and formed HAp thin layers. We previously studied the

morphological details of HAp nanocrystals on the zeolite surface.^{14, 15}

Fig. 6.4 shows the SEM image of FAp powder obtained by the spray dryer and calcined at 800°C for 3hrs. The FAp powder was spherical in shape, and the particle size was about 1-10 µm. The XRD pattern showed only diffractions of FAp. Calcination at 800°C was necessary to increase the crystallinity of FAp. This powder was employed for the starting material of the PECS method.

6-3-2. Characterization of LTA with HAp coating layers/FAp sintered bodies

Fig.6.5 shows the XRD pattern of the sintered body of LTA with HAp thin layers and FAp. The XRD pattern identified only FAp phase, which is explained by a phase change of LTA to amorphous by the PECS method. From the results of XRD and Fourier-transform infrared spectroscopy, we confirmed that the Ca-LTA after hydrothermal treatments almost changed to LTA with NH_4^+ ($\text{NH}_4\text{-LTA}$).¹⁴ Chandrasekhar *et al.* reported that the $\text{NH}_4\text{-LTA}$ calcined at 850°C had an amorphous structure whereas the structure remained intact at 750°C, and mullite started crystallizing at 950°C.¹⁶ In the present study, the temperature increased to 900°C at a heating rate of 50°C/min and held for 10 min. The heating rate and holding time were much less than the rate of 3°C/min and 3 hrs in a furnace described by Chandrasekhar *et al.*¹⁶ We conclude from these results that the LTA in the sintered bodies changes to an amorphous phase under the sintering condition. Therefore, the diffraction pattern of LTA in the sintered bodies was not detected by XRD.

Fig. 6.6a shows the SEM image of the surface of sintered bodies, and Fig. 6.6b-e shows

EDX mapping results of the Si, Al, P and Ca elements. The sintered body was well densified, and the grains were very small ($<1\ \mu\text{m}$). There is no significant difference in the crystal morphology of FAp and LTA. Thus, the elemental mapping analyses of Si, Al, Ca and P on the surface of the sintered body were useful to distinguish the components. The main components of LTA were Si and Al, which located in the same positions in their distribution. The particle size of the amorphous parts was about $5\ \mu\text{m}$ that corresponds with that of LTA with HAp thin layers as shown in Fig. 6.3. The Ca and P were distributed in the same positions, which were the main component of FAp and HAp. These results indicated that the amorphous phase was completely covered by FAp and HAp. The HAp thin layers on LTA surface play an important role for preventing the binding among zeolite powders. Fig. 6.7 shows the STEM image of the sintered body of LTA with HAp thin layers and FAp. The HAp thin layers were clearly observed at the interface between amorphous LTA and FAp. The shape and size of HAp thin layers were needle-like crystals about $150\ \text{nm}$ in length. The size was almost matched to that of HAp grown on the surface of LTA as shown in Fig. 6.3. The FAp crystals in the sintered bodies were well sintered, and the grain size was small ($<300\ \text{nm}$). Micropores were not observed among the three different phases. It indicates that the three different phases are completely sintered, and the HAp layers play an important role for improving the affinity between FAp and amorphous LTA. When the mixed powder of LTA and FAp without HAp thin layers was sintered under the same condition, the sintered bodies obtained were with cracks and/or destroyed in

ejecting. Fig. 6.8 shows the mapping images obtained by EDX equipped with STEM. Si and Al were distributed in the position of amorphous LTA, and P was distributed in the positions of HAp and FAp. Ca was distributed mainly in the positions of FAp and HAp, but the distribution was less dominant in the position of LTA. These results indicate that Ca ions barely remain in the LTA, which correspond with those obtained by EDX analyses as shown in Fig. 6.6.

6-3-3. Mechanical properties of LTA with HAp coating layers/FAp composites

Fig. 6.9 shows optical microscope images of indentations of pyramidal indenters (115°) on LTA (a), FAp (b) and the interface between LTA and FAp (c) on the sintered bodies. Table 6.1 shows the load (P_G :gf), depth (D : μm) and dynamic hardness (DH) calculated from indentations. The DH in a pyramidal indenter is defined by the following formula: $DH = 37.838 P_G/D^2$. The DH of FAp was 612, which was larger than those of amorphous LTA (a) (DH=448) and the interface (c) (DH=441). We considered that the LTA changed to an amorphous phase is weak in strength, and the interface between the phase and FAp is similarly weak in strength.

The average three-point bending strength was 54 MPa, and the Young's modulus was 30 GPa which was considerably lower than that of FAp sintered bodies (three point bending strength: 162 MPa, Young's modulus: 85 GPa). These results indicate that the interface between an amorphous LTA and FAp is similarly weak in strength.

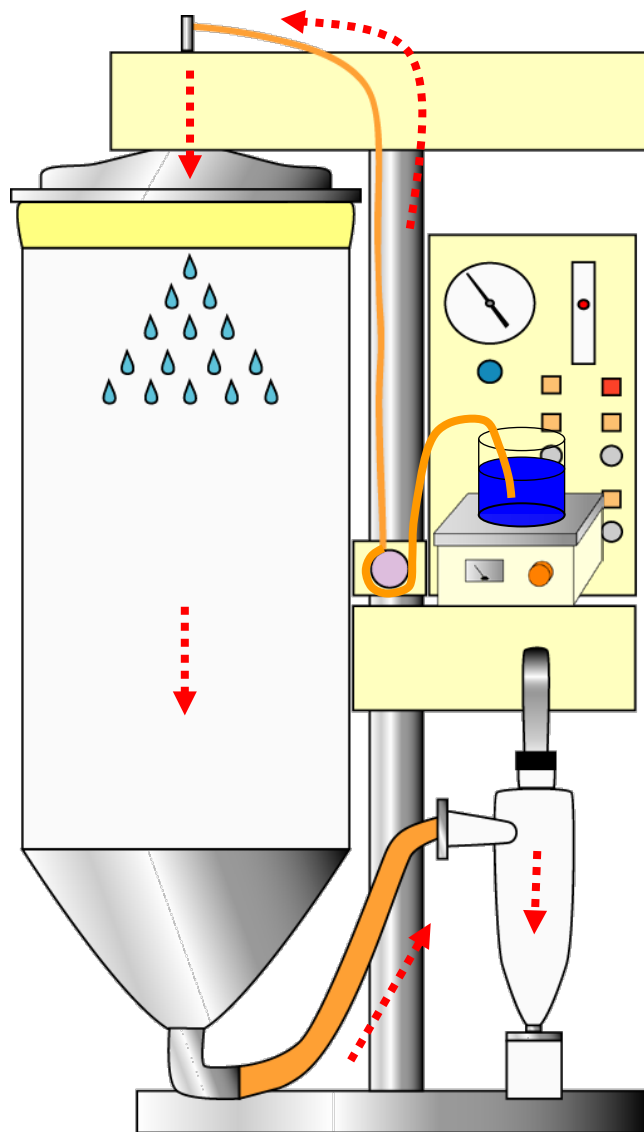
6-4. CONCLUSION

The fabrication of sintered body of LTA with HAp thin layers and FAp was succeeded by using the PECS method at 900°C. The LTA phase changed to an amorphous phase under this condition. The amorphous LTA in the sintered bodies was completely surrounded by HAp and FAp. The microstructural observations indicated that the three different phases (the amorphous LTA, HAp and FAp) were completely sintered. The HAp thin layers played an important role for improving the affinity between FAp and LTA in sintering. The microhardness of the amorphous LTA and the interface of amorphous LTA and FAp were lower than that of FAp, and three point bending strength was also lower than that of FAp. The sintered bodies of LTA with HAp thin layers and FAp are a promising material as a long-term assurance material for the disposal of radioactive waste.

Table 6.1. The load, depth and dynamic hardness calculated from indentations of FAp and HAp and the interface.

	P_G (gf)	D (μm)	DH
FAp	20	1.11	612
LTA	20	1.31	448
Interface	20	1.30	441

P_G : Load, D: Depth DH: Dinamic Hardness



EXPERIMENTAL CONDITIONS

Pressurre : 1.5 MPa at a
Flow rate : 500 ml/hrs
Inlet temperature : 180 °C
Outlet temperature : 180 °C

Fig. 6.1. Spray Dryer (DL-41, YAMATO Sci. Co., Ltd, Japan.)

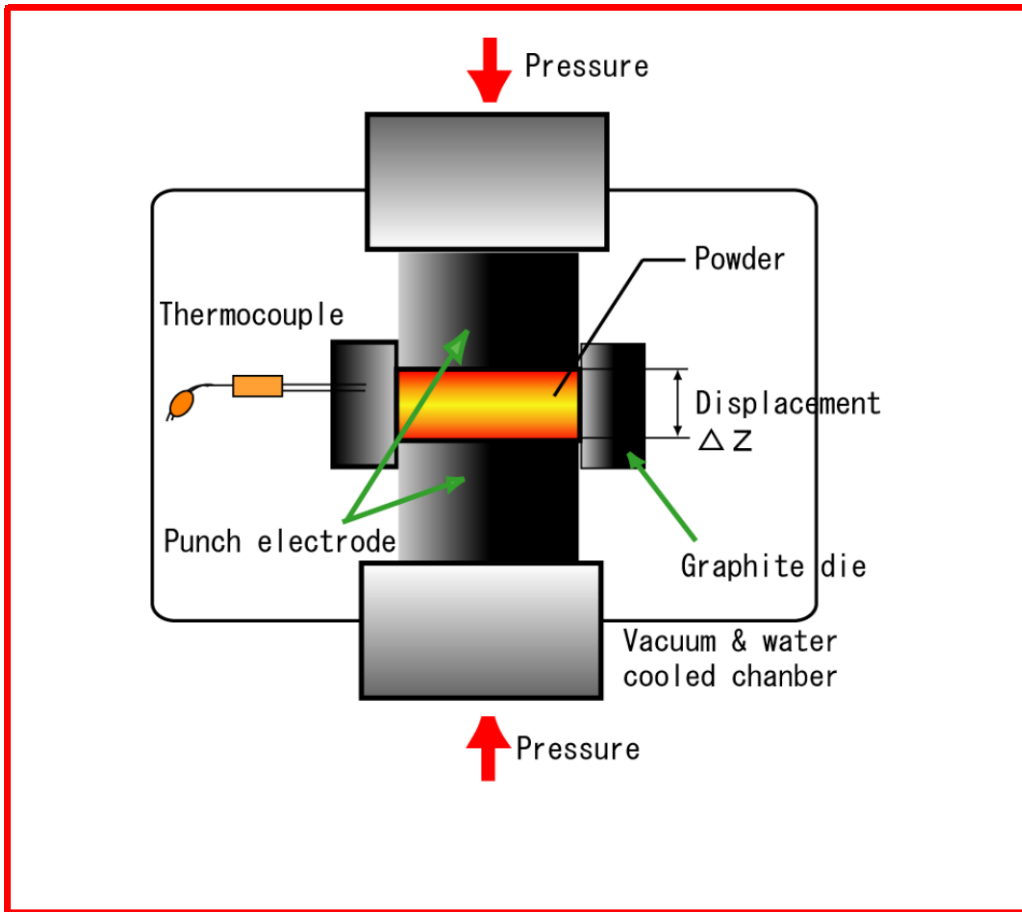


Fig.6.2 The pulse electronic current sintering system

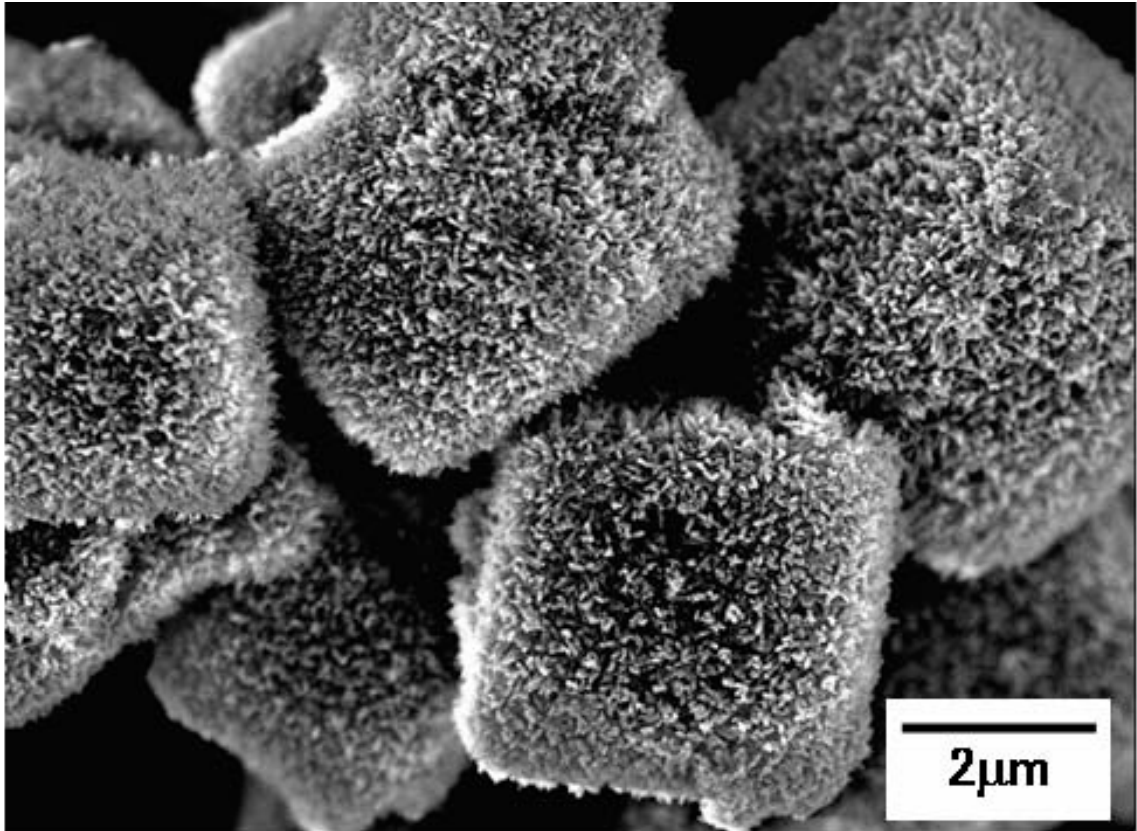


Fig. 6.3. The SEM image of LTA with HAp thin layers prepared by the hydrothermal treatment at 120°C.

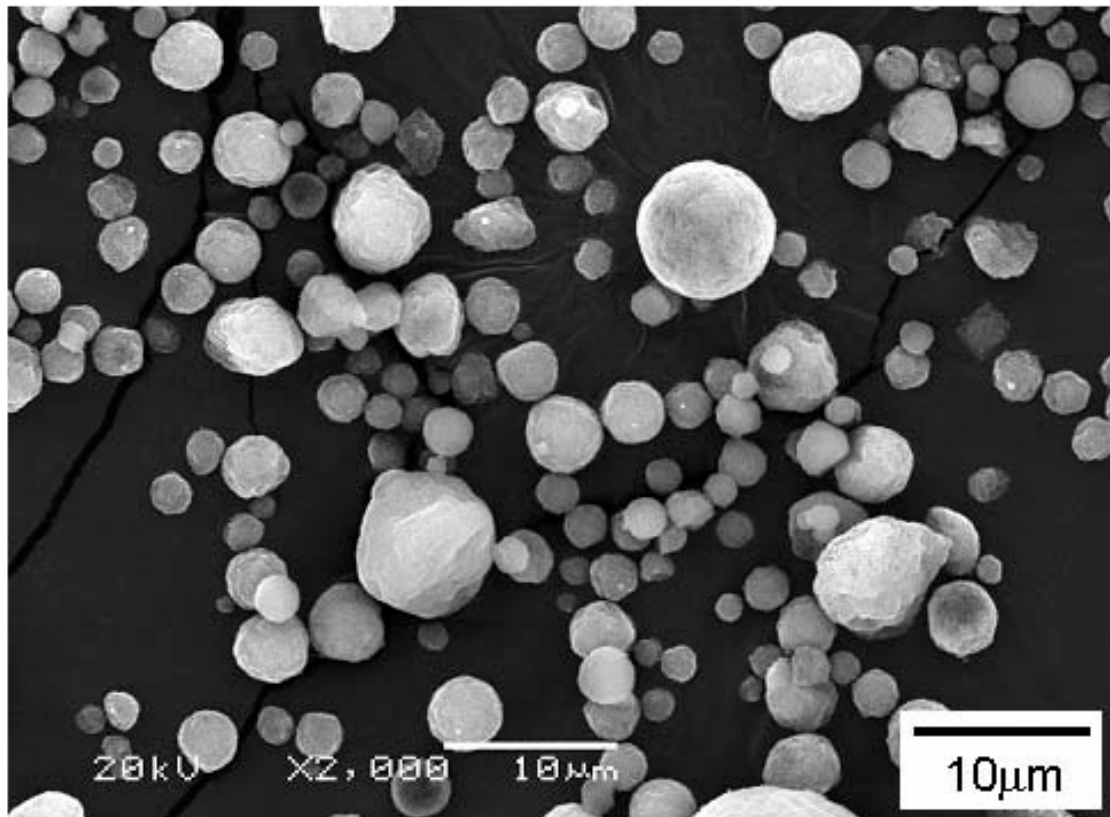


Fig. 6.4. The SEM image of spherical FAp particles prepared by the spray dryer.

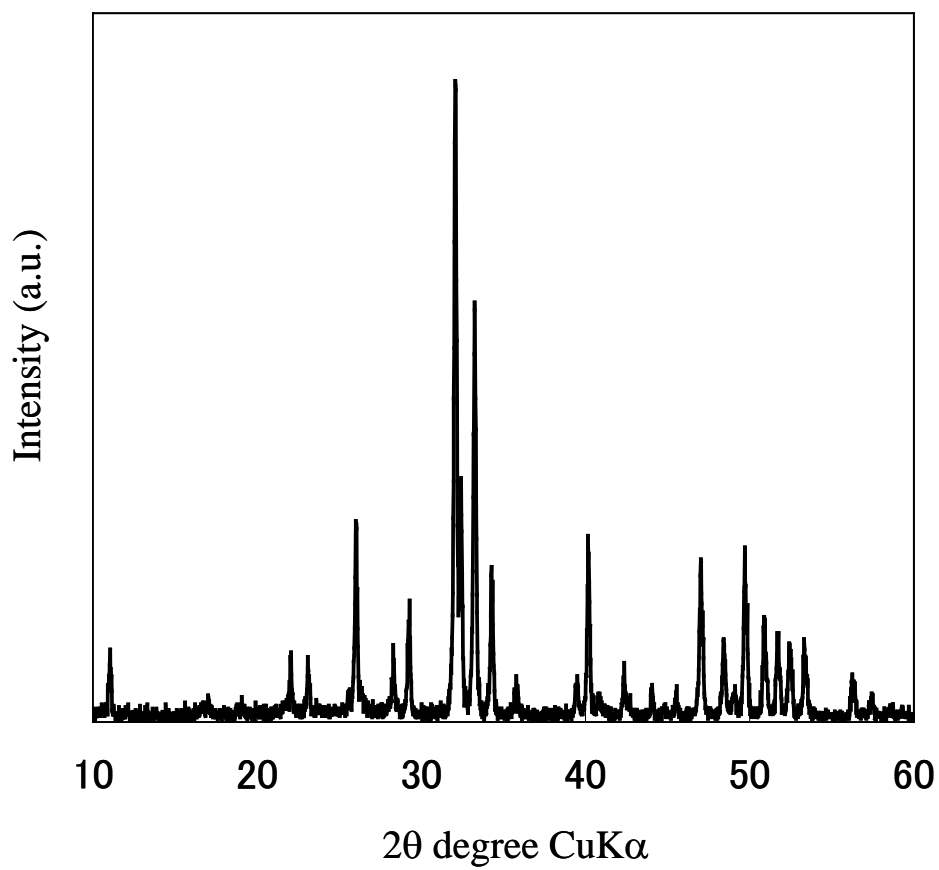


Fig. 6.5. The XRD patterns of the sintered body obtained at 900°C.

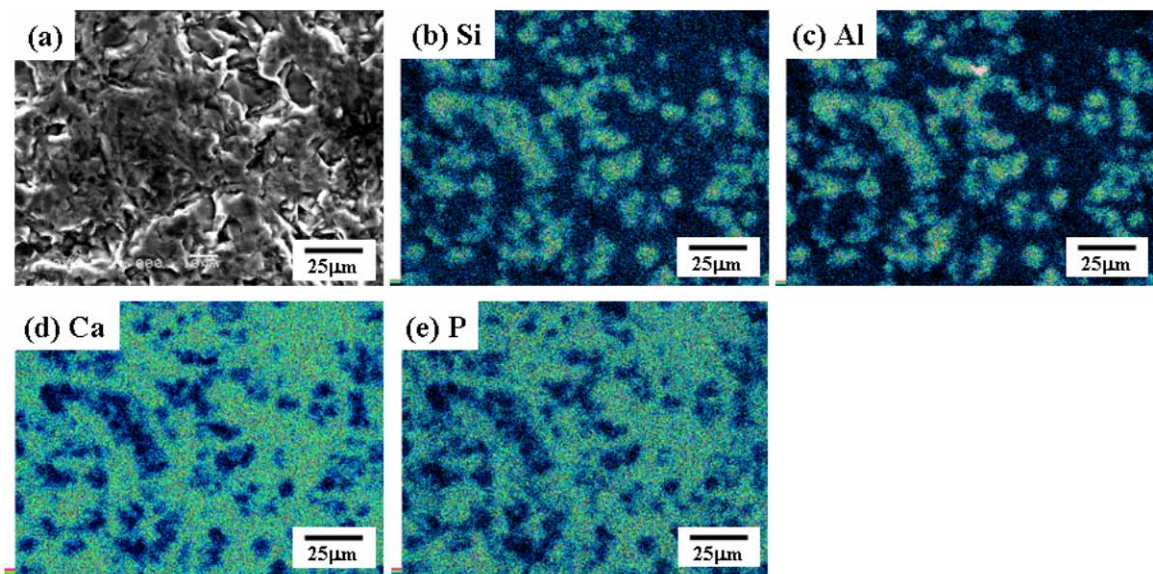


Fig. 6.6. The SEM image (a) and EDS mappings (Si (b), Al (c), Ca (d) and P (e)) of the sintered body obtained at 900°C by PECS.

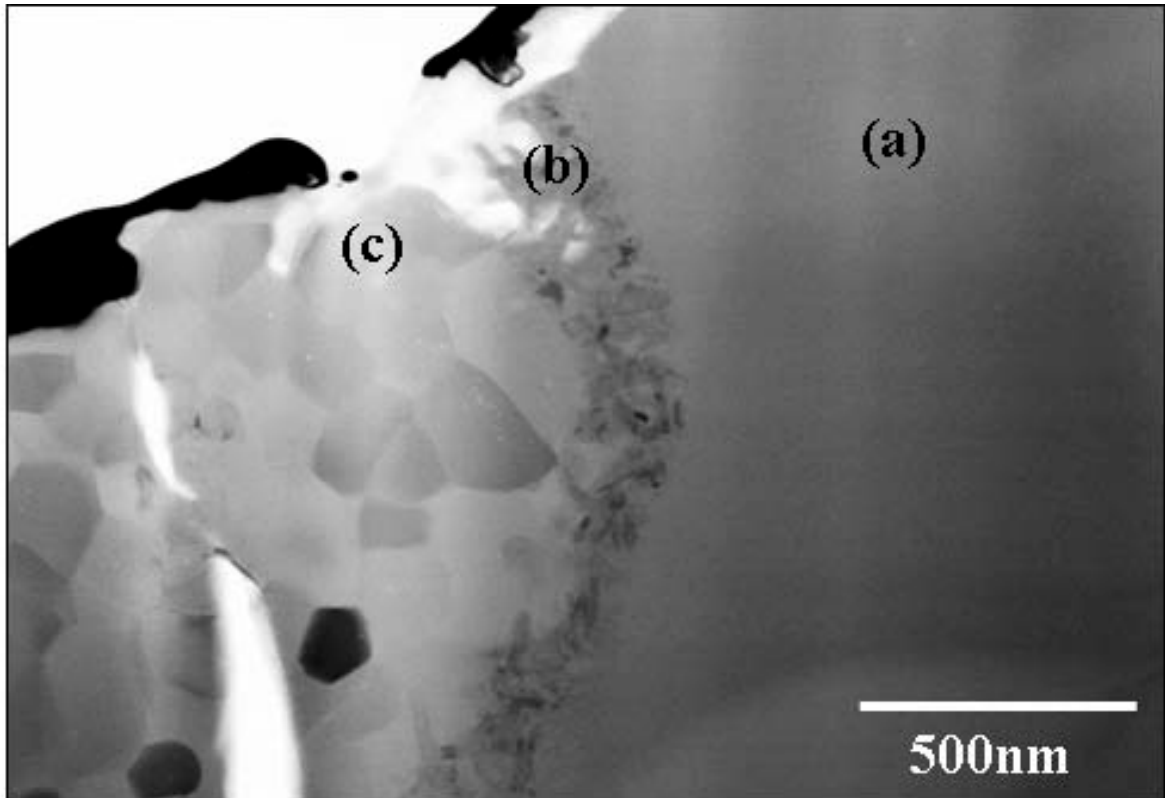


Fig. 6.7. The STEM image (a) and EDS mappings (Si (b), Al (c), Ca (d) and P (e)) of the sintered body obtained at 900°C by PECS.

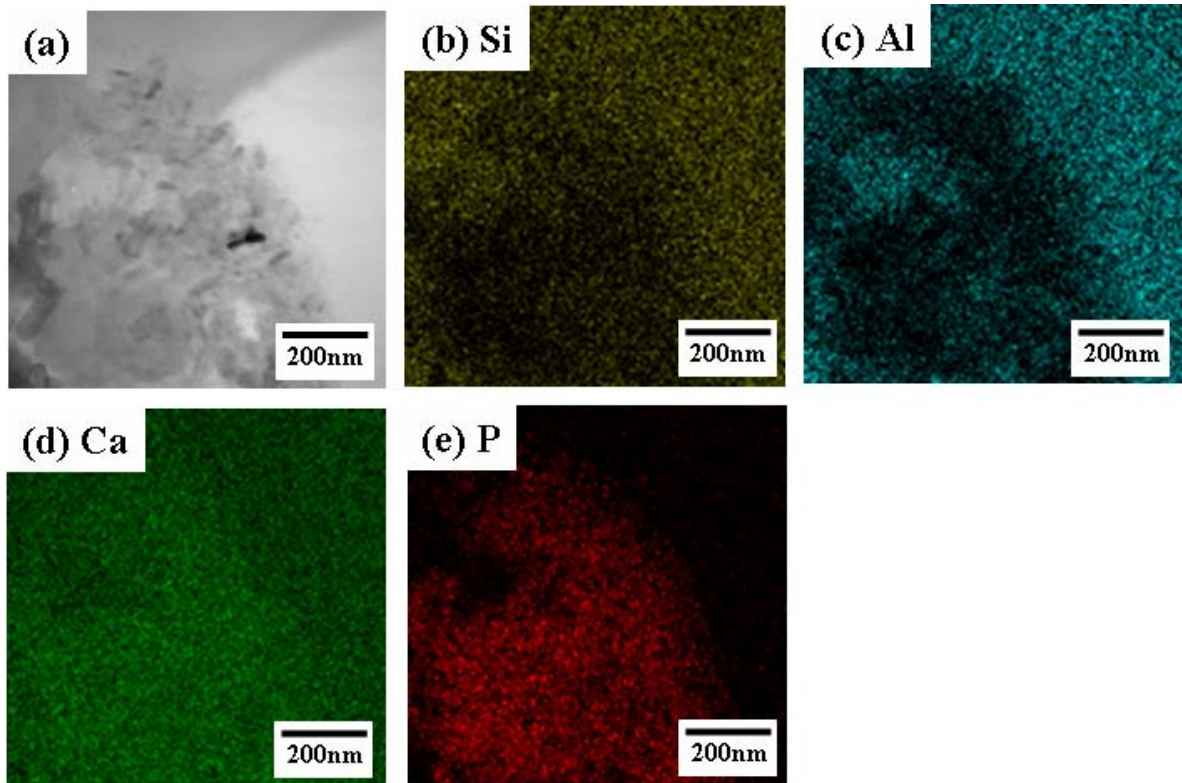


Fig. 6.8. The STEM image (a) and EDS mappings (Si (b), Al (c), Ca (d) and P (e)) of the sintered body obtained at 900°C by PECS.

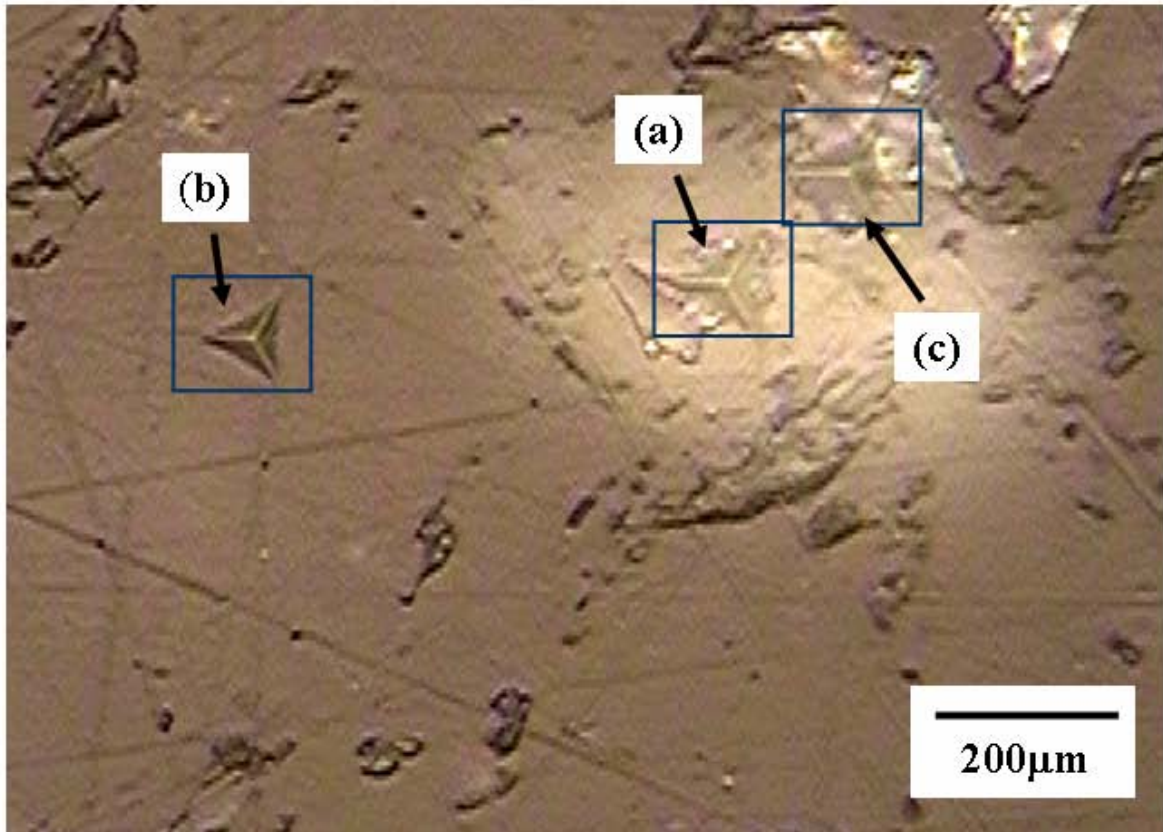


Fig. 6.9. The optical microscope images of indentations of pyramidal indenters (115°) on (a) LTA, (b) FAp and (c) the interface between LTA and FAp in the sintered body by a dynamic-ultra-microhardness tester.

6-13. REFERENCES

- 1) W. M. Meier, D. H. Olson, and C. Baerlocher, *Zeolites*, 17, 1(1996).
- 2) D. W. Breck, In *Zeolite Molecular Sieves*, Eds. D. W. Breck. Wiley, New York, 83(1974).
- 3) Y. Watanabe, H. Yamada, H. Kokusen, J. Tanaka, Y. Moriyoshi and Y Komatsu, *Sep. Sci. Technol.*, 38[7], 1519(2003).
- 4) Y. Watanabe, H. Yamada, J. Tanaka, Y. Komatsu and Y. Moriyoshi, *Sep. Sci. Technol.*, 39, 2091(2004).
- 5) Y. Watanabe, H. Yamada, H. Kokusen, J. Tanaka, Y. Moriyoshi, and Y. Komatsu, In *Proceedings of The 18th International Japan-Korea Seminar on Ceramics*, 543(2001).
- 6) H. Mimura and K. Akiba, *J. Nucl. Sci. Technol.*, 30[5], 436(1993).
- 7) K. C. Song, H. K. Lee, H. Moon and K. J. Lee, *Sep. Purif. Technol.*, 12[3], 215 (1997).
- 8) E. C. Moreno, M. Kresak and R. T. Zaharadnik, *Nature*, 24[5435], 64(1974).
- 9) I. Yanagisawa, J. Izumi, N. Tomonaga, H. Kitao, A. Neyama, and K. Katurai, *Journal of Nuclear Fuel Cycle and Environment*, 6, 67(1999).
- 10) Y. W. Gu, N. H. Loh, K. A. Khor, S. B. Tor, and P. Cheang, *Biomaterials*, 23, 37(2002).
- 11) A. Nakahira, M. Tamai, H. Aritani, S. Nakamura, and K. Yamashita, *J. Biomed. Mater. Res.* **62**, 550(2002).
- 12) M. Akao, H. Aoki, and K. Kato, *J. Mater. Sci.* 16, 809(1981).
- 13) K. Takikawa, and M. Akao, *J. Mater. Sci.-Mater. Med.* **7**, 439(1996).

- 14) Y. Watanabe, Y. Moriyoshi, T. Hashimoto, Y. Suetsugu, T. Ikoma, T. Kasama, H. Yamada, and J. Tanaka, *J. Am. Ceram. Soc.*, 87, 1395(2004).
- 15) Y. Watanabe, Y. Moriyoshi, T. Hashimoto, T. Kasama, Y. Suetsugu, T. Ikoma, H. Yamada, and J. Tanaka, In *Proceedings of The 20th International Japan-Korea Seminar on Ceramics*, 213(2003).
- 16) S. Chandrasekhar, and P. N. Pramada, *Ceram. Int.*, 27, 351(2001).

CHAPTER 7.

CONCLUSIONS

7-1. GENERAL CONCLUSION

The results of this study showed that various zeolite and zeolite/apatite composites were promising materials for removing harmful ions such as NH_4^+ , Cd^{2+} , and Pb^{2+} , and for fixing radioactive ions such as Cs^+ , Sr^{2+} , and I for a long period of time.

Following conclusions were derived.

7-2. Ammonium adsorption with various zeolites

Various natural zeolites mined from Shimane and Akita prefectures, Japan, and Mount Gipps, Australia have been shown to have a high ammonium adsorption capacity. Of these zeolites, Akita zeolite, which is rich in clinoptilolite, was shown to have the highest ammonium adsorption capacity of 1.318 mmol/g. Regarding ion exchange of Na^+ on natural zeolites, Na^+ was used as an alternative to ammonium ions in an ammonium chloride solution, and H^+ ions in distilled water and hydrochloric acid. The order of ammonium ion exchange selectivity for cations on zeolites was $\text{Na}^+ \gg \text{K}^+ > \text{Ca}^{2+} > \text{Mg}^{2+}$. The amount of ammonium ions adsorbed in this experiment quantitatively corresponded to the theoretically expected amount of adsorbed ions given a mole balance on the zeolites at high ammonium concentrations. This result indicates that ammonium adsorption occurs by ion exchange with Na^+ , K^+ , Mg^{2+} , and Ca^{2+} in cation-exchange sites on zeolites.

The ammonium ion exchange activity of synthetic zeolites (Na-SOD, NaCs-RHO, Na-LTA, and Na-FAU) was dependent on their open-window sizes, pore structures, and cation exchange capacities. The Na-FAU, which has the largest open-windows among

these zeolites, showed the highest exchange capacity of ammonium ions.

Natural zeolitic rocks, such as mordenite and clinoptilolite with traces of quartz and feldspar, were treated hydrothermally with 0.1, 0.3, 1.0, and 3.0 M NaOH solutions at temperatures below 150°C. The phase change of these zeolites depended on reaction conditions such as hydrothermal temperature and NaOH concentration, as well as the chemical compositions of the starting materials. The amount of ammonium ions up-taken by the product modified from MOR3 at 100°C in 3 M NaOH solution, which contained mainly phillipsite, was twofold larger (1.92 mmol/g) than that up-taken by the starting material. This result is explained by higher CEC of phillipsite framework in comparison to mordenite and clinoptilolite. The mechanism of ammonium up-take by phillipsite involved ion-exchange of Na⁺ ions with ammonium ions. The framework structure of phillipsite was stable in an ammonium ion solution, and therefore we conclude that phillipsite is ideal for an industrial ion-exchanger to remove ammonium ions from wastewater.

7-3. The preparation of zeolite/apatite composites for removing of harmful ions and for fixing radioactive ions

We successfully obtained the nanocomposites by a new concept which applied an ion exchange reaction. The thin layers of hydroxyapatite needle-like crystals with 100-200 nm in diameter and 30 nm in thickness were formed on the surface of type-A zeolite by a reaction between discharged Ca²⁺ ions from type-A zeolite and an ammonium phosphate

solution in hydrothermal treatment. The *c*-axes of the hydroxyapatite crystals preferentially oriented along the direction perpendicular to the LTA surface. The ion exchange of Ca^{2+} on LTA for NH_4^+ in an ammonium phosphate solution is a driving force of the formation and the preferential orientation of hydroxyapatite.

The ion exchange ability in 0-10 mM NaCl solutions was investigated for a novel type-A zeolite (NH_4^+ type) covered with a hydroxyapatite layer prepared by hydrothermal treatment. The silicon and aluminum ions dissolved from the zeolite framework were less than 0.1 wt%, and the structure was not collapsed. The Na^+ ions in the solutions were exchanged for NH_4^+ ions in cation exchange sites on the type-A zeolite since the exchanged amount of Na^+ ions for NH_4^+ ions was almost coincident. This result indicates that the type-A zeolite with hydroxyapatite layers maintains ion-exchange ability.

The structure of LTA was not destroyed by the hydrothermal treatment at 25-160°C for 8 hrs and also at 120°C for 1 to 72 hrs. The yield of LTA with HAp thin layers synthesized at 120°C for 8hrs showed a maximum value of 0.82. The specific surface area was maintained in the treatment at 25 and 40°C for 8 hrs as compared with that of Ca-LTA, but over 80°C, the value decreased with an increase of temperature. These nanocomposites obtained are novel materials for the simultaneous adsorption and capsulation of both harmful and radioactive ions, which has the excellent characteristics of both zeolite and hydroxyapatite.

The fabrication of sintered body of LTA with HAp thin layers and FAp was succeeded

by using the PECS method at 900°C. The LTA phase changed to an amorphous phase under this condition. The amorphous LTA in the sintered bodies was completely surrounded by HAp and FAp. The microstructural observations indicated that the three different phases (the amorphous LTA, HAp, and FAp) were completely sintered. The HAp thin layers played an important role for improving the affinity between FAp and LTA. The microhardness of the amorphous LTA, and the interface of amorphous LTA and FAp were weaker than that of FAp, and three point bending strength was also weaker than that of FAp. The sintered bodies of LTA with HAp thin layers and FAp are promising materials as a long-term assurance material for the disposal of radioactive waste.

List of publication

1. 論文リスト

1.1 受理済論文（審査付）

- 1) Yujiro Watanabe, Junichi Minato, Hirohisa Yamada, Junzo Tanaka, Yu Komatsu and Yusuke Moriyoshi “Environmental Purification Materials: Removal of Phosphate and Ammonium Ion in Water System” *Trans. Mater. Res. Soc. Jpn.*, **29**[5], 2309-2312 (2004).
- 2) Yujiro Watanabe, Toshiyuki Ikoma, Yasushi Suetsugu, Hirohisa Yamada, Junzo Tanaka, and Yusuke Moriyoshi “Fabrication of Transparent Hydroxyapatite Sintered Body with High Crystal Orientation by Pulse Electric Current Sintering” *J. Am. Ceram. Soc.*, **88**[1] 243-245 (2005).
- 3) Yujiro Watanabe, Hirohisa Yamada, Junzo Tanaka and Yusuke Moriyoshi “Hydrothermal modification of natural zeolites to improve up-take of ammonium ions” *Journal of Chemical Technology and Biotechnology*, **80**[4], 376-380 (2005).
- 4) Yujiro Watanabe, Hirohisa Yamada, Junzo Tanaka, Yu Komatsu and Yusuke Moriyoshi “The Adsorption of Ammonium Ions on Synthetic Zeolites: Ammonium Ion Exchange of Synthetic Zeolites: The Effect of Their Open-Window Sizes, Pore Structures, and Cation Exchange Capacities” *Sep. Sci. Technol.*, **39**[9], 2091-2104 (2004).
- 5) Yujiro Watanabe, Yusuke Moriyoshi, Tadashi Hashimoto, Yasushi Suetsugu, Toshiyuki Ikoma, Takeshi Kasama, Hirohisa Yamada and Junzo Tanaka “Hydrothermal Preparation of Type-A Zeolite with hydroxyapatite Surface Layers” *J. Am. Ceram. Soc.*, **87**[7] 1395-1397 (2004).
- 6) Yujiro Watanabe, Hirohisa Yamada, Hisao Kokusen, Junzo Tanaka, Yusuke Moriyoshi and Yu Komatsu, “Ion Exchange Behavior of Natural Zeolites in Distilled Water, Hydrochloric Acid, and Ammonium Chloride Solution” *Sep. Sci. Technol.*, **38**[7], 1519-1532 (2003).
- 7) Yujiro Watanabe, Hirohisa Yamada, Junichi Minato, Masami Sekita, Junzo Tanaka, Yu Komatsu, Geoffrey W. Stevens and Yusuke Moriyoshi “Ammonium Ion Exchange Behaviors on Natural Clinoptilolites” *Journal of Ion Exchange*, **14**, 217-220 (2003).
- 8) Junichi Minato, Yujiro Watanabe, Keisuke Fukushi, Kenji Tamura and Hirohisa Yamada “Nanoporous glass by pseudomorphi transformation of zeolite” *Trans. Mater. Res. Soc. Jpn.*, **29**[5] 2183-2186 (2004).
- 9) Junichi Minato, Yujiro Watanabe, Tadashi Hashimoto and Hirohisa Yamada “Adsorption of Ammonium Ion on Non-crystalline Pseudomorph after Na-LTA Zeolite”, *Journal of Ion Exchange*, **14**, 121-124 (2003).
- 10) Tadashi Hashimoto, Yujiro Watanabe, Hirohisa Yamada, Junichi Minato, Masami Sekita, Junzo Tanaka, Yu Komatsu and Yusuke Moriyoshi “Modification of Natural Mordenite by Alkali Hydrothermal Treatments”, *Journal of Ion Exchange*, **14**, 125-128 (2003).
- 11) Takeshi Kasama, Yujiro Watanabe, Hirohisa Yamada and Takashi Murakami “Sorption of Phosphates on Al-Pillared Smectites and Mica at Acidic to Neutral pH” *Appl. Clay Sci.*, **25**, 167-177 (2004).
- 12) Junichi Minato, Yun-Jong Kim, Hirohisa Yamada, Yujiro Watanabe, Kenji Tamura, Shingo Yokoyama, Sung Baek Cho, Yu Komatsu, and Geoffrey W. Stevens “Alkali-Hydrothermal Modification of Air-Classified Korean Natural Zeolite and Their Ammonium Adsorption Behaviors” *Sep. Sci. Technol.* **39**[16], 3739-3751 (2004).

1.2 投稿中論文（審査付）

- 1) Yujiro Watanabe, Toshiyuki Ikoma, Yasushi Suetsugu, Hirohisa Yamada, Kenji Tamura, Junzo Tanaka, and Yusuke Moriyoshi “Type-A zeolites with hydroxyapatite surface layers formed by an ion exchange reaction” Submitted to J. Eur. Ceram. Soc. (2004).
- 2) Yujiro Watanabe, Toshiyuki Ikoma, Yasushi Suetsugu, Hirohisa Yamada, Kenji Tamura, Junzo Tanaka, and Yusuke Moriyoshi “The densification of zeolite/apatite composites using a pulse electric current sintering method: A long-term assurance material for the disposal of radioactive waste” Submitted to J. Eur. Ceram. Soc. (2004).
- 3) Yujiro Watanabe, Toshiyuki Ikoma, Hirohisa Yamada, Yasushi Suetsugu, Kenji Tamura, Junzo Tanaka, and Yusuke Moriyoshi “Synthesis of Nano-Apatite Crystals on The Surface of Phillipsite” Submitted to Phosphorous Research Bulletin 17 (2004).
- 4) Hirohisa Yamada, Yujiro Watanabe, Tadashi Hashimoto, Kenji Tamura, Toshiyuki Ikoma, Shingo Yokoyama, Junzo Tanaka and Yusuke Moriyoshi “Synthesis and characterization of LDH-coated zeolite-LTA” Submitted to J. Eur. Ceram. Soc. (2004).

1.3 国際学会 Proceedings

- 1) Yujiro Watanabe, Yusuke Moriyoshi, Tadashi Hashimoto, Takashi Kasama, Yasushi Suetsugu, Toshiyuki Ikoma, Hirohisa Yamada and Junzo Tanaka. “Characterization of Type-A Zeolite with Hydroxyapatite Surface Layer Prepared by Hydrothermal Treatment” Proceedings of The 20th International Japan-Korea Seminar on Ceramics, 2003, 11 p213.
- 2) Yujiro Watanabe, Hirohisa Yamada, Takeshi Kasama, Junzo Tanaka, Yu Komatsu and Yusuke Moriyoshi “Adsorption Behavior of Phosphorus on Synthetic Boehmite” Proceedings of The 19th International Korea-Japan Seminar on Ceramics, 2002, 11 p80.
- 3) Yujiro Watanabe, Hirohisa Yamada, Hisao Kokusen, Junzo Tanaka, Yusuke Moriyoshi and Yu Komatsu “Adsorption of Ammonium Ion on Natural Zeolites Treated at Hydrothermal Conditions” Proceedings of The 18th International Japan-Korea Seminar on Ceramics, 2001,11 p548.
- 4) Yujiro Watanabe, Hirohisa Yamada, Hisao Kokusen, Junzo Tanaka, Yusuke Moriyoshi and Yu Komatsu “Effect of Cage-Size on Ammonium Adsorption by Synthetic Zeolites” Proceedings of The 18th International Japan-Korea Seminar on Ceramics, 2001,11 p543.
- 5) Junichi Minato, Yun-Jong Kim, Yujiro Watanabe, Sung Back Cho, Taik-Nam Kim and Hirohisa Yamada “Adsorption of Ammonium Ion on Korean Natural Zeolite: Untreated and Treated at Hydrothermal Condition” Proceedings of The 20th International Japan-Korea Seminar on Ceramics, 2003, 11 p209.
- 6) Junichi Minato, Yujiro Watanabe, Keisuke Fukushi, Kenji Tamura and Hirohisa Yamada “Formation of Noncrystalline Pseudomorph after NaA Zeolite at Acid Condition” Proceedings of The 20th International Japan- Korea Seminar on Ceramics, 2003, 11 p107.
- 7) Hirohisa Yamada, Yujiro Watanabe and Kenji Tamura “Synthesis of Characterization of High-Crystallinity Mg-Smectite” Proceedings of The 19th International Korea-Japan Seminar on Ceramics, 2002, 11 p367.

2. 特許

- 1) 田中順三、守吉佑介、渡辺雄二郎、橋本正、池上隆康、山田裕久、末次寧、生

- 駒俊之、“アパタイト系化合物で被覆されたゼオライト系化合物の製造方法” 特願 2003-104755
- 2) 湊淳一、山田裕久、田村堅志、渡辺雄二郎、橋本正、“多孔質ガラス微小粒子およびその製造方法” 特願 2003-345253
 - 3) 山田裕久、田村堅志、田中順三、生駒俊之、守吉佑介、渡辺雄二郎、橋本正、“層状複水酸化物／ゼオライト複合体及びその製造法” 特願 2004-081920
 - 4) 山田裕久、田村堅志、田中順三、生駒俊之、末次寧、守吉佑介、渡辺雄二郎 ”放射性元素含有廃棄物の吸着剤および放射性元素の固定化方法” 特願 2004-169135
 - 5) 山田裕久、田村堅志、田中順三、生駒俊之、末次寧、守吉佑介、渡辺雄二郎 ”放射性元素含有廃棄物の吸着剤および放射性元素の固定化方法” 特願 2004-169137
 - 6) 生駒俊之、渡辺雄二郎、末次寧、田中順三、守吉佑介 ”配向アパタイト焼結体の製造方法” 特願 2004-159052

3. 口頭発表リスト

3.1 国際会議

- 1) Yujiro Watanabe, Toshiyuki Ikoma, Yasushi Suetsugu, Hirohisa Yamada, Kenji Tamura, Junzo Tanaka, and Yusuke Moriyoshi “Type-A zeolites with hydroxyapatite surface layers formed by an ion exchange reaction” Eindhoven in the Netherlands. International Symposium on Inorganic and Environmental Materials 2004, 2004, 10.
- 2) Yujiro Watanabe, Toshiyuki Ikoma, Yasushi Suetsugu, Hirohisa Yamada, Kenji Tamura, Junzo Tanaka, and Yusuke Moriyoshi “The densification of zeolite/apatite composites using a pulse electric current sintering method: A long-term assurance material for the disposal of radioactive waste” Eindhoven in the Netherlands. International Symposium on Inorganic and Environmental Materials 2004, 2004, 10.
- 3) Yujiro Watanabe, Toshiyuki Ikoma, Yasushi Suetsugu, Junzo Tanaka and Yusuke Moriyoshi. “Fabrication of Transparent Hydroxyapatite Sintered Bodies with High Crystal Orientation by Spark Plasma Sintering” Sydney in Australia. 7th World Biomaterials Congress 2004, 5.
- 4) Yujiro Watanabe, Yusuke Moriyoshi, Tadashi Hashimoto, Takashi Kasama, Yasushi Suetsugu, Toshiyuki Ikoma, Hirohisa Yamada and Junzo Tanaka. “Characterization of Type-A Zeolite with Hydroxyapatite Surface Layer Prepared by Hydrothermal Treatment” Shimane in Japan. The 20th International Japan-Korea Seminar on Ceramics. 2003, 11.
- 5) Yujiro Watanabe, Hirohisa Yamada, Junzo Tanaka, Yu Komatsu and Yusuke Moriyoshi. “Environmental Purification Materials: Removal of Phosphate and Ammonium Ion in Water System” Yokohama. IUMRS-ICAM2003. 2003, 10.
- 6) Yujiro Watanabe, Hirohisa Yamada, Junichi Minato, Masami Sekita, Junzo Tanaka, Yu Komatsu, Geoffrey W. Stevens, Yusuke Moriyoshi “Ammonium Ion Exchange Behaviors on Natural Clinoptilolites” Kanazawa. The 3rd International Conference on Ion Exchange. 2003, 7.
- 7) Yujiro Watanabe, Hirohisa Yamada, Junichi Minato, Junzo Tanaka and Yusuke Moriyoshi “Eco-function Materials: The Removal of Phosphate and Ammonium in Wastewater” Yokohama. International Symposium on Nanotechnology and Materials

- for the Environment 2003, 3.
- 8) Yujiro Watanabe, Hirohisa Yamada, Takeshi Kasama, Junzo Tanaka, Yu Komatsu, Yusuke Moriyoshi “Adsorption Behavior of Phosphorus on Synthetic Boehmite” soul in Korea. The 19th International Korea-Japan Seminar on Ceramics. 2002, 11.
 - 9) Yujiro Watanabe, Hirohisa Yamada, Junzo Tanaka, Yu Komatsu, Yusuke Moriyoshi “Synthesis and Characterization of Phillipsite from Natural Mordenite” Tokyo, International Symposium on Advanced Technology ISAT-1st : Nanotechnology & its Related Sciences. 2002,11.
 - 10) Yujiro Watanabe, Hirohisa Yamada, Hisao Kokusen, Junzo Tanaka, Yusuke Moriyoshi, Yu Komatsu “Effect of Cage-size on Ammonium Adsorption by Synthetic Zeolites” Kagoshima The 18th International Japan-Korea Seminar on Ceramics. 2001, 11.
 - 11) Yujiro Watanabe, Hirohisa Yamada, Hisao Kokusen, Junzo Tanaka, Yusuke Moriyoshi, Yu Komatsu “Adsorption of Ammonium Ion on Natural Zeolites Treated at Hydrothermal Conditions” Kagoshima The 18th International Japan-Korea Seminar on Ceramics. 2001,11.
 - 12) Yujiro Watanabe, Yu komatsu, “Adsorption of Ammonium Ions on Porous Silicates” 18th International Symposium on Separation Chemistry, Ibaraki, National Institute for Research in Inorganic Materials, 2000, 11.
 - 13) Hirohisa Yamada, Yujiro Watanabe, Tadashi Hashimoto, Kenji Tamura, Toshiyuki Ikoma, Shingo Yokoyama, Junzo Tanaka and Yusuke Moriyoshi “Synthesis and characterization of LDH-coated zeolite-LTA” Eindhoven in the Netherlands. International Symposium on Inorganic and Environmental Materials 2004, 2004, 10.
 - 14) Hirohisa Yamada, Yujiro Watanabe, Kenji Tamura “Environmental Purification Materials in Ecomaterials Center/NIMS” Third NIMS-NEERI Workshop on Environmental Materials 2004, 7.
 - 15) Hirohisa Yamada, Yujiro Watanabe, Kenji Tamura, Masaki Nakamura, Hisao Kokusen and Yu Komatsu “Recent Topics of Eco-Functional Materials for Environmental Purification” The 23rd International Symposium on Separation Chemistry, Kanazawa, Japan 2003, 2.
 - 16) Kenji Tamura, Hirohisa Yamada, Yujiro Watanabe and Yu Komatsu “Application of The Langmuir-Blodgett Technique to Prepare Functional Nano-Structured Films” The 23rd International Symposium on Separation Chemistry, Kanazawa, Japan 2003, 2.
 - 17) Yu. Komatsu, Yujiro Watanabe, Hirohisa. Yamada, Junzo. Tanaka, Yusuke Moriyoshi, Hisohisa. Kokusen “Ion Exchange Behavior of Ammonium Ion on Natural Zeolite” 10th Asian Chemical Congress, Hanoi, Betonamu 2003, 11.
 - 18) Junichi Minato, Yun-Jong Kim, Yujiro Watanabe, Sung Back Cho, Taik-Nam Kim and Hirohisa Yamada “Adsorption of Ammonium Ion on Korean Natural Zeolite: Untreated and Treated at Hydrothermal Condition” Shimane in Japan. The 20th International Japan-Korea Seminar on Ceramics. 2003, 11.
 - 19) Junichi Minato, Yujiro Watanabe, Keisuke Fukushi, Kenji Tamura and Hirohisa Yamada “Formation of Noncrystalline Pseudomorph after NaA Zeolite at Acid Condition” Shimane in Japan. The 20th International Japan-Korea Seminar on Ceramics. 2003, 11.
 - 20) Junichi Minato, Kenji Tamura, Hirohisa Yamada and Yujiro Watanabe “Nanoporous glass by pseudomorphi transformation of zeolite” IUMRS-ICAM2003 & The 6th International Conference on Ecomaterials, Yokohama, Japan 2003, 10.
 - 21) Tadashi Hashimoto, Yujiro Watanabe, Hirohisa Yamada, Junichi Minato, Masami Sekita, Junzo Tanaka, Yu Komatsu, Yusuke Moriyoshi “Modification of Natural

- Mordenite by Alkali Hydrothermal Treatments” Kanazawa. The 3rd International Conference on Ion Exchange 2003, 7.
- 22) Junichi Minato, Yujiro Watanabe, Tadashi Hashimoto and Hirohisa Yamada “Adsorption of Ammonium Ion on Non-crystalline Pseudomorph after Na-LTA Zeolite” Kanazawa. The 3rd International Conference on Ion Exchange 2003, 7.
 - 23) Junichi Minato, Yujiro Watanabe and Hirohisa Yamada “Formation of Non-crystalline Pseudomorph after Na-LTA at Acidic Solution” Yokohama. International Symposium on Nanotechnology and Materials for the Environment 2003,3.
 - 24) Hirohisa Yamada, Yujiro Watanabe, Kenji Tamura “Synthesis and Characterization of high-crystallinity Mg-smectite” Seoul in Korea. The 19th International Korea-Japan Seminar on Ceramics. 2002, 11.
 - 25) Hirohisa Yamada, Yujiro Watanabe, Yu Komatsu “Synthesis of new aluminosilicate adsorbent for ammonium ions” The 19th International Symposium on Separation Chemistry. Kanazawa 2002, 6.
 - 26) Hirohisa Yamada, Yujiro Watanabe, Yu Komatsu “Synthesis of new aluminosilicate adsorbent for ammonium ions” The 19th International Symposium on Separation Chemistry. Kanazawa 2002, 6.
 - 27) Yusuke Moriyoshi, Yujiro Watanabe, Yoshiki Shimizu, Yosuke Suganuma and Hideki Monma “Reaction Products between Sepiolite and Sulfuric acid” Budapest 2001, 6.

3.2 国内会議

- 1) 渡辺雄二郎、生駒俊之、末次寧、山田裕久、田中順三、守吉佑介 ”パルス通電加圧焼結法による水酸アパタイト透明配向緻密体の作製と評価” 日本バイオマテリアル学会シンポジウム、茨城、2004年11月
- 2) 渡辺雄二郎、生駒俊之、末次寧、山田裕久、田村堅志、小松 優、田中順三、守吉佑介 ”ヨウ素含有ゼオライトAのアパタイトコーティング効果” 第109回無機マテリアル学会、仙台、2004年11月
- 3) 渡辺雄二郎、生駒俊之、末次寧、山田裕久、田村堅志、田中順三、守吉佑介 ”イオン交換プロセスを用いた各種ゼオライトのアパタイトコーティング” 第20回日本イオン交換学会、山梨、2004年9月
- 4) 渡辺雄二郎、生駒俊之、末次寧、山田裕久、田村堅志、田中順三、守吉佑介 ”パルス通電加圧焼結法によるベーマイト/アパタイト複合焼結体の作製” 第48回粘土科学討論会、新潟、2004年9月
- 5) 渡辺雄二郎、橋本正、山田裕久、田村堅志、生駒俊之、田中順三、守吉佑介 ”ゼオライト/LDHコンポジットの合成” 第108回無機マテリアル学会、東京、2004年6月
- 6) 渡辺雄二郎、生駒俊之、末次寧、田中順三、守吉佑介 ”パルス通電加圧焼結法による水酸アパタイト透明配向焼結体の作製” 第25回日本バイオマテリアル学会、大阪、2003年12月
- 7) 渡辺雄二郎、生駒俊之、末次寧、山田裕久、田中順三、小松優、守吉佑介 ”イオン交換プロセスを用いたA型ゼオライトと水酸アパタイトの複合化” 第16回イオン交換セミナー・ポスター研究発表会、東京、2003年10月
- 8) 渡辺雄二郎、末次寧、生駒俊之、山田裕久、田中順三、守吉佑介 ”放射性元素固定化に関する研究～水酸アパタイトを表層に有するゼオライトの特徴とその性能評価～” 第107回無機マテリアル学会、名古屋、2003年10月

- 9) 渡辺雄二郎、福士圭介、笠間丈史、湊淳一、山田裕久、田中順三、守吉佑介 “合成ベーマイトのリン吸着に及ぼす表面サイト構造の影響” 第 47 回粘土科学討論会、広島、2003 年 9 月
- 10) 渡辺雄二郎、末次寧、生駒俊之、山田裕久、田中順三、守吉佑介 ”水熱処理法による水酸アパタイトを表層に有するA型ゼオライトの作製” 第 106 回無機マテリアル学会、東京、2003 年 6 月
- 11) 渡辺雄二郎、山田裕久、田中順三、小松優、守吉佑介 “合成ゼオライトのアンモニウムイオン吸着:細孔径依存性” 第 105 回無機マテリアル学会、高知、2002 年 11 月
- 12) 渡辺雄二郎、山田裕久、田中順三、守吉佑介、小松優 “天然モルデナイトから合成したフィリップサイトのアンモニウムイオン吸着挙動” 第 18 回日本イオン交換学会、千葉 2002 年 10 月
- 13) 渡辺雄二郎、山田裕久、笠間丈史、田中順三、小松優、守吉佑介 “結晶性の異なるベーマイトのリン酸イオン吸着挙動” 第 46 回粘土科学討論会、仙台、2002 年 9 月
- 14) 渡辺雄二郎、山田裕久、田中順三、小松優、守吉佑介 “天然ゼオライトの水熱処理による高機能化とそのアンモニウムイオン吸着能” 第 104 回無機マテリアル学会、長岡、2002 年 6 月
- 15) 渡辺雄二郎、山田裕久、國仙久雄、田中順三、守吉佑介、小松優 “環境汚染物質の捕獲法(1): ケイ酸塩によるアンモニア及びリンの捕獲” 日本分析化学会第 50 年会、熊本、2001 年 11 月
- 16) 渡辺雄二郎、山田裕久、國仙久雄、田中順三、守吉佑介、小松優 “クロボクによるリン酸イオンの捕獲挙動” 第 17 回日本イオン交換学会、仙台、2001 年 10 月
- 17) 渡辺雄二郎、山田裕久、國仙久雄、田中順三、守吉佑介、小松優 “天然ゼオライトへのアンモニウムイオンの吸着” 第 45 回粘土科学討論会、千葉、2001 年 9 月
- 18) 渡辺雄二郎、小松優 “生活排水中の河川汚染物質除去法の開発” しまね・つくば研究者ネットワーク、茨城、つくば国際会議場 2000 年 9 月
- 19) 大澤倫子、渡辺雄二郎、守吉佑介、門間英毅、山田裕久、生駒俊之、田中順三 “複酸化物とリン酸塩の反応によるアパタイトの合成” 第 109 回無機マテリアル学会、仙台、2004 年 11 月
- 20) 大嶋俊一、國仙久雄、渡辺雄二郎、Kathy A Northcott、小松優 “メソポーラスケイ酸塩MCM-41 の二価金属イオン吸着材としての機能評価” 第 109 回無機マテリアル学会、仙台、2004 年 11 月
- 21) 横山信吾、渡辺雄二郎、宇野光、田村堅志、山田裕久、佐藤努 ”膨張性雲母粘土鉱物を用いたアンモニウムイオンの吸着” 第 48 回粘土科学討論会、新潟、2004 年 9 月
- 22) 田村堅志、山田裕久、横山信吾、渡辺雄二郎、山岸皓彦 ”LB法を用いたゼオライト薄膜の合成” 第 48 回粘土科学討論会、新潟、2004 年 9 月
- 23) 田村堅志、山田裕久、横山信吾、渡辺雄二郎 ”膨張性イライト/エポキシコンポジットの合成” 第 48 回粘土科学討論会、新潟、2004 年 9 月
- 24) 湊淳一、Yun-Jong Kim、山田裕久、渡辺雄二郎、横山信吾、田村堅志、Sung-Baek

- Cho, Geoffrey W. Stevens, 小松優 ”空気分級した韓国産ゼオライトのアルカリ水熱処理とそのアンモニウムイオン吸着挙動” 第 48 回粘土科学討論会、新潟、2004 年 9 月
- 25) 湊淳一、Yun-Jong Kim、山田裕久、渡辺雄二郎、横山信吾、田村堅志、Sung-Baek Cho, Geoffrey W. Stevens, 小松優 ”空気分級した韓国産ゼオライトのアンモニウムイオン吸着” 日本鉱物学会 2004 年度年会、岡山、2004 年 9 月
- 26) 宇野光、渡辺雄二郎、横山信吾、田村堅志、山田裕久、守吉佑介 ”フィリップサイトの合成とその特徴づけ” 第 48 回粘土科学討論会、新潟、2004 年 9 月
- 27) 山田裕久、渡辺雄二郎、田村堅志、下村周一 ”水浄化における無機材料” 新技術フォーラムin群馬 2004、群馬、2004 年 3 月
- 28) 奥戸昭雄、渡辺雄二郎、橋本正、神山広志、守吉佑介、門間英毅 “セピオライトを原料とするリン酸塩の合成” 第 19 回日本アパタイト研究会、東京、2003 年 12 月
- 29) 牧野言、渡辺雄二郎、國仙久雄、山田裕久、田中順三、守吉佑介、小松優 “クロボクによるリン酸イオンの回収” 第 18 回日本イオン交換学会、千葉 2002 年 10 月
- 30) 湊淳一、渡辺雄二郎、橋本正、山田裕久 “Na 型 LTA の非晶質仮像メカニズム” 日本鉱物学会 50 周年記念年会、大阪、2002 年 10 月
- 31) 湊淳一、渡辺雄二郎、橋本正、山田裕久 “ゼオライト A の‘アモルファス結晶（仮像）’化” 第 46 回粘土化学討論会、仙台、2002 年 9 月
- 32) 橋本正、渡辺雄二郎、湊淳一、山田裕久、田中順三、守吉佑介 “アルカリ水熱処理による天然ゼオライトの相変化” 第 46 回粘土化学討論会、仙台、2002 年 9 月
- 33) 小松優、渡辺雄二郎、守吉佑介 “天然ゼオライトを捕獲材としたアンモニウムイオンの吸着挙動” 日本分析化学会中部支部北陸地区講演会、金沢、2002 年 6 月
- 34) 小松優、渡辺雄二郎、山田裕久、田中順三 “快適な水空間創製のための資源循環型水浄化材料” セラミックス協会年会、大阪、2000 年 10 月
- 35) 小松優、渡辺雄二郎、山田裕久、矢島祥行、田中順三、守吉佑介 “多孔質ケイ酸塩によるアンモニウムイオンの吸着挙動” 第 16 回日本イオン交換学会、東京、2000 年 10 月
- 36) 小松優、山田裕久、田中順三、渡辺雄二郎、守吉佑介、 ”快適な水空間～資源循環型水浄化材料” 第三回テクノコンフォート研究会、茨城、金属材料研究所 2000 年 7 月

3.3 招待講演

- 1) 渡辺雄二郎、大島俊一、秋葉和也、有磯貴志、梶山哲人、國仙久雄、田中順三、小松優 “陰イオン捕獲材・島根・八ヶ岳産クロボクの性能評価” 第 11 回生活環境研究会金沢工業大学 2004 年 4 月
- 2) Yujiro Watanabe, Toshiyuki Ikoma, Yasushi Suetsugu, Hirohisa Yamada, Yu Komatsu, Junzo Tanaka, Yusuke Moriyoshi “A novel material for removal of both harmful and radioactive ions: Characterization of type A zeolite coated with hydroxyapatite” The

- 23rd International Symposium on Separation Chemistry, 金沢工業大学 2004年2月
- 3) 渡辺雄二郎 “水浄化材料:ゼオライトとクロボクのパフォーマンスとその評価法” 第6回生活環境研究会金沢工業大学 2003年3月
 - 4) 渡辺雄二郎、守吉佑介 “環境浄化材料によるアンモニウムイオン除去に関する研究”第2回生活環境研究会 金沢工業大学 2002年3月

4. 受賞

- 1) 渡辺雄二郎、生駒俊之、末次寧、山田裕久、田中順三、小松優、守吉佑介 第16回イオン交換セミナー・ポスター研究発表会 優秀賞

ACKNOWLEDGMENTS

I sincerely appreciate Professor Yusuke Moriyoshi of Hosei University, who passionately supervised me during this study. I wish express my thanks for valuable discussions and helpful advice on the writing of this thesis to Professors Shoichi Okouchi, Yusei Maruyama, and Hiromi Hamanaka of Hosei University and Professor Hideki Monma of the Kogakuin University.

I wish to express my special gratitude for valuable discussions, helpful advice and warm supports on this work to Dr. Junzo Tanka of Biomaterials Center of National Institute for Materials Science, Dr. Hirohisa Yamada of Ecomaterials Center of National Institute for Materials Science, Drs. Toshiyuki Ikoma and Yasushi Suetugu of Biomaterials Center of National Institute for Materials Science, Dr. Kenji Tamura of Ecomaterials Center of National Institute for Materials Science, and Professors Yu Komatsu and Hisao Kokusen of Kanazawa Institute of Technology.

I express my utmost gratitude to Dr. Hiroshi Watanabe for help with English and valuable discussions. I wish to express my special thanks for technical supports and valuable discussions to Drs. Toshiyuki Nishimura and Shingo Yokoyama, Mrs Yoshiyuki Yajima, Keiji Kurashima, and Hiroharu Komori, and Ms. Hiroko Aoki of National Institute for Materials Science, Dr. Takeshi Kasama of University of Cambridge, and Dr. Keisuke

Fukushi of National Institute of Advanced Industrial Science and Tecnology for their warm supports on this work. I wish to express my thanks to all other staffs of my laboratory of Hosei University and Biomaterials Centers of National Institute for Materials Science for their warm supports on this work.

Finally, my heartly gratitude goes to my parents who have supported me up to now.